International Energy Agency
Programme on
Energy in Buildings and Communities

Annex 59: High Temperature Cooling & Low Temperature Heating in Buildings

Final Report

III. Novel flow paths of outdoor air handling equipment

2015

Published by Department of Building Science and Technology, Tsinghua University, 100084 Beijing, P.R. China

Participating countries in EBC:
Australia, Austria, Belgium, Canada, P.R. China, Czech Republic, Denmark, Finland, France, Germany, Ireland, Italy, Japan, Republic of Korea, the Netherlands, New Zealand, Norway, Portugal, Singapore, Spain, Sweden, Switzerland, United Kingdom and the United States of America.

Additional copies of this report may be obtained from:

EBC Executive Committee Support Services Unit (ESSU)
C/o AECOM Ltd
The Colmore Building
Colmore Circus Queensway
Birmingham B4 6AT
United Kingdom
Web: www.iea-ebc.org
Email: essu@iea-ebc.org

Preface

The International Energy Agency

The International Energy Agency (IEA) was established in 1974 within the framework of the Organisation for Economic Co-operation and Development (OECD) to implement an international energy programme. A basic aim of the IEA is to foster international co-operation among the 30 IEA participating countries and to increase energy security through energy research, development and demonstration in the fields of technologies for energy efficiency and renewable energy sources.

The IEA Energy in Buildings and Communities Programme

The IEA co-ordinates international energy research and development (R&D) activities through a comprehensive portfolio of Technology Collaboration Programmes. The mission of the IEA Energy in Buildings and Communities (IEA EBC) Technology Collaboration Programme is to develop and facilitate the integration of technologies and processes for energy efficiency and conservation into healthy, low emission, and sustainable buildings and communities, through innovation and research. (Until March 2013, the IEA EBC Programme was known as the IEA Energy Conservation in Buildings and Community Systems Programme, ECBCS.)

The R&D strategies of the IEA EBC Programme are derived from research drivers, national programmes within IEA countries, and the IEA Future Buildings Forum Think Tank Workshops. These R&D strategies aim to exploit technological opportunities to save energy in the buildings sector, and to remove technical obstacles to market penetration of new energy efficient technologies. The R&D strategies apply to residential, commercial, office buildings and community systems, and will impact the building industry in five areas of focus for R&D activities:

- Integrated planning and building design
- Building energy systems
- Building envelope
- Community scale methods
- Real building energy use

The Executive Committee

Overall control of the IEA EBC Programme is maintained by an Executive Committee, which not only monitors existing projects, but also identifies new strategic areas in which collaborative efforts may be beneficial. As the Programme is based on a contract with the IEA, the projects are legally established as Annexes to the IEA EBC Implementing Agreement. At the present time, the following projects have been initiated by the IEA EBC Executive Committee, with completed projects identified by (*) and joint projects with the IEA Solar Heating and Cooling Technology Collaboration Programme by (☼):

Annex 1: Load Energy Determination of Buildings (*)
Annex 2: Ekistics and Advanced Community Energy Systems (*)
Annex 3: Energy Conservation in Residential Buildings (*)
Annex 4: Glasgow Commercial Building Monitoring (*)
Annex 5: Air Infiltration and Ventilation Centre
Annex 6: Energy Systems and Design of Communities (*)
Annex 7: Local Government Energy Planning (*)
Annex 8: Inhabitants Behaviour with Regard to Ventilation (*)
Annex 9: Minimum Ventilation Rates (*)
Annex 10: Building HVAC System Simulation (*)
Annex 11: Energy Auditing (*)
Annex 12: Windows and Fenestration (*)
Annex 13: Energy Management in Hospitals (*)
Annex 14: Condensation and Energy (*)

Annex 15: Energy Efficiency in Schools (*)
Annex 16: BEMS 1- User Interfaces and System Integration (*)
Annex 17: BEMS 2- Evaluation and Emulation Techniques (*)
Annex 18: Demand Controlled Ventilation Systems (*)
Annex 19: Low Slope Roof Systems (*)
Annex 20: Air Flow Patterns within Buildings (*)
Annex 21: Thermal Modelling (*)
Annex 22: Energy Efficient Communities (*)
Annex 23: Multi Zone Air Flow Modelling (COMIS) (*)
Annex 24: Heat, Air and Moisture Transfer in Envelopes (*)
Annex 25: Real time HVAC Simulation (*)
Annex 26: Energy Efficient Ventilation of Large Enclosures (*)
Annex 27: Evaluation and Demonstration of Domestic Ventilation Systems (*)
Annex 28: Low Energy Cooling Systems (*)
Annex 29: ☼ Daylight in Buildings (*)
Annex 30: Bringing Simulation to Application (*)
Annex 31: Energy-Related Environmental Impact of Buildings (*)
Annex 32: Integral Building Envelope Performance Assessment (*)
Annex 33: Advanced Local Energy Planning (*)
Annex 34: Computer-Aided Evaluation of HVAC System Performance (*)
Annex 35: Design of Energy Efficient Hybrid Ventilation (HYBVENT) (*)
Annex 36: Retrofitting of Educational Buildings (*)
Annex 37: Low Exergy Systems for Heating and Cooling of Buildings (LowEx) (*)
Annex 38: ☼ Solar Sustainable Housing (*)
Annex 39: High Performance Insulation Systems (*)
Annex 40: Building Commissioning to Improve Energy Performance (*)
Annex 41: Whole Building Heat, Air and Moisture Response (MOIST-ENG) (*)
Annex 42: The Simulation of Building-Integrated Fuel Cell and Other Cogeneration Systems (FC+COGEN-SIM) (*)
Annex 43: ☼ Testing and Validation of Building Energy Simulation Tools (*)
Annex 44: Integrating Environmentally Responsive Elements in Buildings (*)
Annex 45: Energy Efficient Electric Lighting for Buildings (*)
Annex 46: Holistic Assessment Tool-kit on Energy Efficient Retrofit Measures for Government Buildings (EnERGo) (*)
Annex 47: Cost-Effective Commissioning for Existing and Low Energy Buildings (*)
Annex 48: Heat Pumping and Reversible Air Conditioning (*)
Annex 49: Low Exergy Systems for High Performance Buildings and Communities (*)
Annex 50: Prefabricated Systems for Low Energy Renovation of Residential Buildings (*)
Annex 51: Energy Efficient Communities (*)
Annex 52: ☼ Towards Net Zero Energy Solar Buildings (*)
Annex 53: Total Energy Use in Buildings: Analysis and Evaluation Methods (*)
Annex 54: Integration of Micro-Generation and Related Energy Technologies in Buildings (*)
Annex 55: Reliability of Energy Efficient Building Retrofitting - Probability Assessment of Performance and Cost (RAP-RETRO) (*)
Annex 56: Cost Effective Energy and CO_2 Emissions Optimization in Building Renovation (*)
Annex 57: Evaluation of Embodied Energy and CO_2 Equivalent Emissions for Building Construction (*)
Annex 58: Reliable Building Energy Performance Characterisation Based on Full Scale Dynamic Measurements (*)
Annex 59: High Temperature Cooling and Low Temperature Heating in Buildings (*)
Annex 60: New Generation Computational Tools for Building and Community Energy Systems (*)
Annex 61: Business and Technical Concepts for Deep Energy Retrofit of Public Buildings (*)
Annex 62: Ventilative Cooling (*)
Annex 63: Implementation of Energy Strategies in Communities (*)

Annex 64: LowEx Communities - Optimised Performance of Energy Supply Systems with Exergy Principles (*)
Annex 65: Long-Term Performance of Super-Insulating Materials in Building Components and Systems
Annex 66: Definition and Simulation of Occupant Behavior in Buildings (*)
Annex 67: Energy Flexible Buildings
Annex 68: Indoor Air Quality Design and Control in Low Energy Residential Buildings
Annex 69: Strategy and Practice of Adaptive Thermal Comfort in Low Energy Buildings
Annex 70: Energy Epidemiology: Analysis of Real Building Energy Use at Scale
Annex 71: Building Energy Performance Assessment Based on In-situ Measurements
Annex 72: Assessing Life Cycle Related Environmental Impacts Caused by Buildings
Annex 73: Towards Net Zero Energy Resilient Public Communities
Annex 74: Competition and Living Lab Platform
Annex 75: Cost-effective Building Renovation at District Level Combining Energy Efficiency and Renewables
Annex 76: ☼ Deep Renovation of Historic Buildings Towards Lowest Possible Energy Demand and CO_2 Emissions
Annex 77: ☼ Integrated Solutions for Daylight and Electric Lighting
Annex 78: Supplementing Ventilation with Gas-phase Air Cleaning, Implementation and Energy Implications
Annex 79: Occupant Behaviour-Centric Building Design and Operation
Annex 80: Resilient Cooling

Working Group - Energy Efficiency in Educational Buildings (*)
Working Group - Indicators of Energy Efficiency in Cold Climate Buildings (*)
Working Group - Annex 36 Extension: The Energy Concept Adviser (*)
Working Group - HVAC Energy Calculation Methodologies for Non-residential Buildings
Working Group - Cities and Communities
Working Group - Building Energy Codes
Working Group - International Building Materials Database

Authors: Masaya Okumiya (Nagoya University), Xiaohua Liu (Tsinghua University), Yi Jiang (Tsinghua University), Michal Pomianowski (Aalborg University), Yuwei Zheng (Tsinghua University), Tao Zhang (Tsinghua University), Satoru Iizuka (Nagoya University), Teruyuki Saito (Nagoya University)

Editors: Tao Zhang, Xiaohua Liu, Masaya Okumiya

Contents

A short introduction

Air flow rate influencing the recovery efficiency

1. Typical outdoor air handling processes in each country

1.1. Weather conditions in different countries

Fig. 1-1 shows the climate conditions all over the world. There are significant discrepancies between different countries.

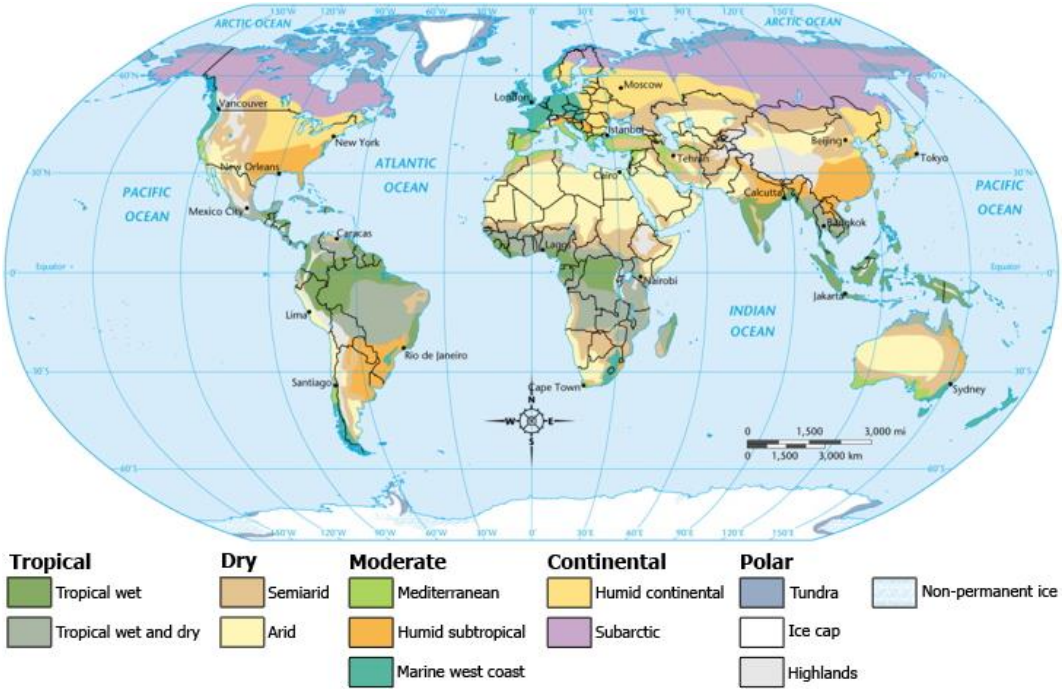

Fig. 1-1 Global climate analysis.

1.1.1. European countries

Most part of Europe is located in the 35 °–60 ° north latitude range, belonging to the Mediterranean climate. Outdoor air parameters in various cities of Europe are listed in Appendix A, which shows the outdoor humidity ratio is lower in northern area but higher in the southern. In many northern cities, outdoor humidity design ratios are approximately 11~13 g/kg in the summertime. Due to the dry outdoor air, there is only a necessity for cooling in many buildings with little to no dehumidification. While in the southern area, such as Italy, the outdoor humidity design ratio is approximately 20 g/kg, and thus, both cooling and dehumidification are needed in the summertime.

1.1.2. Japan

Japan covers a range within 25 ° in latitude from north to south, where a main feature is the four distinctive seasons. Fig. 1-2 shows summertime outdoor humidity design ratios for the main cities in Japan. As the figure indicates, a damp climate in summer with an outdoor humidity design ratio of 17–22 g/kg exists, and thus dehumidification of the outdoor air is required.

(Note: data out of brackets is parameter for no assurance of 0.4% and in brackets is 1.0%)

Fig. 1-2 Design outdoor humidity ratios in main cities of Japan (unit: g/kg).

1.1.3. China

The outdoor conditions in Chinese cities vary tremendously. The map of cities in China and the outdoor design condition are shown in Appendix A. In northwestern China, where the outdoor climate is sufficiently dry, the primary task of an air conditioner is to just cool the outdoor air rather than perform both cooling and dehumidification processes. For this situation, direct or indirect evaporative cooling technology can be utilized. However, the outdoor air will need to be both heated and humidified during the winter. In eastern China, the outdoor climate is humid; therefore, the main task of the air conditioner is to provide efficient cooling and dehumidification during the summer. In northeastern China, the air needs to be heated and humidified during wintertime while in southeastern China little heating of the outdoor air in winter is necessary.

1.1.4. United States

Temperate and subtropical climate can be found in most parts of the United States (Source: Chapter 27 Climatic Design Information of ASHRAE Handbook.). Due to the vast and varied range of local terrain, climate variation is complex.

Fig. 1-3 shows the outdoor humidity design ratios in various cities of the United States. And the values are with no assurance of 0.4% (without guaranteeing for 35 hours) and 1.0% (without guaranteeing for 88 hours). The outdoor humidity ratio is lower in the Western United States and higher in the eastern section. The summer outdoor humidity design ratio in the eastern part of the United States is approximately 17–21 g/kg; while in the western areas, such as Los Angeles, San Francisco and Seattle, the outdoor humidity design ratio is just 11 to 12 g/kg. Thus, for the Western United States during summer months, air conditioning systems

for buildings only need to provide cooling with no dehumidification.

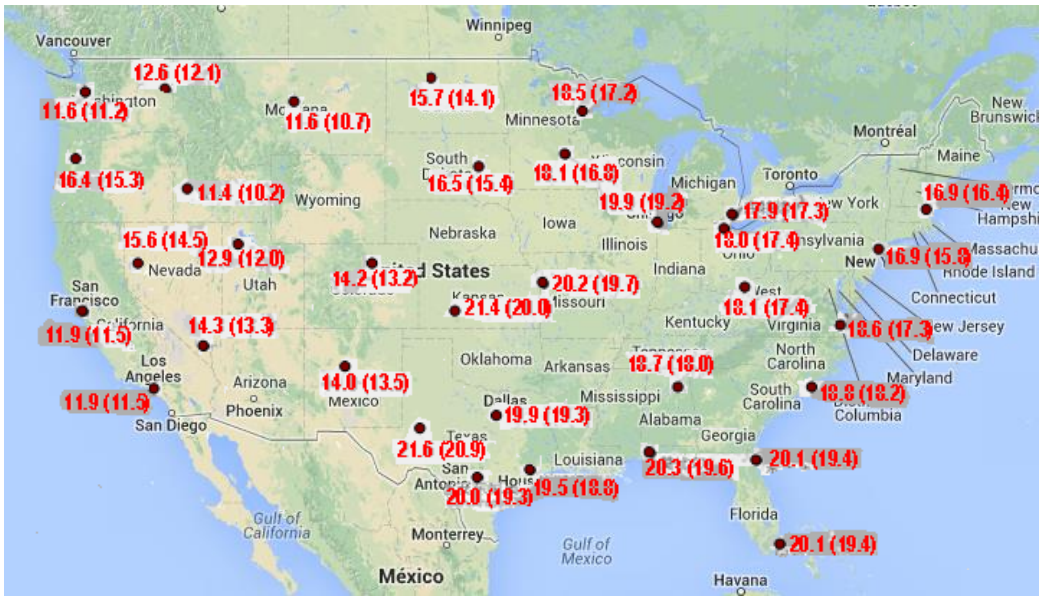

(Note: data out of brackets is parameter for no assurance of 0.4% and in brackets is 1.0%)

Fig. 1-3 Outdoor humidity design ratios for major cities in the continental United States (units: g/kg).

1.2. Outdoor air handling unit

There are many types of air handling processes that allow for mixing outdoor air with return air or keep outdoor air separated from other air streams. Outdoor air that is handled by an air handling unit (AHU) after mixing with return air is shown in Fig. 1-4(a). Outdoor air can be handled independently by an Outdoor Air Handling Unit (OAHU). Fig. 1-4(b) shows a one-line diagram where the outdoor air is mixed with return air in the AHU while Fig. 1-4(c) shows the outdoor air being directly supplied to room.

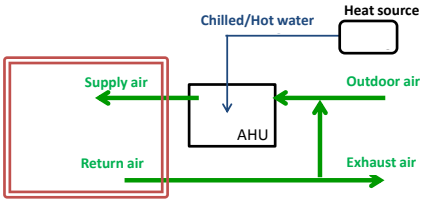

(a)

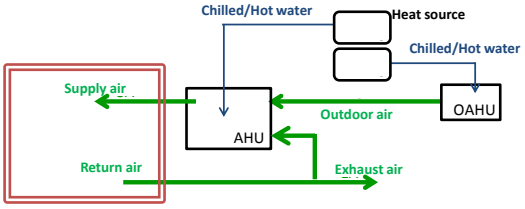

(b)

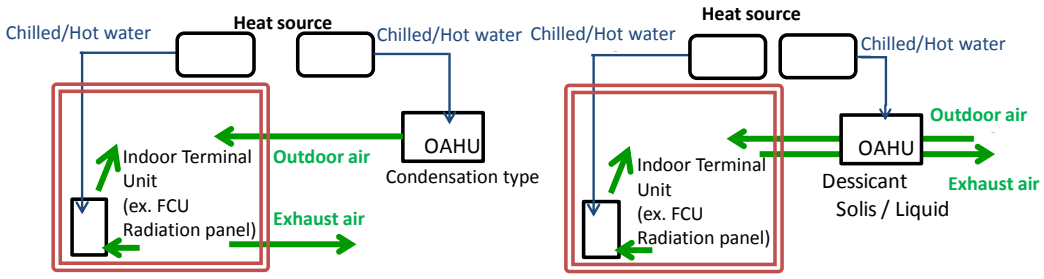

(c)

Fig. 1-4 Air handling processes in air-conditioning system: (a) Outdoor air mixed with return air before handled by AHU; (b) Outdoor air handled by the OAHU before mixing with return air; (c) Outdoor air directly supplied to the indoor space after being handled by the OAHU.

There are three common kinds of methods for handling outdoor air by an OAHU with dehumidification: condensation method, absorption method (liquid desiccant), and the adsorption method (solid desiccant). A sensible or total heat exchanger (HEX) is typically equipped with an AHU and a condensation type OAHU. A HEX is also used to direct the outdoor air into a room as shown in Fig. 1-5.

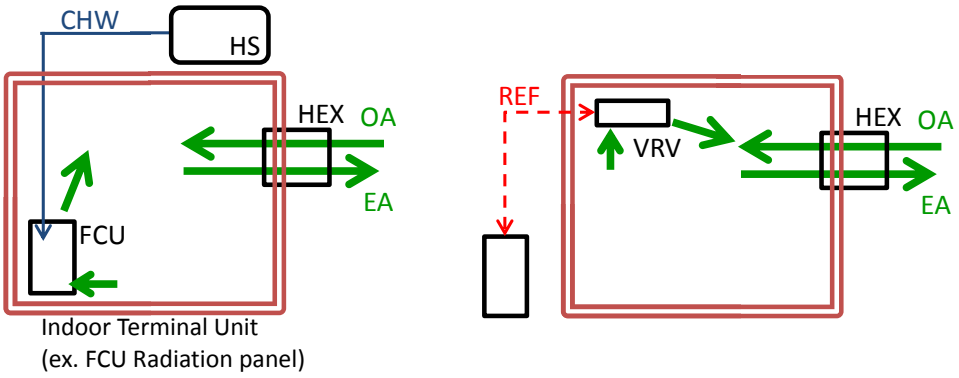

Fig. 1-5 Sensible or total heat exchanger adopted for outdoor air handling process

OAHU's are used to condition outdoor air to ensure proper sensible and latent heat loads. In the case that the OAHU is used with a radiant panel in the room, the OAHU should be designed to handle latent room heat by avoiding condensation on the panel.

2. Main parts of outdoor air handling processors

2.1. Heat recovery devices

Heat recovery devices are very useful for reducing the energy consumption of the outdoor air handling process especially in hot and humid climates. They work between outdoor air and indoor exhaust air sufficiently recovering cooling or heat from exhaust air depending on the room's environmental conditions. Heat recovery devices can be classified

into two types: sensible heat recovery devices and enthalpy recovery devices.

Sensible heat recovery devices include plate heat exchangers, heat pipe exchangers, sensible heat recovery wheels, etc. Sensible heat recovery devices can only recover sensible heat from the exhaust air. Enthalpy recovery devices, however, can recover both sensible heat and latent heat from the indoor exhaust air. This type of device demonstrates greater performance than sensible heat recovery devices. Enthalpy recovery devices include plate enthalpy heat exchangers, devices using rotary wheels and liquid desiccants. Performance and operating characteristics of common heat recovery devices are shown in Table 2-1.

Table 2-1 Performance comparison of common heat recovery devices

	Plate	Heat pipe	Desiccant wheel	Plate enthalpy	Liquid desiccant
heat recovery type	Sensible	Sensible	Sensible/Enthalpy	Enthalpy	Enthalpy
Medium	Metal/ non-Metal	Metal	Metal/ non-Metal	non-Metal	Solution
Performance index	Sensible heat efficiency	Sensible heat efficiency	Sensible/total heat efficiency	total heat efficiency	total heat efficiency
Recovery efficiency (%)	50-80	50-70	50-85	50-75	50-85
Face velocity	1.0-5.0	2.0-4.0	2.0-5.0	1.0-3.0	1.5-2.5
Pressure loss (Pa)	100-1000	100-500	100-300	100-500	150-370
Leakage (%)	0-5	0-5	0.5-10	0-5	-
Maintenance	harder	easy	harder	hard	middle
Air volume	low	middle	high	low	low

Source: Heat recovery equipment selection and installation for air-conditioning systems, China Architecture & Building Press, 2006

2.1.1. Sensible heat recovery devices

An example of a sensible heat recovery device is a plate heat exchanger as depicted in Fig. 2-1. Metal corrugated plates are positioned between two airflows forming hot and cold channels. Heat is transferred from the high temperature airflow to the low temperature airflow. The sensible heat recovery efficiency, as defined by Eq. (2-1), can be used to evaluate the plate heat exchanger performance. Corrugated plates increase the available heat exchanger area resulting in heat recovery efficiencies that can reach 50%–80%.

$$\eta = \frac{T_{outdoor,out} - T_{outdoor,in}}{T_{indoor,in} - T_{outdoor,in}} \tag{2-1}$$

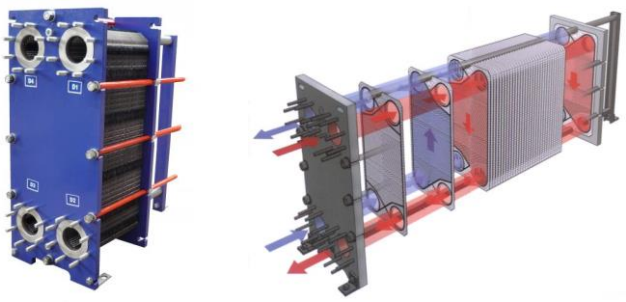

Fig. 2-1 Diagram of plate heat exchanger

2.1.2. Plate enthalpy heat exchanger

For plate enthalpy heat exchangers, air channels with triangular or U-shape sectional shapes are divided between outdoor air and indoor exhaust air using partitions, as shown in Fig. 2-2. Membranes are applied to facilitate heat and mass transfer between two airflows to maximize heat recovery.

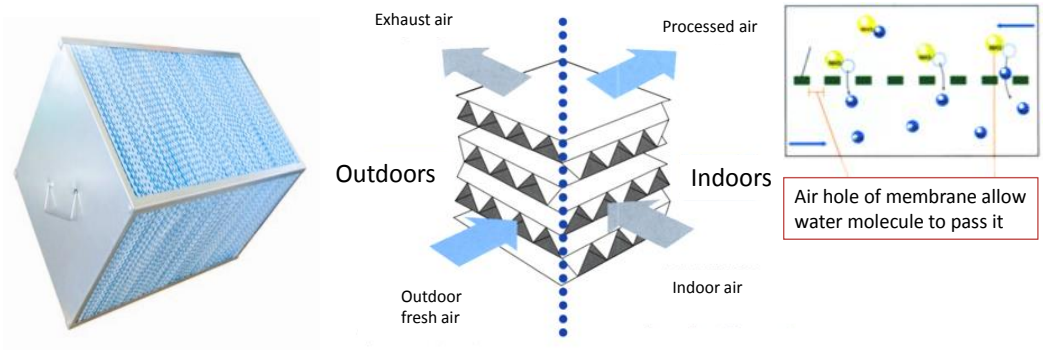

Fig. 2-2 Diagram and principle of plate enthalpy heat exchangers

2.1.3. Enthalpy recovery wheel

The enthalpy recovery device with a rotary wheel has a honeycomb cylinder structure made of paper that is coated with desiccant material as shown in Fig. 2-3. Rotation speed is typically 8–10 rpm (480–600 r/h) for this style of heat recovery device. When the water vapor pressure and temperature of the solid desiccant on the wheel are lower than that of the outdoor air, the moisture transfer direction and the heat transfer direction are both from the outdoor air to the desiccant. This process makes air dehumidification possible. With the rotation of the wheel, the fully adsorbed desiccant rotates to the indoor exhaust air zone and is dried and cooled by the exhaust air. In this process, exhaust air and outdoor air flow through the top and bottom sections of the wheel, respectively, with a counter-flow configuration to achieve enthalpy recovery.

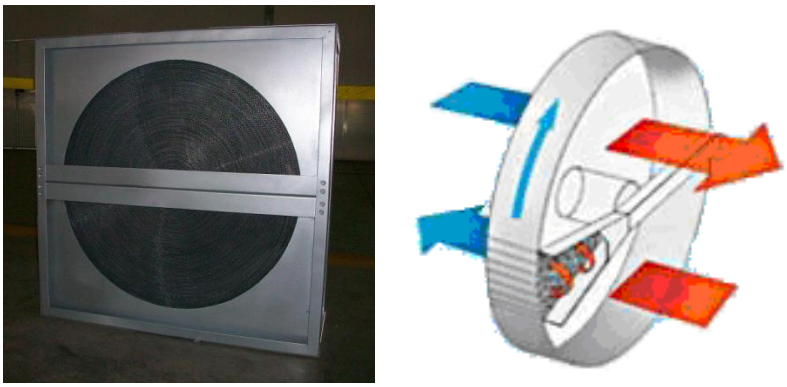

Fig. 2-3 Desiccant wheel used for heat recovery

2.2. Dehumidification device

Outdoor air humidity control is the key part of outdoor air handling process. In summer, high temperature and high humidity outdoor air should be cooled and dehumidified before supplied into rooms. Dehumidification methods include condensing dehumidification, and those using solid desiccant and liquid desiccant. The former uses cooling source with temperature lower than air dew-point temperature to cool and dehumidify the hot and moist air simultaneously. The latter produce partial vapor pressure difference (humidity ratio difference) between desiccant surface and the air by solid (silica gel, zeolite, molecular sieve, et al) or liquid desiccant (salt solution of LiBr, LiCl, $CaCl_2$, et al).

2.2.1. Condensation dehumidification methods

Condensation dehumidification uses chilled water or refrigerant with a temperature low enough to cool the humid air; as the air temperature drops below its dew point temperature, the moisture condenses and the air is dehumidified. The operating schematic of the condensation dehumidification method is demonstrated in Fig. 2-4.

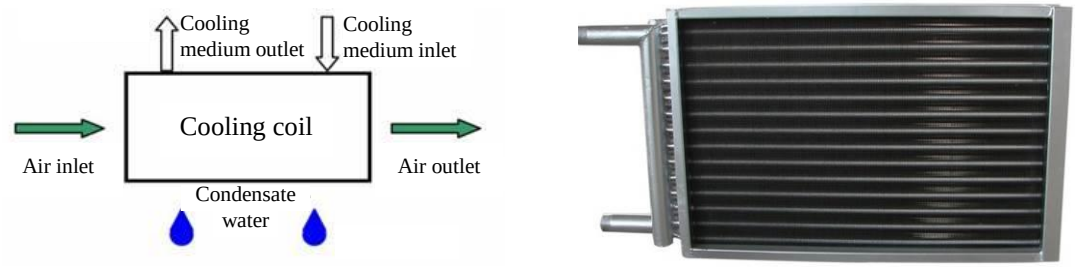

(a) (b)

Fig. 2-4 Operating schematic of the condensation dehumidification method: (a) operating principle; and (b) picture of the cooling coil.

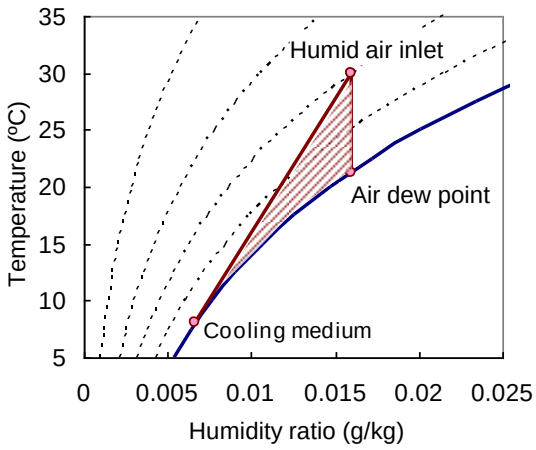

Fig. 2-5 Reachable air outlet region of the condensation dehumidification method.

The relatively low-temperature cooling medium flows into the cooling coil, and then the temperature of the humid air flowing through the coil decreases. When the saturation condition is achieved, the humid air is dehumidified and the moisture continues to be condensed as the temperature continues to decrease. Fig. 2-5 shows the reachable handling region (nearly a triangular region) of the outlet air state using the condensation dehumidification method. The temperature and humidity ratio of the processed outlet air are both lower than those of the inlet, and the state of the processed outlet air usually approaches the saturation state.

2.2.2. Dehumidification devices using liquid desiccant

The operating principle of the typical dehumidification-regeneration cycle using liquid desiccant is shown in Fig. 2-6. The left side of this figure is the air dehumidification process, and the right side is the desiccant regeneration process. In the air dehumidification process, moisture transfers from the gas phase (air) to the liquid phase (solution) because the partial pressure of water vapor in the air is greater than that in the solution. With the help of the mass transfer process, the humidity ratio of the moist air is reduced, i.e., the air is dehumidified, and the solution is diluted due to moisture absorption. Thus, the partial pressure of the water vapor in the solution is gradually increased, so that the water vapor pressure difference between the solution and the air is gradually reduced. As a result, the dehumidification ability of the solution is weakened, and regeneration of the diluted solution is required. As shown in the right part of Fig. 2-6, hot water provides the heat required for the desiccant regeneration process. A solution-to-solution heat exchanger is usually adopted in this air handling system to precool the solution flowing into the dehumidifier, and to preheat the solution flowing into the regenerator. Thus, the heat recovery process between solutions of different temperatures is realized, and the energy performance is improved.

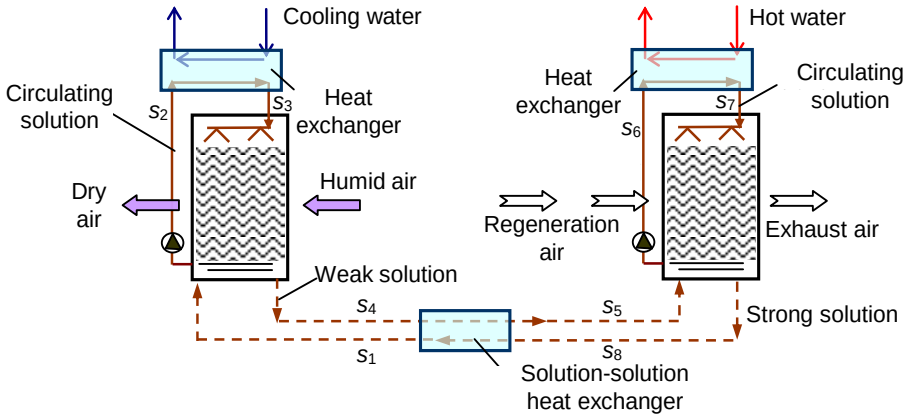

Fig. 2-6 Principle of the typical liquid desiccant dehumidification-regeneration cycle.

2.2.3. Dehumidification devices using solid desiccant

There are two types of dehumidification methods that use solid desiccant: those with rotary wheels and those with fixed desiccant beds. Desiccant wheels are widely used due to their ability to achieve continuous dehumidification and regeneration. The operating principle of a desiccant wheel is shown in Fig. 2-7. Dehumidification wheels are similar to the enthalpy recovery desiccant wheels introduced in Section 2.1, which have a honeycombed channel coated with desiccant material. Heat and mass transfer processes proceed simultaneously in the channels. In desiccant wheels used for air dehumidification, most of the surface area is used for dehumidification, and the remainder is used for regeneration. An optimal rotation speed is around 0.2~0.5 rpm (12~30 r/h).

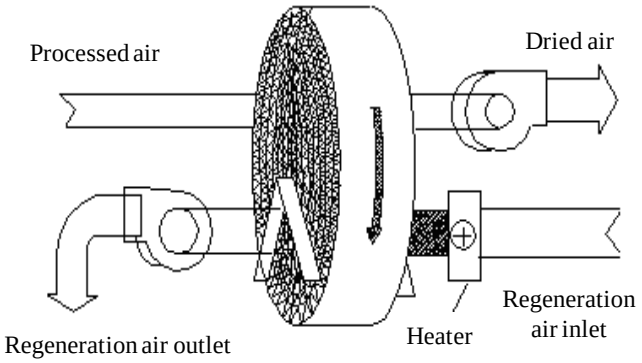

Fig. 2-7 Operating principle of the desiccant wheel used for dehumidification.

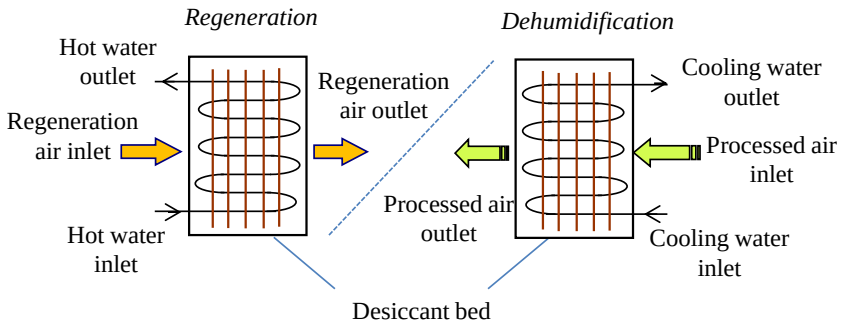

Fig. 2-8 Operating principle of the fixed desiccant bed (the first half of the cycle).

The fixed desiccant bed is another kind of dehumidification device that utilizes solid desiccant. In contrast to the rotation mode of desiccant wheels, desiccant beds realize the shifting between dehumidification and regeneration modes by shifting the air flow direction. Fig. 2-8 illustrates the working principle of a fixed descant bed (Suzuki K and Oya N, 1983; Zhang LZ, 2005). During the first half of the cycle, the left desiccant bed works in regeneration mode, while the right bed works in dehumidification mode. Humid air enters the right bed, and cooling water enters the right bed to take away the adsorption heat. Regeneration air enters the left bed, and hot water enters the left bed to provide desorption heat. During the second half of the cycle, the left bed works in dehumidification mode (with cooling water entering it), and the right bed works in regeneration mode. During the dehumidification period, the supplied air humidity ratio changes periodically due to the shifting of fan valves and water valves, and this instability of the supplied air parameters limits the use of fixed desiccant beds to some extent.

- DESICA

The internal-cooling desiccant bed is a novel kind of dehumidification device that utilizes solid desiccant, coordinating with a heat pump. The running schematic is shown in Fig. 2-9. And it's running at about 6-minute period. The solid desiccant is coated on the evaporator and condenser of the heat pump. And the moist outdoor air goes through the evaporator, and is cooled and dehumidified. The regeneration air goes through the condenser. After half period, a four-way valve changes the refrigerant line and evaporator and condenser change their ability with each other. Meanwhile, a four-way air valve exchanges two air flows, ensuring outdoor air goes through the evaporator at this half period.

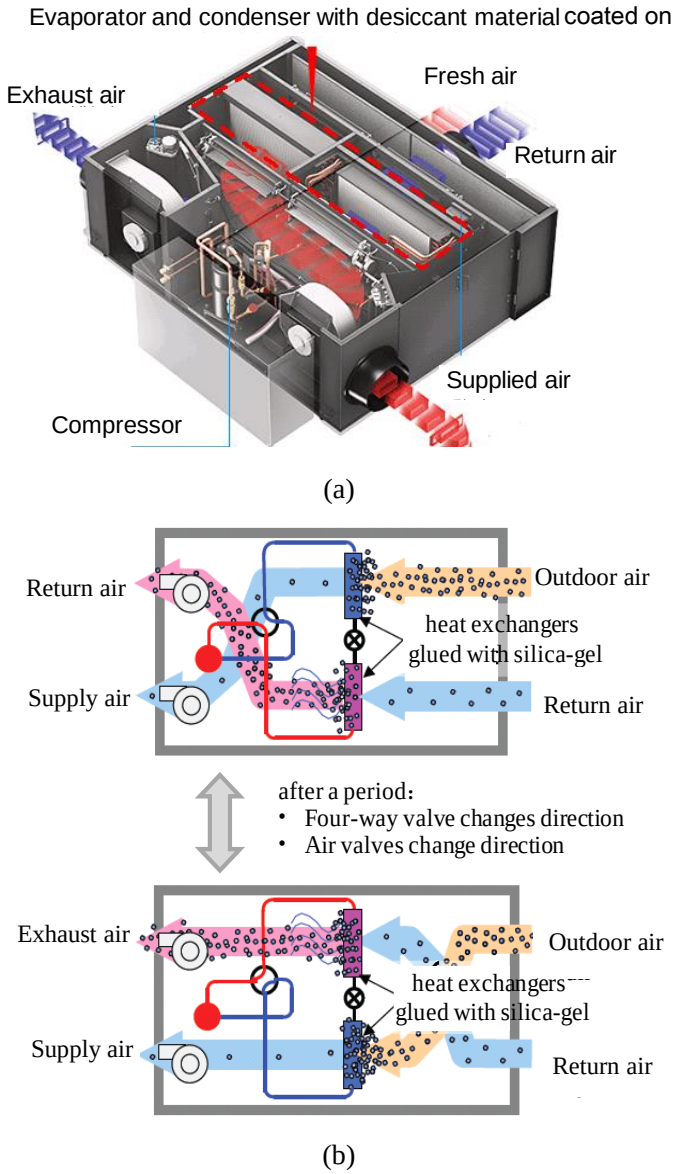

Fig. 2-9 Operating schematic of DESICA: (a) schematic diagram; and (b) operating principle.

2.3. Evaporative cooling device

In the summertime, the air is hot and either moderately dry or humid very often requiring cooling before it can be supplied to the room. One of the methods to supply cool air is evaporative cooling. Evaporative cooling can either be done by direct evaporative cooling (DEC) or by indirect evaporative cooling (IEC). The cooling process can also consist of a combination of DEC and IEC or a combination of DEC and IEC with a drying process utilizing desiccant.

2.3.1. Direct evaporative cooling

In the DEC coil, outdoor air is blown through water-saturated pads and air has direct contact with wet pads. The water in the pads evaporates due to a change in state from liquid to gas. The phase change process requires heat transfer from the air to the water. Therefore, the

air temperature drops when passing through the wet pads. From the thermodynamic point of view, the heat transfer process that occurs in the DEC coil is the same as occurs in a wet film humidifier as shown in Fig 2-10. While both processes perform the same steps of air-cooling and humidification resulting in raising both the relative humidity and absolute humidity of the air, the two processes differ in their primary purpose. The primary purpose of DEC is to cool the air while humidification is a secondary consideration. In the wet film humidification process, the primary purpose is to humidify air with a secondary effect of cooling the air.

The potential for evaporative cooling is important in hot and dry climates where the outdoor air has a significant capacity for additional water vapor. The process is an isenthalpic process since enthalpy remains constant due to no heat transfer occur. This isenthalpic process is only observed however, when the water temperature sprayed onto the pads is equal to the wet-bulb temperature of the air entering the DEC coil. A pictorial diagram of the DEC coil is presented in Fig. (a) while Fig. (b) shows the theoretical thermodynamic process for DEC on a psychrometric chart.

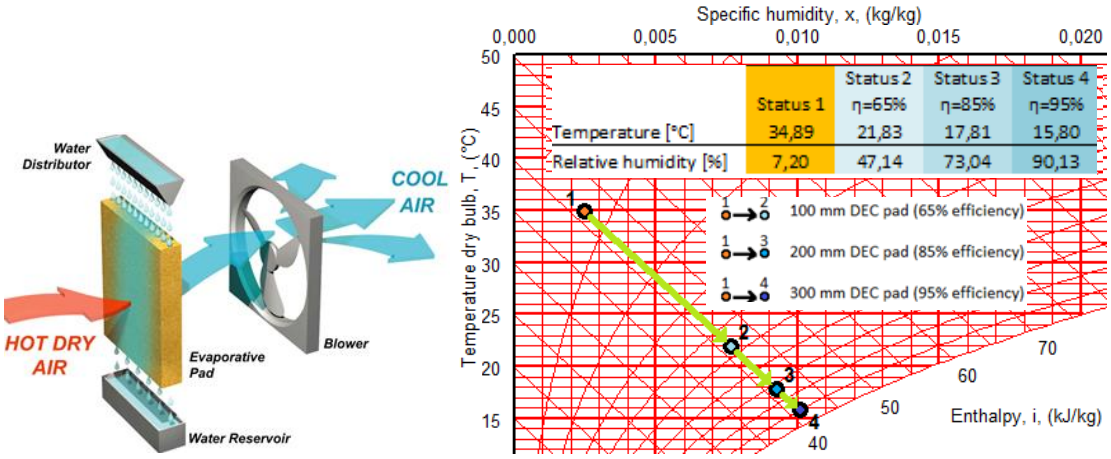

(a) (b)

Fig. 2-10 Direct evaporative cooling: (a) Operating schematic, (b) Thermodynamic proces of isenthalpic direct evaporative cooling.

As can be observed, the efficiency of the cooling depends on the thickness of the pads. In the presented example, the efficiency of a 100 mm pad is assumed to be 65% , a 200 mm pad is assumed to be 85% and a 300 mm pad is assumed to be 95% as these values are based on commercialy available products. The efficiency can be calculated using Eq. (2-2).

$$\eta = \frac{\omega_{after\,DEC} - \omega_{before\,DEC}}{\omega_{saturated} - \omega_{before\,DEC}} \tag{2-2}$$

The absolute humidity for saturated conditions can be found when extending the

isenthalpic process to 100% relative humidity.

The pads used in DEC are frequently made of aspen fiber and cellulose and characterized by a large surface area. The design of the pads should take into account several critical features including as small a pressure drop across the pads as possible while achieving a maximum saturation effect of water into the air. In addition, the pads should not decompose due to contact with water and air. Finally the pads should not support growth of algae nor be suspect to clogging. It is standard design practice to install a filter before the DEC pads to extend the life expectancy of the pads. This filter will also act to prevent accumulation of organic particles, which could lead to bacteria growth.

2.3.2. Indirect evaporative cooling

In an IEC coil, the primary air and wetted secondary air are blown through a heat exchanger however; by design, the primary air has no direct contact with the water. The secondary air is cooled by the water and subsequently cools the primary air in the heat exchanger. Consequently, no moisture is transferred to the primary air but its dry and wet bulb temperatures are reduced. IEC has several advantages including heat recovery from the exhaust air and preheating of the primary air during winter. When used for heating, the secondary air is not sprayed with water. Operating schematics of two types of IEC coils are presented in Fig. 2-11 while Fig. 2-12 illustrates the thermodynamic process on an I-x diagram and psychrometric chart.

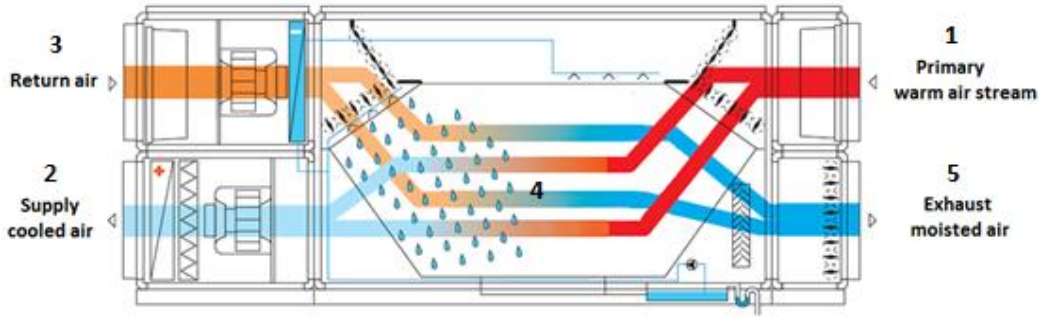

a)

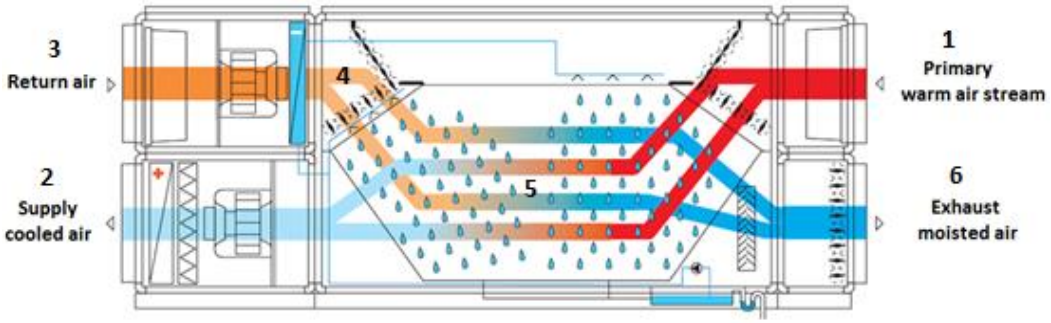

b)

Fig. 2-11 Operating schematic of indirect evaporative cooling.

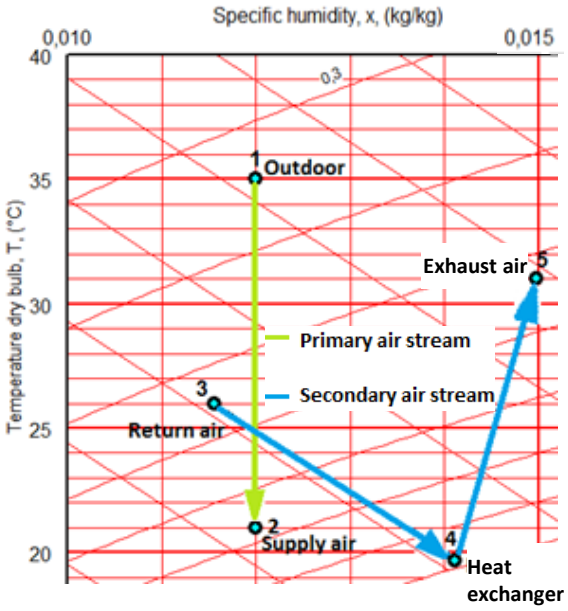

(a)

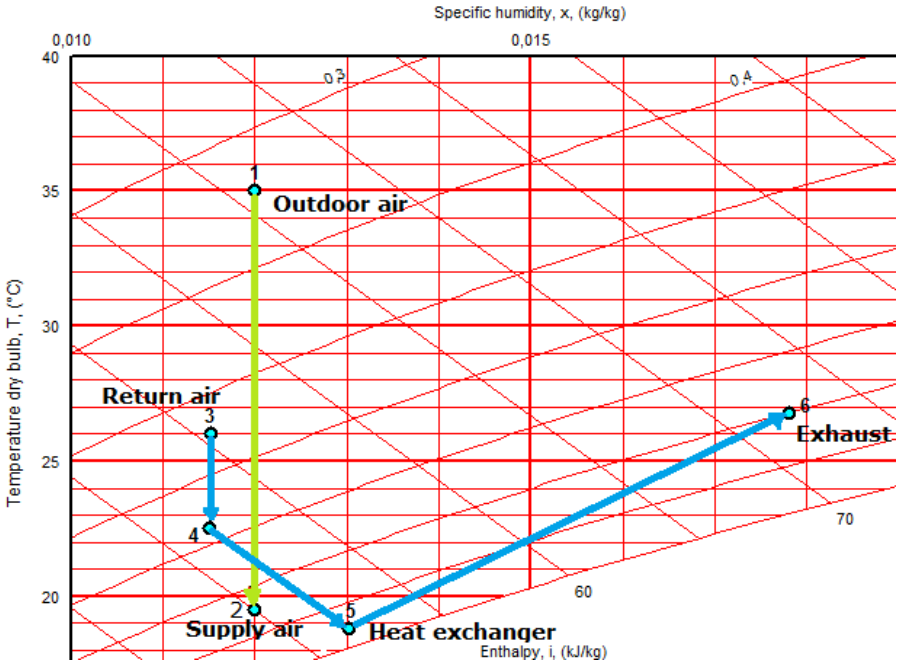

(b)

Fig. 2-12 Thermodynamic proces of isenthalpic indirect evaporative cooling.

Two representations of indirect evaporative cooling systems are presented in Fig. 2-12 A and B. In System A, the temperature of the primary air can not be decreased below 20 ℃ due to the dew point temperature limit of the secondary air as indicated by Point #2. In System B, the primary air will fall below 20 ℃ due to two stage cooling of the secondary air. The two stage cooling is achieved first by cooling the secondary air in the cooling coil that uses high temperature water. This results in decreasing the dew point temperature of the secondary air

as indicated by Point #4. Then secondary air is then humidified and cooled further as indicated by the path from Point #4 to Point #5. In the heat exchanger, heat is transferred from the hot outdoor air (primary air) to the cooled return air (secondary air). The counterflow or crossflow heat exchnager where heat transfer occurs is usually made of thin polypropylene plates.

2.3.3. Combined direct and indirect evaporative cooling

In some cases DEC and IEC are combined together when either method used independent of the other is not sufficient to meet required cooling loads. The schematic of the combined systems is presented in Fig. 2-13. The thermodynamic process of combined DEC and IEC is presented in Fig. 2-14.

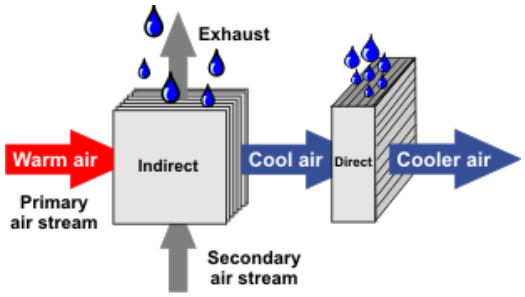

Fig. 2-13 Operating schematic of indirect and direct evaporative cooling system.

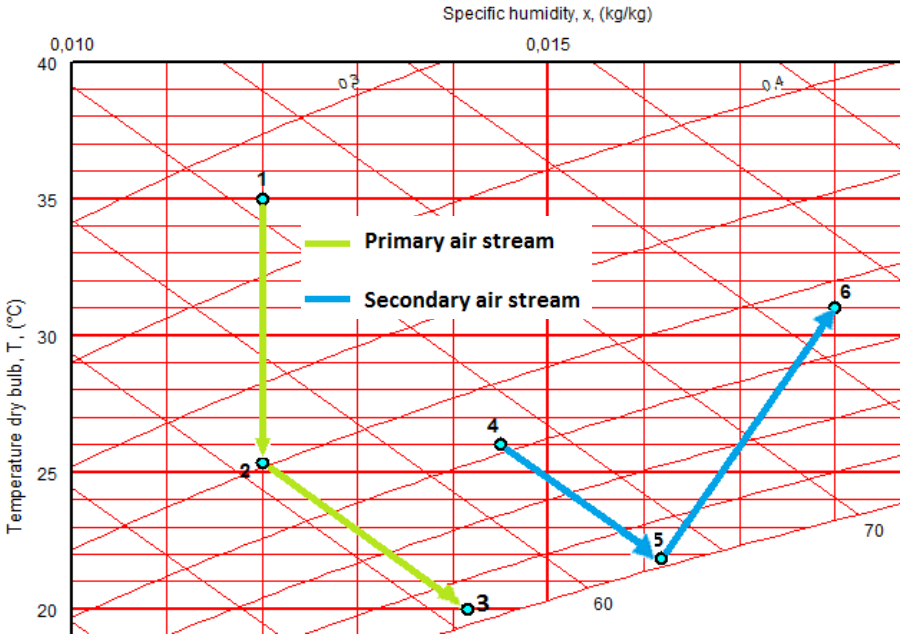

Fig. 2-14 Thermodynamic proces ofcombined direct and indirect evaporative cooling.

The primary air is first cooled in the IEC coil without changing its absolute humidity as shown Fig 2-14. Secondly, additional cooling of the primary air is obtained in the DEC coil where the air is also humidified. The secondary air in the system could be the return air

depending on the type of combined system. The advantage of a combined DEC and IEC system is the ability for the system to be used in wintertime. However, secondary airflow could not be used to increase the humidity of the supply air. To overcome this limitation, heat from return air in the IEC heat exchanger could be recovered to heat the primary outdoor air and then the DEC coil could be used to increase the humidity. The specification and materials of combined DEC and IEC is the same as for systems operating separately.

3. Heat recovery device

To evaluate the performance of heat recovery devices, a key parameter is the recovery efficiency since it directly reflects the effectiveness of the heat and mass transfer process. In general, outdoor heat recovery devices are utilized to reduce the cooling/heating capacity requirements expected from indoor exhaust air. However, while heat recovery devices save in cooling/heat capacity, more fan energy is consumed. Therefore, a more intuitive parameter is introduced to determine if the energy saved from the heat recovery devices greater than the energy consumed by the fans.

3.1. Evaluation of heat recovery device

3.1.1. COP definition

The coefficient of performance (COP), as defined by Eq. (3-1), represents the refrigeration and heating performance of chillers. In a similar way, the heat recovery COP of devices can be defined by Eq. (3-2), where Q_r represents the energy recovered and W_{fan} represents the fan power. Thus, the overall heat recovery COP considers the heat recovery and the fan's power.

$$COP_{chiller} = \frac{Q}{W_{compressor}} \tag{3-1}$$

$$COP_{recovery} = \frac{Q_r}{W_{fan}} \tag{3-2}$$

3.1.2. Reference COP

For a conventional air-conditioning system without a heat recovery device, the consumption power is composed of the compressor power, the pump's power, the cooling tower power, and the fan's power. After adding a heat recovery device, the recovery device assumes part of cooling demand (Qr). Additionally, the cooling quantity of chillers will decrease (Qe-Qr). Therefore, the compressor power will decrease and the fan power will increase due to a high-pressure loss across the heat recovery device. Only when total power consumption decreases will the heat recovery device save energy. The derivation process is

provided in Eqs. (3-3)-(3-9) resulting in the determination of the reference COP.

$$W'_{compressor} + W'_{pump} + W'_{tower} + W'_{fan} < W_{compressor} + W_{pump} + W_{tower} + W_{fan} \quad (3\text{-}3)$$

$$\frac{Q_e - Q_r}{COP_{source}} + (W_{fan} + W^*_{fan}) < \frac{Q_e}{COP_{source}} + W_{fan} \quad (3\text{-}4)$$

$$\frac{Q_e - Q_r}{COP_{source}} + W^*_{fan} < \frac{Q_e}{COP_{source}} \quad (3\text{-}5)$$

$$\frac{Q_e - Q_r}{COP_{source}} + \frac{Q_r}{COP_{\mathrm{recovery}}} < \frac{Q_e}{COP_{source}} \quad (3\text{-}6)$$

$$\frac{Q_r}{COP_{source}} < \frac{Q_r}{COP_{source}} \quad (3\text{-}7)$$

$$COP_{\mathrm{recovery}} > COP_{source} \quad (3\text{-}8)$$

$$COP_{reference} = COP_{source} = \frac{Q_e}{W_{source}} = \frac{Q_e}{W_{compressor} + W_{pumps} + W_{towers}} \quad (3\text{-}9)$$

Increase in fan power can be derived by the heat recovery COP and the heat recovery capacity. To determine if heat recovery devices can save energy, the reference COP is used to compare with the heat recovery COP as defined by Eq. (3-9). If the heat recovery COP is higher than the reference COP, then the increase in required fan power is less than the decrease in required compressor and pump power. Therefore, heat recovery devices can reduce total energy consumption of an HVAC system. Alternately, when the fan consumes more energy than the compressor and pumps can save, heat recovery devices are not needed.

The heat recovery COP may be influenced by device characteristics and operating conditions. Device characteristics include the heat exchanger area, the heat transfer coefficient and pressure loss across the system. Operating conditions include indoor and outdoor air conditions and the volume of the two airflows that represents the heat transfer potential. For a given heat recovery device, the device characteristics have already been determined. Therefore, changes to the heat recovery COP will occur when changes to the air parameters take place. Heat recovery devices are less efficient methods than chillers when the heat recovery COP is lower than the reference COP. In this situation, heat recovery devices should be bypassed thereby preventing excess consumption of fan power.

3.2. Experimental data

3.2.1. Plate enthalpy exchanger

A plate enthalpy exchanger was experimentally evaluated in the outdoor environment

chamber at Nagoya University as shown in Fig. 3-1, which illustrates the outline of the experiment chamber. Temperature and humidity of OA (outdoor air), RA (return air), and SA (supply air) was measured in every 10 seconds near the heat exchange unit. The recovery efficiency, COP and the amount of recovery heat were calculated based on the test results.

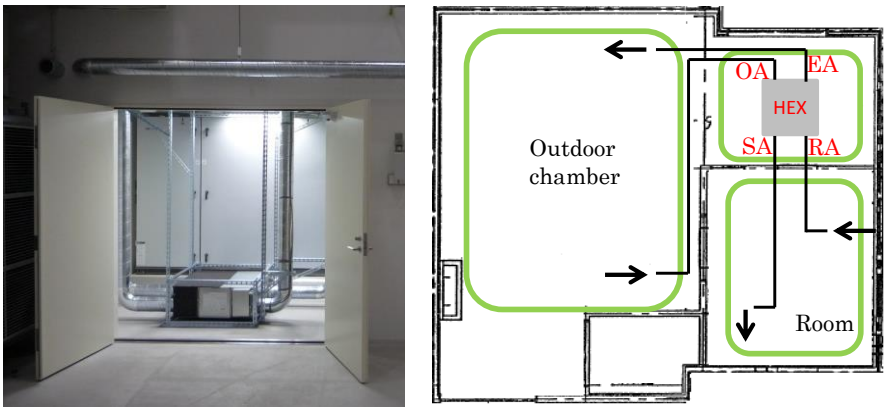

Fig. 3-1 Outline of the experiment chamber for plate enthalpy exchanger

The plate enthalpy exchanger setup underwent four test cases as shown in Table 3-1. The outdoor air temperature and the indoor air temperature were varied for the tests. Two plate enthalpy exchangers were chosen for the test with their rated parameters listed in Table 3-2. The rated airflow rates of the two plate enthalpy exchangers were 230 m^3/h and 140 m^3/h, respectively.

Table 3-1 Operating conditions for the test

	Outdoor chamber		**Room**
	Temperature	Relative humidity	Temperature
Case A	30 ℃	50%	26 ℃
Case B	30 ℃	50%	28 ℃
Case C	35 ℃	50%	26 ℃
Case D	35 ℃	50%	28 ℃

Table 3-2 Specification of the plate enthalpy exchanger

Plate enthalpy exchanger type		**High**	**Low**
Unit type		Concealed unit installed within ceiling void	
Air volume		230m^3/h	140m^3/h
Power consumption		155W	59W
External static pressure		105Pa	28Pa
Temperature exchange efficiency		72.5%	79.5%
Enthalpy exchange efficiency	in cooling	66.2%	73.0%
	in heating	69.0%	76.5%

Based on the test results, the enthalpy recovery efficiency, the heat recovery COP and the enthalpy difference between the OA and RA was calculated. Fig. (a) plots the results for the enthalpy recovery efficiency for the high flow rate plate enthalpy exchanger based on a variable enthalpy difference between the OA and RA. The graph also indicates the regression line. Fig. (b) plots the enthalpy recovery efficiency for the low flow rate plate enthalpy exchanger based on the variable enthalpy difference.

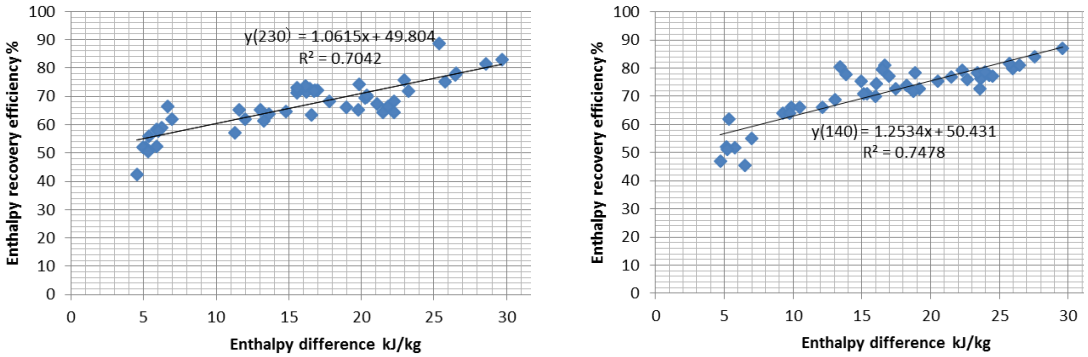

(a) (b)

Fig. 3-2 Tested enthalpy recovery efficiency results based on a variable enthalpy difference: (a) Air flow rate of 230 m^3/h, (b) Airflow rate of 140 m^3/h.

For this type of enthalpy recovery device, the recovery COP is defined as Eq. (3-2), which equals the recovered heating/cooling capacity divided by the input fan power. Fig. 3-3(a) plots the recovery COP based on a varying enthalpy difference between the OA and RA. The recovered heat based on a varying enthalpy difference is shown in Fig. 3-3(b). As indicated by Fig. 3-3(a), the COP of the plate enthalpy exchanger is significantly influenced by the enthalpy difference.

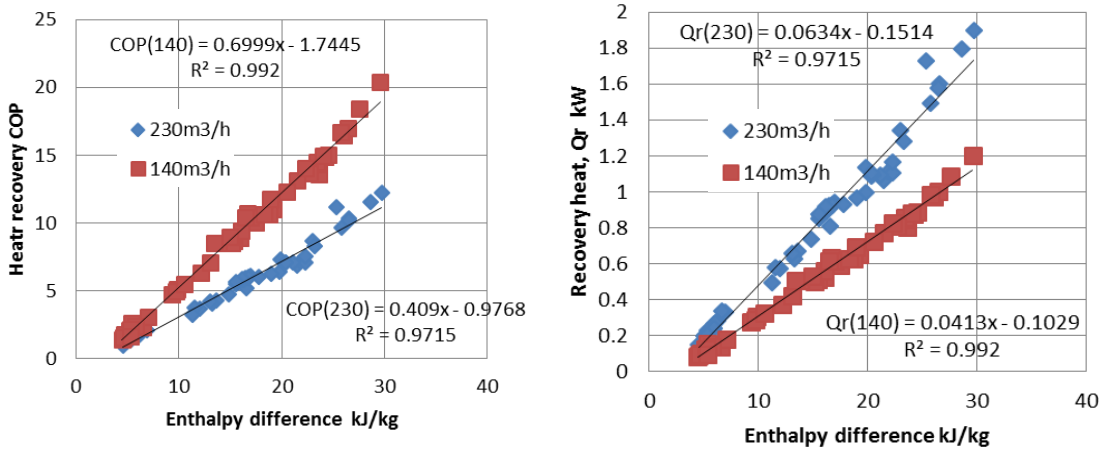

(a) (b)

Fig. 3-3 Experiment results of the plate heat recovery device: (a) Heat recovery COP; (b) Recovered heat.

3.2.2. Enthalpy wheel

1) Experiment introduction

An enthalpy recovery wheel from a manufacturer was experimentally evaluated as shown in Fig. 3-4. The technical specifications and operating parameters are listed in Table 3-3. As indicated in Fig. 3-4, Room 1 and Room 2 of the enthalpy difference laboratory were set at different temperatures and humidity ratios. Room 1 was designated as an indoor space, while Room 2 was designated as an outdoor space. The rotary wheel was controlled with a frequency converter allowing the rotation speed to be varied from 252 r/h to 1260 r/h as the frequency was increased from 10 Hz to 50 Hz. The temperature was measured with thermocouples with an error rate of ±0.1 ℃, and the relative humidity was measured using a temperature and humidity recorder (WSZY-1A) with a ±2% RH error rate. A series of experiments were conducted at different rotation speeds, air inlet parameters, and air volumes.

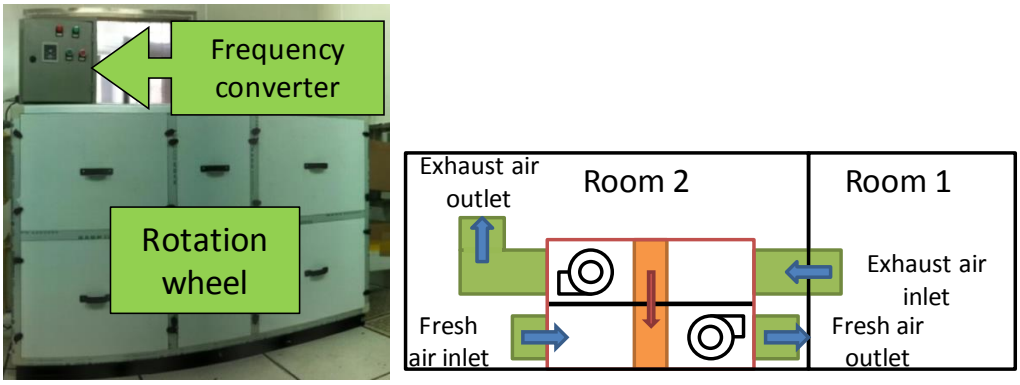

Fig. 3-4 Experimental setup

Table 3-3 Enthalpy wheel technical specifications and operating parameters

Device information		Operating parameters	
Wheel	Radius: 210mm; Thickness: 200mm	Indoor air condition	24 ℃ ~ 28 ℃, 8.4g/kg ~ 13.5g/kg, 600 m^3/h ~ 1260m^3/h
Fans	Rated power: 0.2kW rated air volume: 1400m^3/h	Outdoor air condition	27.5 ℃ ~ 37 ℃, 12.3g/kg ~26.7g/kg, 900m^3/h ~1940m^3/h
Wheel motor	Frequency: 50Hz Power: 0.09kW	Q_{out}/Q_{in}	1 ~ 1.5
		Rotation speed / frequency converter	252r/h ~1260r/h 10 Hz ~ 50 Hz

2) Experimental results

Fig. 3-5 shows experimental results at different operating conditions. Air volume was adjusted by air valve and the fan's power was considered the same as the rated value. For the given technical specifications and operating parameters, the recovery efficiency varied within a range of 40%–70%, the recovery heat varied within a range of 6–14 kW, and the heat

recovery COP varied from 15–30. For a dehumidification desiccant wheel, the recovery COP is defined as Eq. (3-10). The wheel motor power was less than 15% of fan power.

$$COP_{\text{recovery}} = \frac{Q_r}{W_{fan} + W_{motor}} \tag{3-10}$$

As shown in Fig. 3-5(a), the recovery efficiency is relatively unchanged at high rotation speeds, so the recovery heat and COP stay constant. The outdoor humidity ratio and temperature have no impact on recovery efficiency however, they have a significant impact on the recovery heat and COP. This is due to the changing temperature and humidity differences between two airflows as shown in Fig. 3-5(b-c). The larger the differences, the higher the recovery heat and COP. In Fig. 3-5(d) – Air Volume Ratio, the two left hand points provide evidence of the air volume's influence based on the same air volume ratio. The data indicates that the COP increases with decreasing air volumes. Maintaining the outdoor air volume constant while changing the indoor exhaust air volume, the efficiency and COP decrease with decreasing exhaust air.

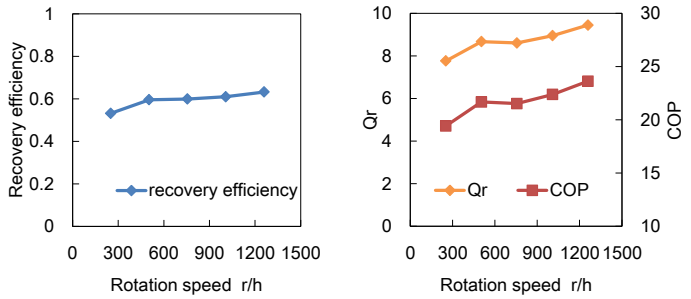

(a)
$Q_{outdoor}$=900 m^3/h
$T_{outdoor}$ =35
$d_{outdoor}$ =26
Q_{indoor}=770 m^3/h
T_{indoor} =25.5
d_{indoor} =11

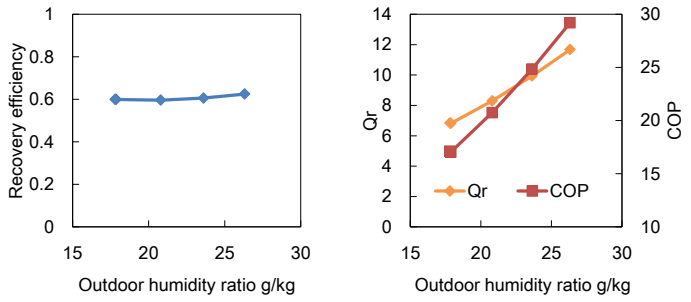

(b)
$Q_{outdoor}$=1000 m^3/h
$T_{outdoor}$ =35
Q_{indoor}=1100 m^3/h
T_{indoor} =25
d_{indoor} =9
Rs=1260 r/h

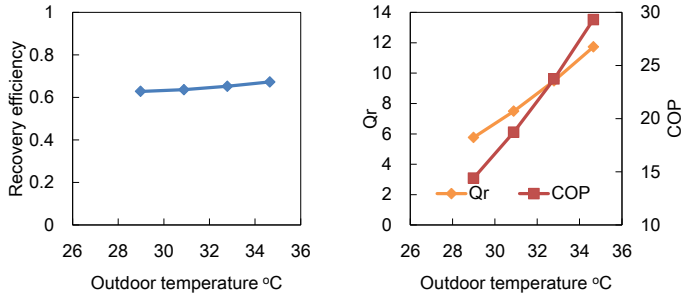

(c)
$Q_{outdoor}$=1000 m^3/h
$\varphi_{outdoor}$ =70%
Q_{indoor}=1100 m^3/h
T_{indoor} =25
d_{indoor} =9
Rs=1260 r/h

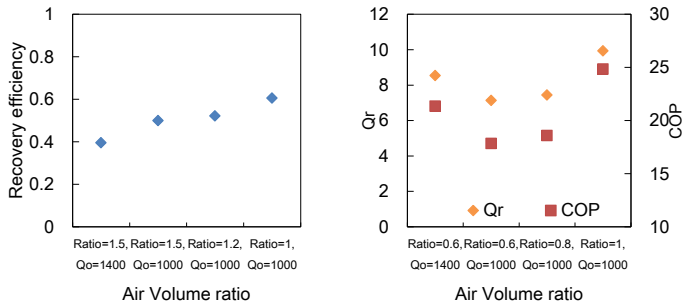

(d)

$T_{outdoor}$ =35

$d_{outdoor}$ =23

T_{indoor} =25

d_{indoor} =9

Rs=1260 r/h

Fig. 3-5 Experimental results (enthalpy recovery efficiency, COP, recovery heat) of enthalpy wheel: (a), At varied rotation speed; (b) At varied outdoor humidity ratio; (c) At varied outdoor temperature; (d) At varied air volumes.

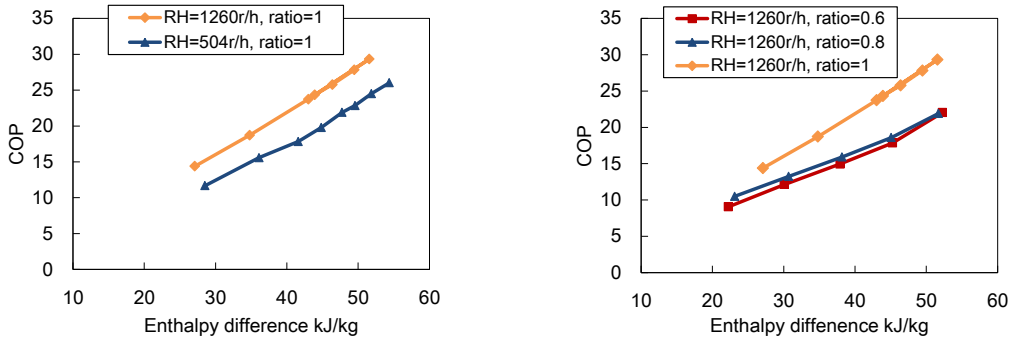

(a) (b)

Fig. 3-6 Experimental results II of enthalpy wheel at different inlet enthalpy differences: (a) At varied rotation speed; (b) At varied air volume ratio, defined by the ratio of indoor air volume to outdoor air volume.

Fig. 3-6 indicates that the inlet parameters such as the enthalpy difference have a significant impact on heat recovery COP. Furthermore, the rotation of the enthalpy wheel and air volume ratio also impact the COP. Hence, the ambient climate of a city is a key influence on the COP. When the outdoor air conditions are similar to indoor air conditions, the enthalpy wheel cannot support high efficient heat recovery.

3.3. Case studies

3.3.1. Plate heat exchanger

Outdoor conditions of 30 ℃ and 30–60% relative humidity and indoor condition with 25 ℃ and 9 g/kg absolute humidity were selected for a case study of a plate heat exchanger. The enthalpy recovery efficiency, heat recovery COP and the amount of recovery heat were calculated with the help of the fitting formulas as previously shown in Fig. 3-3(a). Fig. (a) provides the enthalpy recovery efficiency while the recovery COP and the recovery heat are shown in Fig. (b).

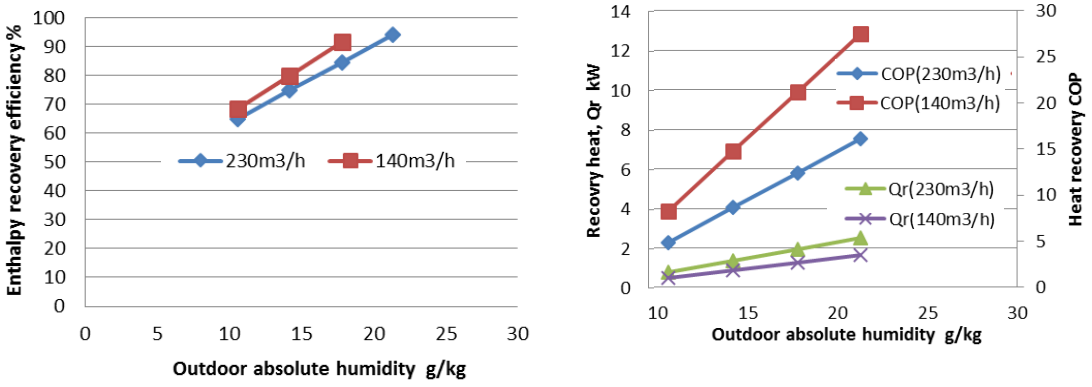

(a) (b)

Fig. 3-7 Calculated results of the plate heat recovery device: (a) Enthalpy recovery efficiency, (b) Heat recovery COP and recovered heat.

For the air volume of 230 m^3/h, the COP correlation formula is determined by the following equation:

$$COP_{recovery} = 0.409 * \Delta h - 0.9768 \quad (3\text{-}11)$$

where Δh is inlet enthalpy difference between indoor and outdoor air.

Fig. (a) shows the rate of enthalpy differences between the outdoor and indoor air conditions when the indoor air conditions are 26 ℃ and 50% relative humidity. Weather data was obtained at Nagoya for July and August 2013 and the data from the timeframe of 0900 to 1800 was used. As indicated by Eq. (3-11), a reference line was obtained at Δh = 12.1 kJ/kg when the reference COP was 4, i.e. the recovery COP is greater than 4 when the enthalpy difference, Δh, is greater than 12.1 kJ/kg. Thus for Nogoya, a plate enthalpy recovery device is useful for approximately 77% of the time when cooling is needed.

3.3.2. Desiccant wheel

Fig. (a) shows the enthalpy difference frequency between indoor air and outdoor air in the cooling season assuming the indoor conditions are constant at 26 ℃ and 50%. The frequency data assumes the reference COP is 4.0, the rotation speed and air volume ratio are 1260 r/h and 1 respectively. Using the data shown in Fig. 3-6(a) the COP correlation formula is determined by the following equation:

$$COP_{recovery} = 0.6067 * \Delta h - 2.2677 \quad (3\text{-}12)$$

where, Δh is inlet enthalpy difference between indoor air and outdoor air, kJ/kg.

By comparing Eq. (3-10) and the reference COP, a reference line can be obtained as shown in Fig. (b). The reference line indicates that during the cooling season, the heat recovery desiccant wheel can be installed in 60% of time. For the other 40% of the time,

installation of a desiccant wheel will not reduce energy consumption of an HVAC system.

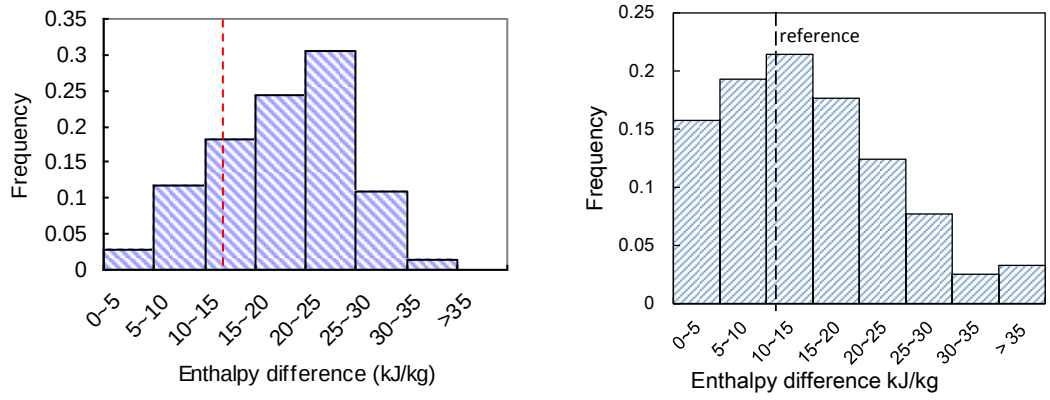

(a) (b)

Fig. 3-8 Enthalpy difference frequency figures in different cities: (a) Nagoya, (b) Beijing.

3.4. Conclusions

Heat recovery devices can reduce energy consumption when running at proper parameters. The recovery efficiency can indicate device performance however; the recovery COP provides a straightforward method for evaluating if a heat recovery device will save energy. This evaluation is based on a comparison of the reference COP that is determined from chillers and pumps with the recovery COP.

For all types of heat recovery devices, the heat recovery COP is influenced by outdoor and indoor air parameters and air volumes. While outdoor air conditions are similar to indoor air conditions, the heat recovery COP may be lower than the reference COP. Under this circumstance, the heat recovery device recovers cooling/heat by consuming more energy than cooling/heat sources indicating the heat recovery devices should be bypassed. Additionally during the transition season, outdoor air can handle indoor cooling/heat load and the heat recovery device must be bypassed to reduce resistance pressure drop.

For the enthalpy wheel, air leakage is a significant element to consider as part of the application. Air leakage can be classified into two types. The first air leakage situation is caused by continuous rotation, as shown in Fig. . When the desiccant wheel rotates from the fresh air side (A0 to A4) to the exhaust air (or regeneration air) side (A5 to A9), air mixing of the two streams occurs. Fresh air entering at Z1-A0 will exit at Z6-A2. Similarly, air entering at Z1-A3 will exit at Z6-A5. A5 represents the entrance of the exhaust air (or regeneration air). Hence, fresh air entering at Z1-A3 to Z1-A4 cannot exit at the appropriate duct and will be blown back by the exhaust air (or regeneration air) from the other duct. For the enthalpy recovery desiccant wheel, the rotation speed is typically in the range of 10–30 r/min (600–1800 r/h), u_a is typically 2–3 m/s, and L is usually 0.2–0.4 m, so the influence of the air

mixing rate is significant (θ = 2%–15%). The allowed maximum air-mixing rate is within 5%, so the greater L and u_a are, the higher the allowed rotation speed. Therefore, this type air leakage cannot be prevented.

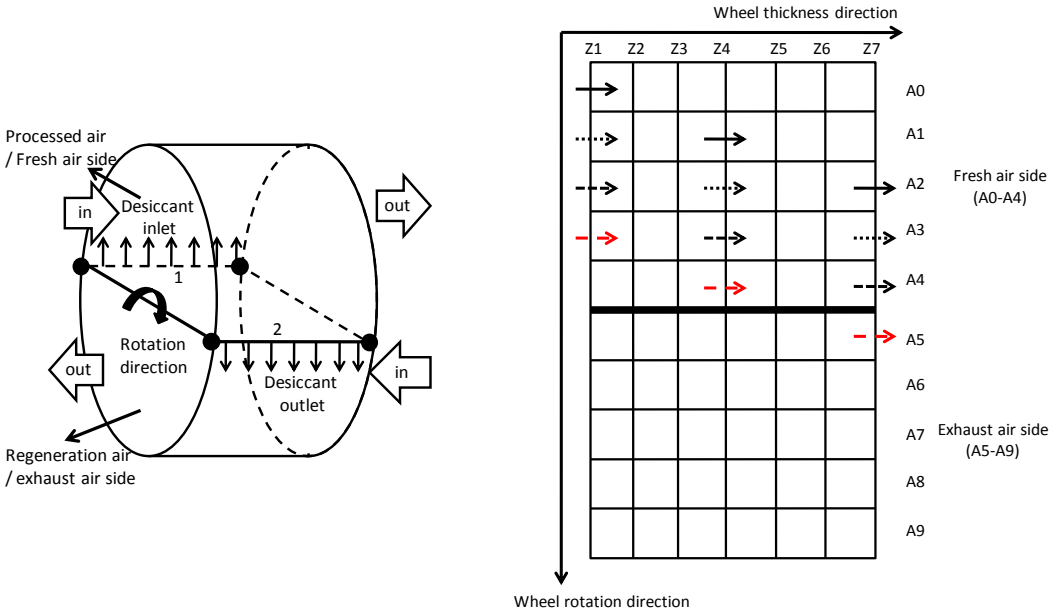

(a) (b)

Fig. 3-9 Air mixing in the desiccant wheel: (a) Desiccant wheel, and (b) Air mixing.

Differential air pressure may cause air leakage in front and at back of wheel, as shown in Fig. 3-10. This occurs due to two fans assisting two separate air flows go through the desiccant wheel. Incorrect installation of the enthalpy wheel components will also cause air leakage. As shown in Fig. 3-10(b), two fans were installed on the same side of rotation wheel. In this situation, the air pressure difference at points A and B is close to pressure head of the fans. A significant quantity of air is transferred from A to B resulting in an air leakage ratio that can reach 80%.

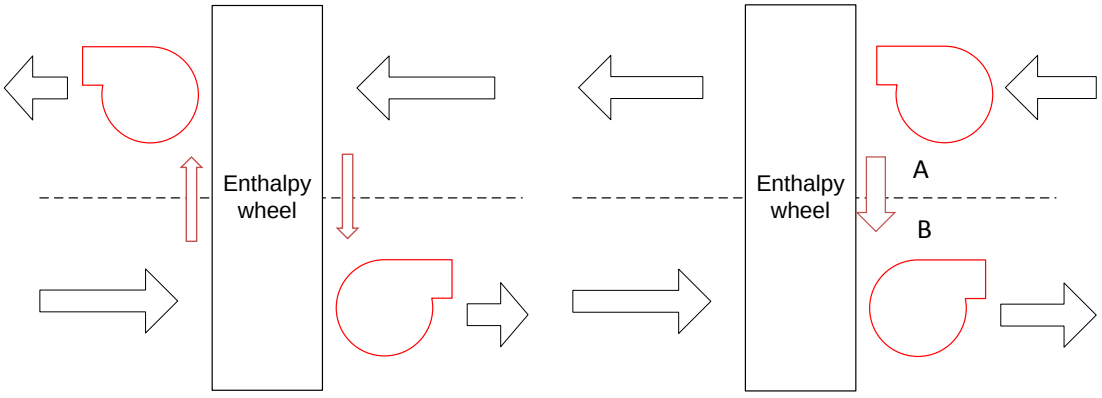

(a) (b)

Fig. 3-10 Air leakage schematic in enthalpy wheel system

4. Dehumidification

4.1. Performance evaluation index

The cooling and heating requirement of different dehumidification methods are shown in Table 4-1. For every method, the cooling source is necessary.

Table 4-1 The cooling and heating requirement.

	Cooling	Heating
Condensing	Yes	-
Solid desiccant	Yes	Yes
liquid desiccant	Yes	Yes

4.2. Performance of typical dehumidification modes

4.2.1. Condensing dehumidification

Condensing dehumidification is the original method of humidity control. For a conventional HVAC system, 7 ℃ chilled water is transported to outdoor air handling units to cool and dehumidify the outdoor air, as shown in Fig. 4-1. The outdoor air is usually handled to a state with a similar humidity ratio as the indoor state before being supplied to the indoor environment.

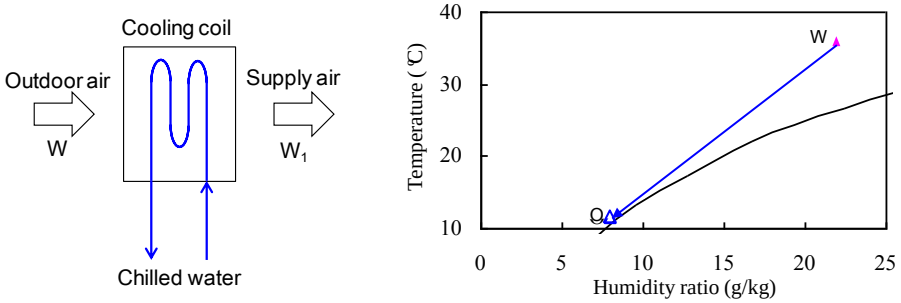

Fig. 4-1 Conventional condensing dehumidification module: (a) operating principle; and (b) air handling process in psychrometric chart.

When the condensation dehumidification method is adopted for the outdoor air handling process, there is a significant temperature difference between the inlet outdoor air and the cooling source. Thus, this low-temperature cooling source leads to an obvious temperature mismatch for the total heat transfer process, resulting in heat transfer loss. To reduce this kind of heat transfer loss caused by the significant temperature difference between the inlet fluids, using an appropriate high-temperature cooling source to precool the outdoor air is a feasible solution, which results in a cascade process and improved energy performance.

1) Precooling the outdoor air with heat recovery from the indoor exhaust air

Setting an appropriate indoor exhaust air system and venting the indoor exhaust air in an organized way, the heat recovery device can be implemented between the indoor exhaust air and the outdoor air, where the energy can be recovered. Fig. 4-2 illustrates the outdoor air

handling process using condensation dehumidification with the enthalpy recovery module. It can be seen that the enthalpy of the outdoor air decreases after the enthalpy recovery process (from state *W* to W_1). Thus, the required enthalpy difference in the dehumidification process decreases, helping to reduce the energy consumption of the outdoor air handling process.

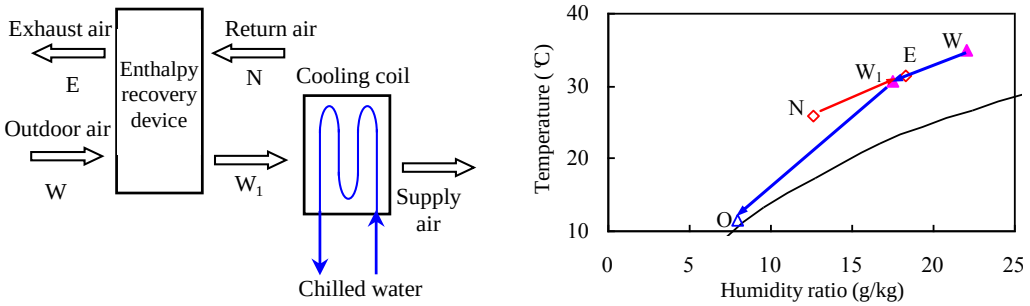

(a) (b)

Fig. 4-2 Condensation dehumidification process with the enthalpy recovery module: (a) operating principle; and (b) air handling process in psychrometric chart.

2) Precooling the outdoor air with high-temperature chilled water

To improve the operating performance of the outdoor air handling process, the high-temperature chilled water (about 16~18 ℃) of the THIC system could be adopted to precool the air. The lower-temperature chilled water could be used to dehumidify the air further, as shown in Fig. 4-3. The high-temperature chilled water could be directly obtained from natural cooling sources such as underground water, and could also be available from the high-temperature water chiller. With the help of the precooling process, the outdoor air could be cooled from the hot and humid state to the saturated state (or approaching the saturated state). The major task of the precooling process is to cool the air from state *W* to state W_1, as shown in Fig. 4-3(b). Low-temperature chilled water is then adopted to dehumidify the air from state W_1 to state *O*, satisfying the humidity ratio requirement of the supplied air. Moreover, using high-temperature chilled water for precooling takes full advantage of the energy efficiency of the high-temperature cooling source. Based on the variances of the outdoor air parameters and the required supply air parameters, the air handling processor can meet the requirement of the supplied air by regulating the flow rate of the low-temperature chilled water and ensuring the use of high-temperature chilled water as much as possible.

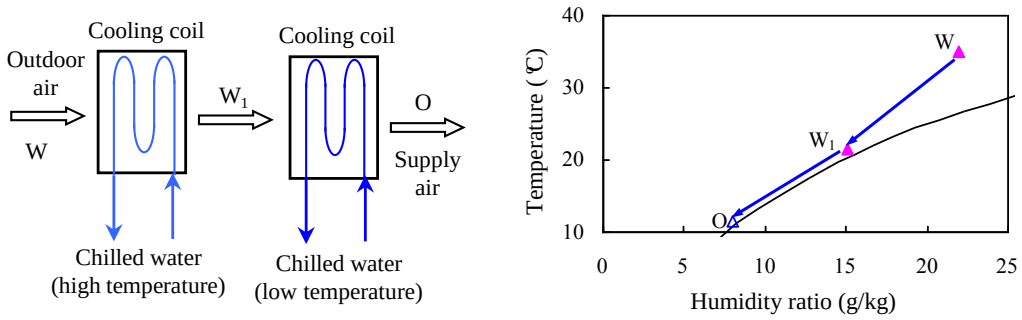

(a) (b)

Fig. 4-3 Condensation dehumidification process using high-temperature chilled water for precooling: (a) operating principle; and (b) air handling process in psychrometric chart.

To make the air handling processor more flexible, Fig. 4-4 illustrates an improved outdoor air handling process using condensation dehumidification. In the handling process, the outdoor air is first precooled by the high-temperature chilled water (16~18 ℃) from the cooling source. The air is dehumidified further by the evaporator of the separate heat pump cycle to meet the humidity ratio requirement. The condenser of the heat pump could be an air-cooled type utilizing indoor exhaust air or a water-cooled type utilizing cooling water. For the outdoor air handling process shown in Fig. 4-4, the refrigerant inside the evaporator evaporates directly, and the air is dehumidified by the heat transfer process between the refrigerant and the moist air. As the separately installed heat pump is responsible for dehumidification, only a single plumbing system for the high-temperature chilled water is required, resulting in a much simpler arrangement of the processors.

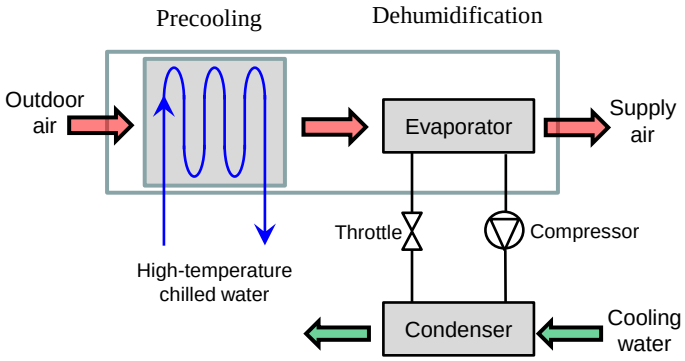

Fig. 4-4 Condensation dehumidification outdoor air handling process with a separate heat pump.

3) Comparison

For above mentioned three condensing dehumidification process (conventional condensing, precooling with heat recovery, precooling with high-temperature chilled water), Table 4-2 lists enthalpy differences and cooling source energy consumption at different outdoor air parameters, where the high-temperature chilled water is 16 ℃. Taking the required

humidity ratio of 8 g/kg (the relative temperature is 11.5℃ with a relative humidity of 95%) as the handling target.

As indicated by the results, precooling process can reduce energy consumption efficiently benefiting from high COP of high-temperature chillers or heat recovery device. In Condensation dehumidification process using enthalpy recovery device for precooling, chillers only undertake the load at second stage, and this part is influenced by outdoor temperature and humidity ratio.

In Condensation dehumidification process using high-temperature chilled water for precooling, the enthalpy difference of the precooling process is significantly higher as the outdoor temperature and humidity ratio are higher. The enthalpy difference of the precooling process accounts for about 50% of the total enthalpy difference during the outdoor air handling process. Thus, precooling using high-temperature chilled water could undertake the load of handling the outdoor air effectively, and is a feasible approach for improving the efficiency of the outdoor air handling process.

In summary, the improvement central theme is using multi-stage cold source to realize dehumidification. Installation of heat recovery device, high-temperature chiller or separated heat pump is recommended.

Table 4-2 Outdoor air enthalpy differences under typical conditions

Outdoor air parameters			conventional condensing		precooling with heat recovery			precooling with high-temperature chilled water		
Temperature (℃)	Humidity ratio (g/kg)	Enthalpy (kJ/kg)	Δh (kJ/kg)	W (kJ/kg)	Δh_1 (kJ/kg)	Δh_2 (kJ/kg)	W (kJ/kg)	Δh_1 (kJ/kg)	Δh_2 (kJ/kg)	W (kJ/kg)
35	22	91.6	59.9	13.0	27.2	32.7	7.11	32.7	27.2	5.9
30	22	86.4	54.7	11.9	23.5	31.2	6.78	29.1	25.6	5.6
35	16	76.2	44.5	9.7	16.4	28.1	6.11	22.0	22.5	4.9
30	16	71.0	39.3	8.5	12.7	26.6	5.78	18.3	21.0	4.6

Notes: Δh_1 is the enthalpy difference during precooling; Δh_2 is the enthalpy difference during dehumidification; W is the energy consumption of chillers.

Notes: COP of low-temperature chillers is assumed at 4.6; COP of high-temperature chillers is assumed at 7.2.

Notes: Enthalpy recovery efficiency of heat recovery device is assumed at 70%; indoor environment is 26 ℃ and 50%.

4) Reheating

For the aforementioned outdoor air handling processes using condensation dehumidification, a common problem is that the supply air temperature is usually too low to be supplied to the indoor environment directly. As the humidity ratio is about 8~10 g/kg, the corresponding air temperature is about 11.5~14.8 ℃. Thus, mixing with return air or reheating is needed to a certain extent. Common reheating methods include electrical reheating, steam reheating, etc. However, these methods lead to additional energy dissipation and much hot and cold offset. Therefore, the design principle is to cancel the hot and cold offset.

Reheating the supplied air after dehumidification using the indoor exhaust air or the outdoor air is a more feasible solution, since it achieves the reheating effect while reducing unnecessary energy consumption. Fig. 4-5 and Fig. 4-6 show two ways to recover heat for heating with indoor exhaust air and outdoor air respectively.

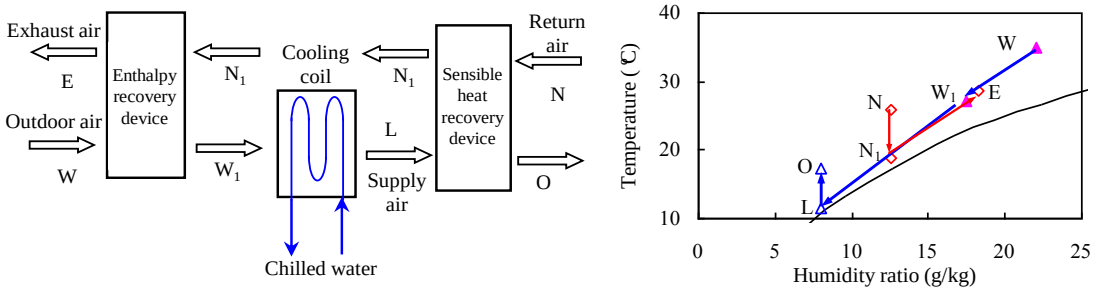

(a) (b)

Fig. 4-5 Condensation dehumidification process using return air for precooling and reheating: (a) operating schematic; and (b) air handling process in psychrometric chart.

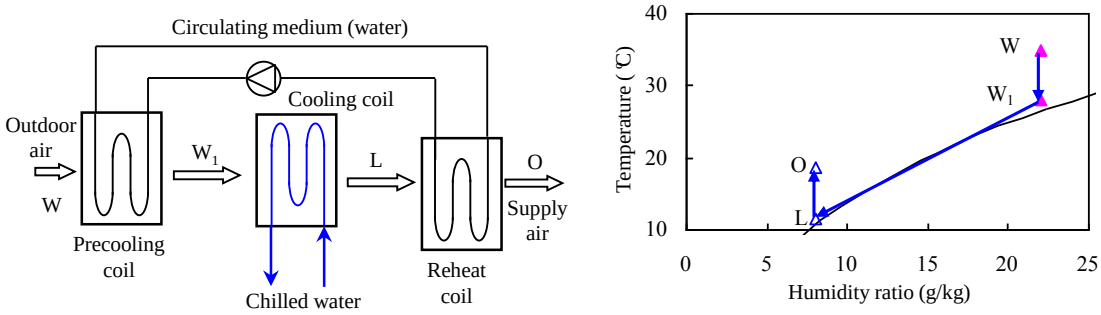

(a) operating schematic (b) air handling process

Fig. 4-6 Outdoor air handling process using intermediate for precooling and reheating: (a) operating schematic; and (b) air handling process in psychrometric chart.

As described in Fig. 4-5, the sensible heat recovery process is conducted between the dehumidified outdoor air and the indoor return air, realizing the reheating of the outdoor air. The return air is cooled by the dehumidified air, and then flows through the enthalpy recovery device. The outdoor air is first precooled by the indoor exhaust air before being dehumidified,

from state W to state W1. In Fig. 4-6, the fluid intermediate acts as the medium for the energy exchange between the outdoor air and the dehumidified air, and it could be adopted for precooling and reheating. The intermediate circulates in a closed loop. The intermediate's major task is to cool or reheat the air in the handling process undertaking the sensible load.

4.2.2. Desiccant wheel

Desiccant wheel is a kind of solid desiccant dehumidifier using rotation wheel to produce dry air continuously. Solid desiccant material is coated on the honeycomb construction of the wheel. The honeycomb construction produces many air channels for air flowing through and transferring heat and mass with solid desiccant on the walls of channels. For the same reason, the specific surface area of honeycomb construction can reach 2000~4000m^2/m^3, and for a certain air face velocity (2.5m/s), the NTU can reach 5~10 of every 10cm thick wheel.

The wheel is generally divided to two sections, one for dehumidification, and another for regeneration, as depicted in Fig. 4-7. Solid desiccant material absorbs water from high humidity air in dehumidification section, and rotates to regeneration section to desorb water to regeneration air, and then back for dehumidification.

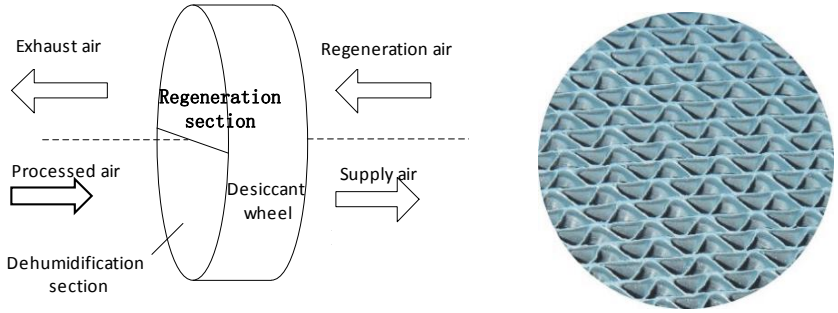

Fig. 4-7 Dehumidification wheel device and honeycomb core

There have been variety kinds of desiccant cooling systems in literature and real applications. The six kinds of desiccant cooling systems, which are mostly used, are mainly analyzed in this report. They are summarized into three types according to the types of processed air, which are all fresh air system, all return air system and mixed air system.

I: all fresh air system

There is one type of all fresh air system, called ventilation cycle, seen in Fig. 4-8, using ambient air as the processed air and return air as the regeneration air.

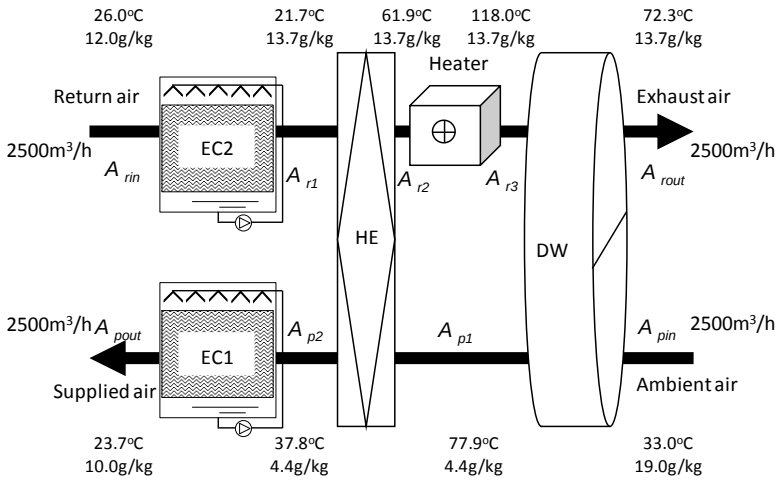

Fig. 4-8 Ventilation cycle

There are two evaporative cooling devices at the inlet of return air side and the outlet of ambient air side, used to cool and humidify the air. A sensible heat exchanger is used to recovery heat between the return air after evaporative cooler and the processed air after the desiccant wheel. A heater used to heat the return air to the required regeneration temperature. A desiccant wheel used to dehumidify the processed air.

The air handling processes are shown in Fig. 4-9.

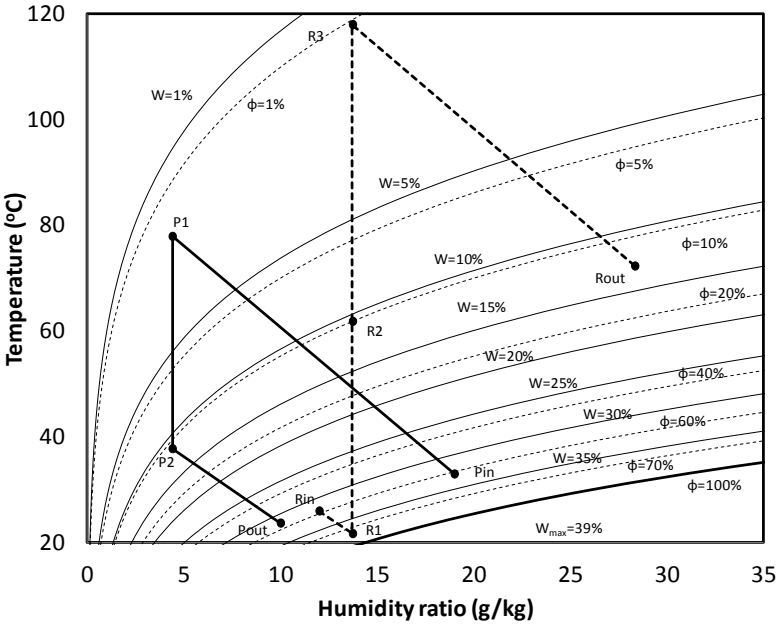

Fig. 4-9 Air handling processes of the ventilation cycle

The processed air is dehumidified and heating by the desiccant wheel first. Then it is cooled in the heat exchanger by the return air. Last, it is cooled and humidified by the evaporative cooler. The return air is cooled and humidified by the evaporative cooler first. And then it is heated in the heat exchanger by the processed air. Then, it is continued heated by the heater to the required regeneration temperature. Last, it is used to regenerate the

desiccant wheel.

II: all return air system

There are two types of all return air system, called recirculation cycle and dunkle cycle, seen in Fig. 4-10 and Fig. 4-12, using ambient air as the regeneration air and return air as the processed air.

The recirculation cycle is the same with ventilation cycle, with the processed air changed from ambient air to return air, and regeneration air changer from return air to ambient air. The air handling processes are shown in Fig. 4-11.

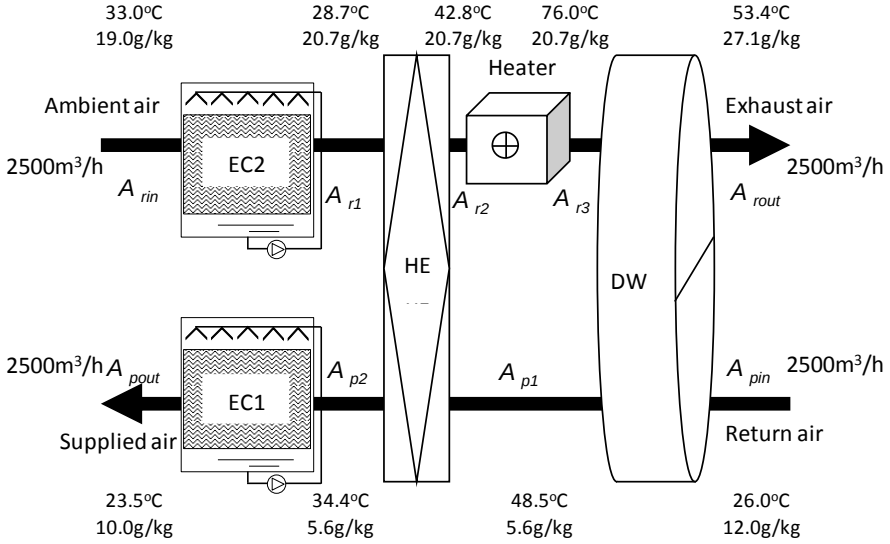

Fig. 4-10 Recirculation cycle

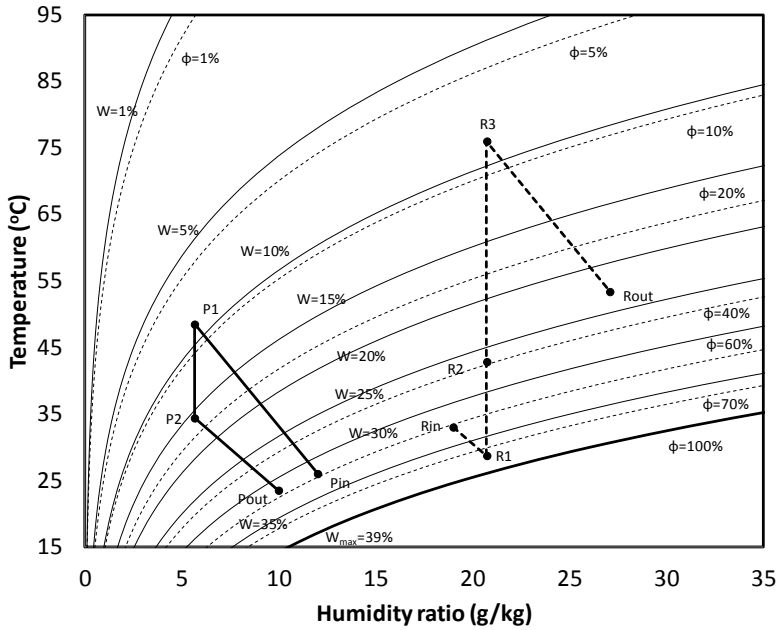

Fig. 4-11 Air handling processes of the recirculation cycle

Fig. 4-12 is the schematic of dunkle cycle, and the air handling process is shown in Fig. 4-13. The processed air is first cooled and humidified by the evaporative cooler. Then it is

heated in the heat exchanger by the processed air after dehumidification. After that, it is dehumidified and heated by the desiccant wheel. Then it is cooled step by step by the ambient air and the return air in two separate heat exchangers. Last, it is cooled and humidified by another evaporative cooler. The ambient air is first heated by the hot and dried processed air. And then it is heated in the heater. Lastly, it is used to regenerate the desiccant wheel.

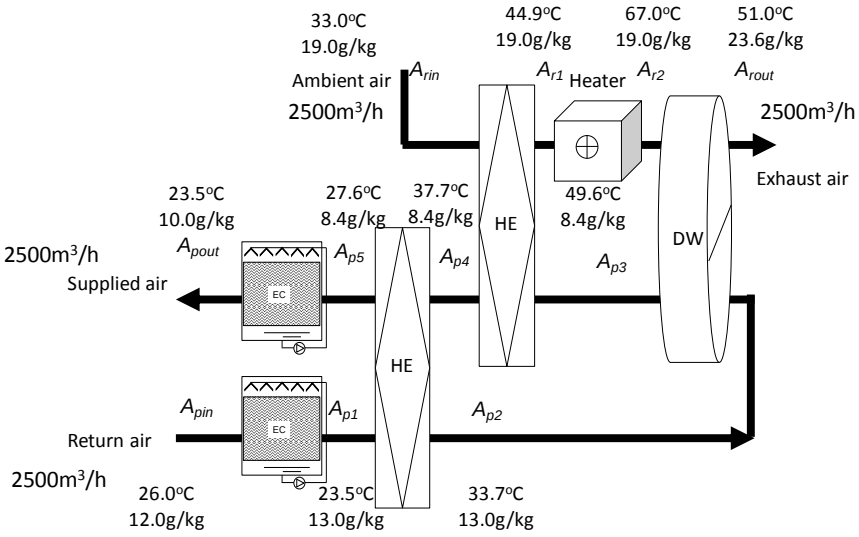

Fig. 4-12 Dunkle cycle

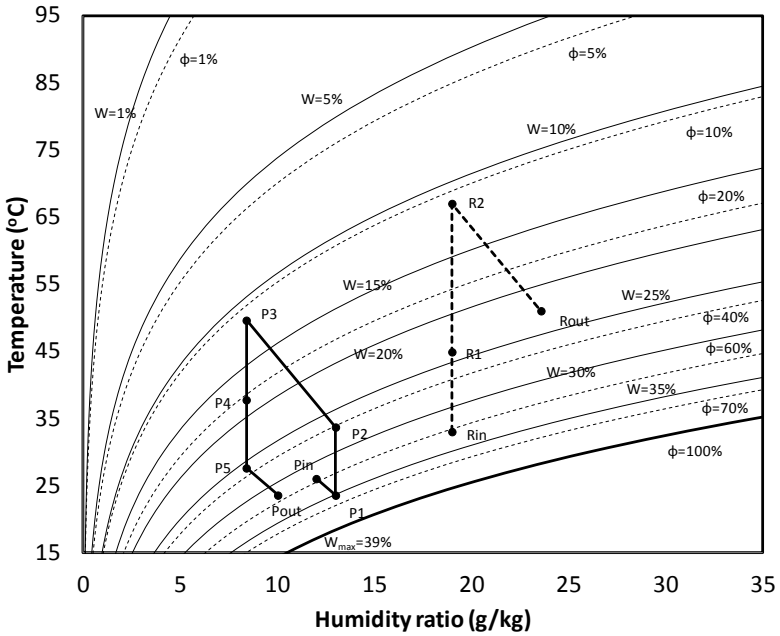

Fig. 4-13 Air handling processes of the dunkle cycle

III: mixed air system

There are three types of mixed air system, called advanced WSHE I cycle, advanced WSHE II cycle and novel WSHE cycle, seen in Fig. 4-14, Fig. 4-16 and Fig. 4-18, using ambient air as the regeneration air and mixed air (mixture of ambient air and return air) as the

processed air. The corresponding air handling processes are shown in Fig. 4-15, Fig. 4-17 and Fig. 4-19.

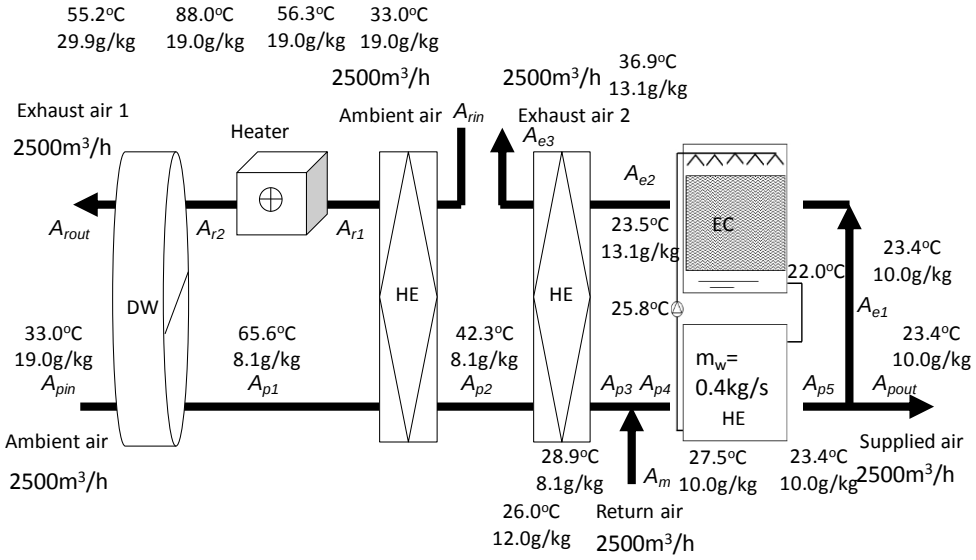

Fig. 4-14 Advanced WSHE I cycle

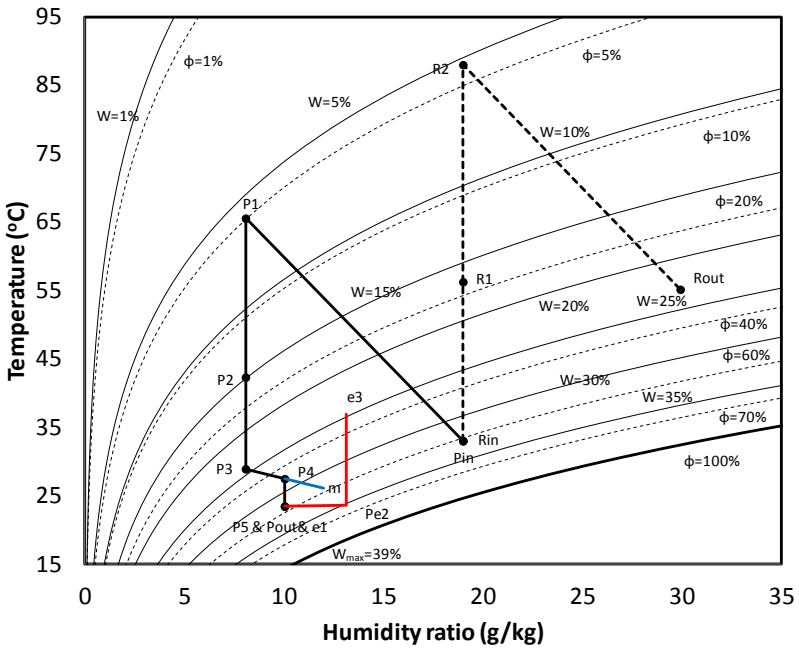

Fig. 4-15 Air handling processes of the advanced WSHE I cycle

As seen in Fig. 4-14, Fig. 4-16 and Fig. 4-18, the air handling processes of the regeneration air are the same. The ambient air is heated in the heat exchanger by the hot and dried processed air. Then it is heated in a heater to the required regeneration temperature. Last, it is used to regenerate the desiccant wheel.

Seen in Fig. 4-14 and Fig. 4-15 that, for the processed air side of the advanced WSHE I cycle, the ambient air is dehumidified by the desiccant wheel. Then, it is cooled in two separate heat exchangers. Then, it is mixed with a stream of return air and cooled in a sensible

heat exchanger by cooled water produced in the evaporative cooler. Then the cooled air is separated into two streams. One streams of the cooled air is supplied into the occupant room, and the other stream of cooled air is introduced into the evaporative cooler to produce cold water. Before being exhausted, the air is used to cool the processed air in the heat exchanger.

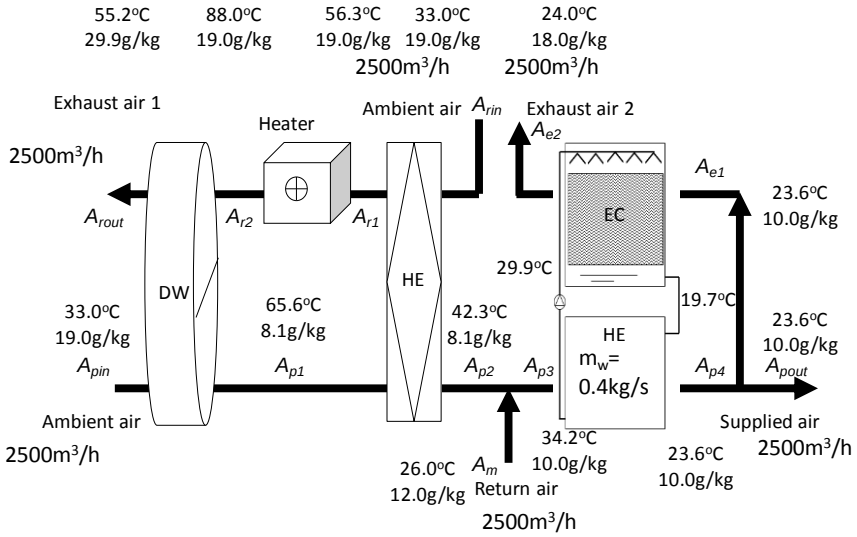

Fig. 4-16 Advanced WSHE II cycle

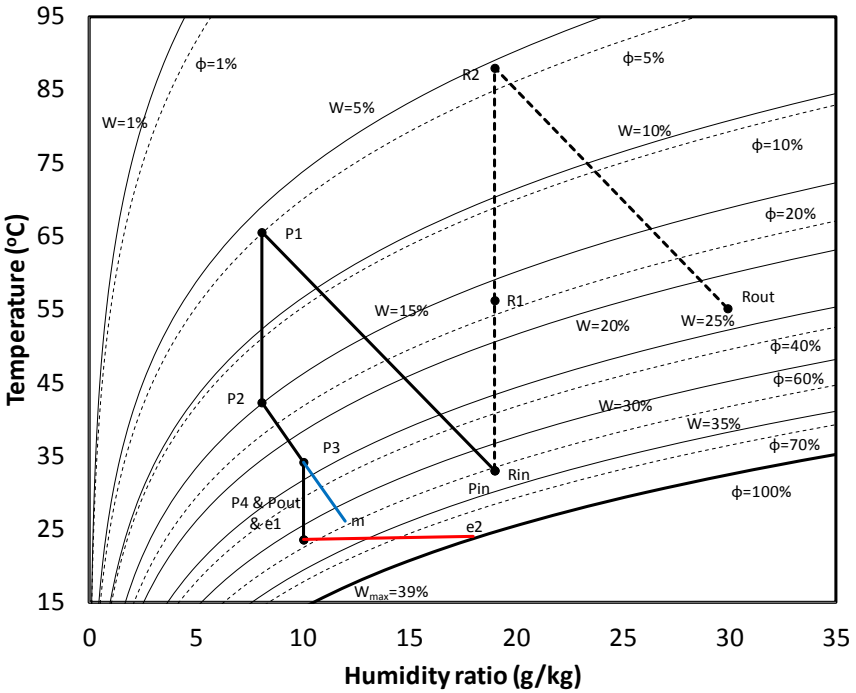

Fig. 4-17 Air handling processes of the advanced WSHE II cycle

The processed air handling process of advanced WSHE II cycle is similare with that of advanced WSHE I cycle. The heat exchanger at the exhaust air 2 side is removed.

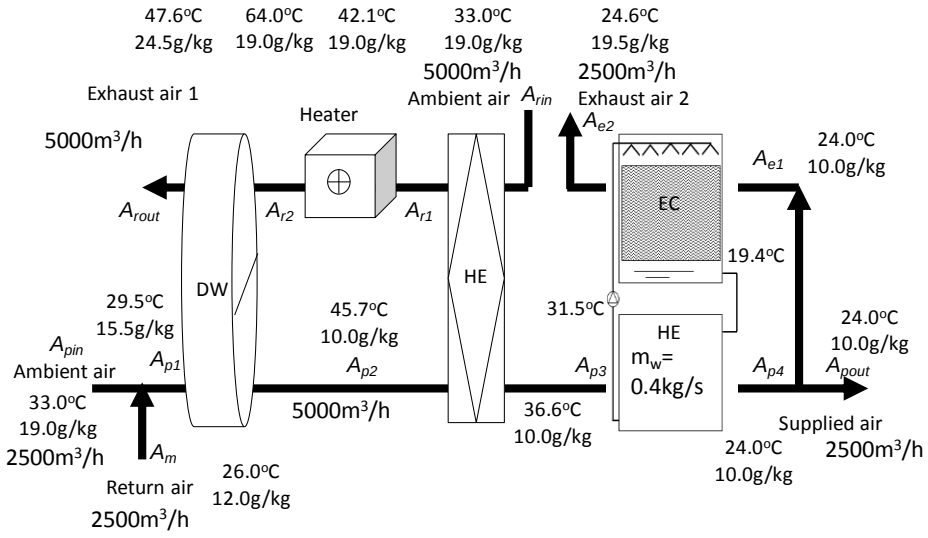

Fig. 4-18 Novel WSHE cycle

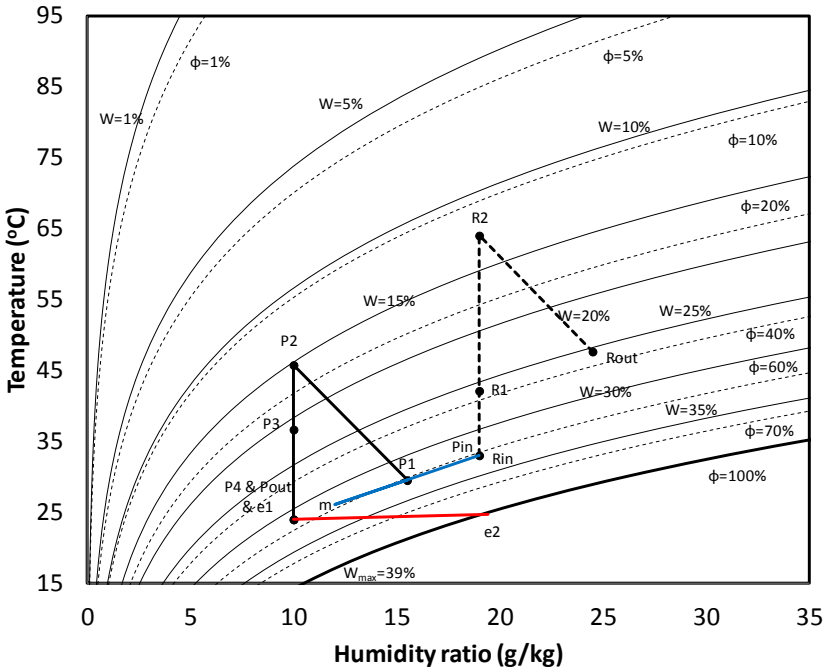

Fig. 4-19 Air handling processes of the novel WSHE cycle

The processed air handling process of novel WSHE cycle is similare with that of advanced WSHE II cycle. The return air is mixed with the ambient air before the desiccant wheel.

The performances of these six types of desiccant cooling systems are cpmpared based on the same supplied air states (humidity ratio, temperature and air flow rate), the same desiccant wheel structure. COP_t is used to evaluate the performance of the desiccant cooling systems, shown in Equ. (4-1).

$$COP_t = \frac{Q_{remove}}{Q_{heater}} = \frac{m_p\left(i_{pout} - i_{rin}\right)}{m_r \Delta t} \quad (4\text{-}1)$$

where m_p is supplied air flow rate; m_r is air flow rate in the heater; i_{pout} and i_{rin} are the processed air outlet enthalpy and the air enthalpy of the indoor occupant room; Δt is temperature rise after heater. COP_t shows the performance of the system to remove the heat from the occupant room.

The working conditions and information of each component are listed in Table 4-3.

Table 4-3 Parameter information

Name	Information
Working conditions	ambient air: 33ºC, 19g/kg return air: 26ºC, 12g/kg supplied air: <24ºC, 10g/kg, 2500m3/h
Desiccant wheel (DW)	thickness=0.2m, diameter=1m evenly divided between the two streams of air air flow rate is the same
Heat exchanger (HE)	NTU=2.5 NTU of each HE is the same
Evaporative cooler (EC)	adjusting NTU to reach satisfied supplied air temperature NTU of each EC is the same
Heater	electrical heating

To reach the required supplied air states, the air states after each component are shown in Fig. 4-8 to Fig. 4-19. For the mixed air system, the mixed air is the mixture of ambient air and return air with the same air flow rate. The required evaporative cooler NTU_m, regeneration temperature and COP_t are shown in Table 4-4.

Table 4-4 simulation results

Name	Working Conditions	Structure	t_{reg} ºC	COPt
VC	PA:ambient air; RA:return air	1 DW; 1 HE, NTU=2.5 each; 2 EC, NTUm=1.17 each	118	0.13
RC	PA:return air; RA:ambient air	1 DW; 1 HE, NTU=2.5 each; 2 EC, NTUm=1.02 each	76	0.23
DC	PA:return air; RA:ambient air	1 DW; 2 HE, NTU=2.5 each; 2 EC, NTUm=1.51 each	67	0.33
AWSHEI	PA:mixed air; RA:ambient air	1 DW; 3 HE, NTU=2.5 each; 1 EC, NTUm=0.47	88	0.24
AWSHEII	PA:mixed air; RA:ambient air	1 DW; 2 HE, NTU=2.5 each; 1 EC, NTUm=1.96	88	0.23
NWSHE	PA:mixed air; RA:ambient air	1 DW; 2 HE, NTU=2.5 each; 1 EC, NTUm=2.58	64	0.16

It can be seen in Table 4-4 that, dunke cycle are of the highest performance while ventilation cycle is of the lowest performance. That is because dunke cycle is used to dehumidify return air, and the regeneration temperature is lower. For the mixed air system,

advanced WSHE I and II cycles are of the relatively higher performance although the regeneration temperature is higher than novel WSHE cycle. That is because m_r of novel WSHE cycle doubles that of advanced WSHE I and II cycles. Comparing advanced WSHE I and II cycles, there air three heat exchangers in advanced WSHE I cycle and two heat exchangers in advanced WSHE II cycle, thus NTU_m of the former is smaller than that of the later.

4.2.3. Desiccant plate

The new device with the adsorbent coating on the surface of the heat exchanger enabled the direct cooling and heating of adsorbent. This new type of heat exchanger combined with adsorbent is shown as Fig. 4-20.

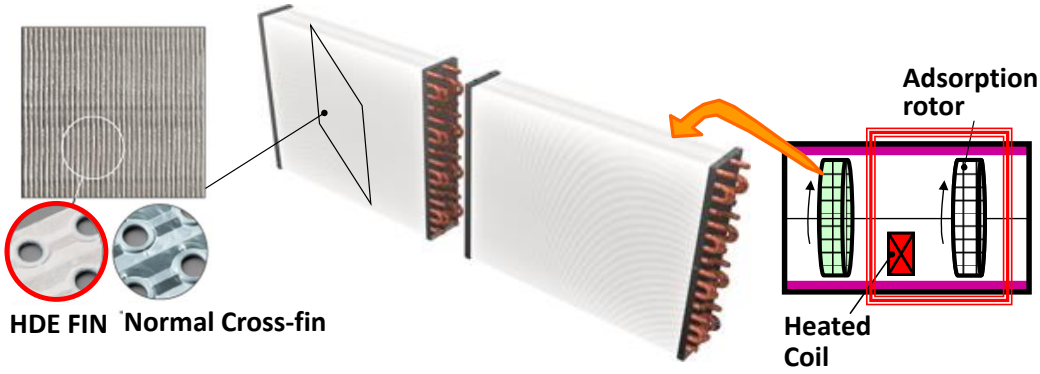

Fig. 4-20 Hybrid desiccant Element (HDE).

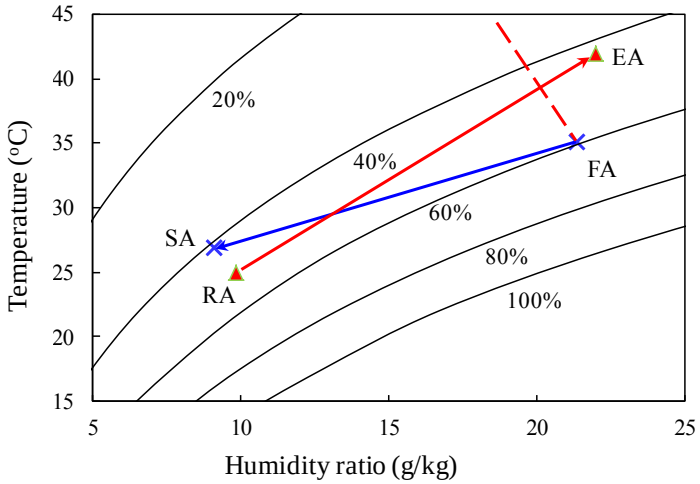

Fig. 4-21 Typical air handling process of DESICA.

The desorption heat required in the conventional desiccant system have to be provided on the air before the adsorption rotor and it makes the temperature very high. High desorption temperature is necessary for high dehumidification capacity and the temperature required for heating the air before the desorption process is up to as high as 70℃. Direct cooling

adsorption and direct heating regeneration were evaluated to utilize lower regeneration temperature. These innovative technologies make the required temperature level to be lower than 40 ℃. The typical air handling process of this novel air handling device(DESICA) is illustrated as Fig. 4-21.

For temperature, performance improvement was easily achieved by raising evaporating temperature. For humidity control, desiccant technology is focused on and the novel air handling device (DESICA) is developed to achieve high performance. Based on the high performance air handling device using desiccant (DESICA) and the VRF with high evaporating temperature, the novel HVAC system (THIC system) could be constructed, with its operating principle illustrated as Fig. 4-22.

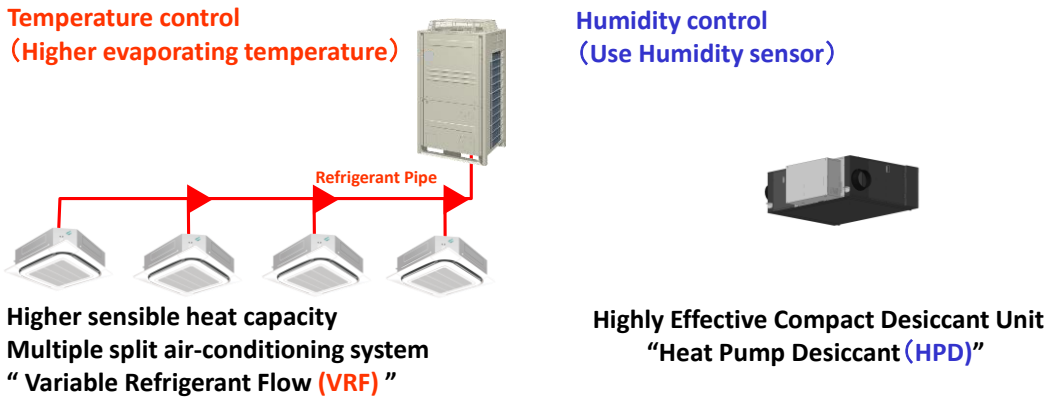

Fig. 4-22 The novel HVAC system combining high evaporating temperature VRF and DESICA.

The demonstration test was conducted in the office space in Nagoya University. Fig. 4-23 gives the tested outline of this demonstration, with the conventional system responsible for the right part while the novel THIC system for the left part.

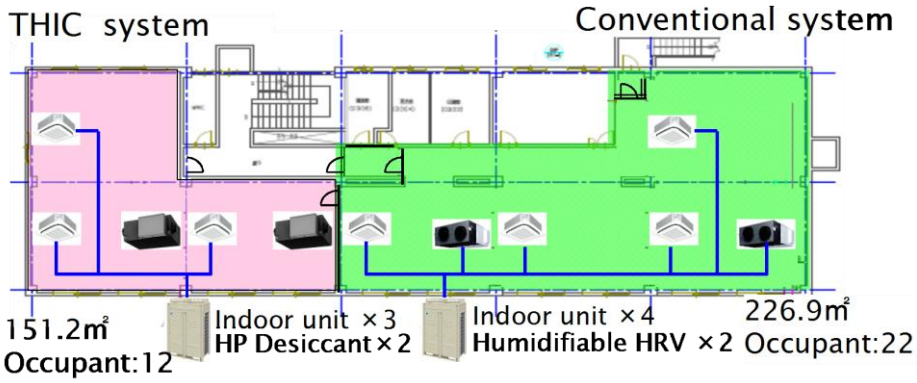

Fig. 4-23 The demonstration test of conventional and novel THIC systems.

From the aspect of comfort, the questionnaire shows that the THIC system can improve

the indoor air conditions, with fewer over-dehumidification or insufficient-dehumidification conditions. Furthermore, Fig. 4-24 shows the energy performances of these two systems and the energy consumption of the novel THIC system using DESICA in summer was reduced by almost half. Thus this novel DESICA device is an energy efficient solution for humid air handling process.

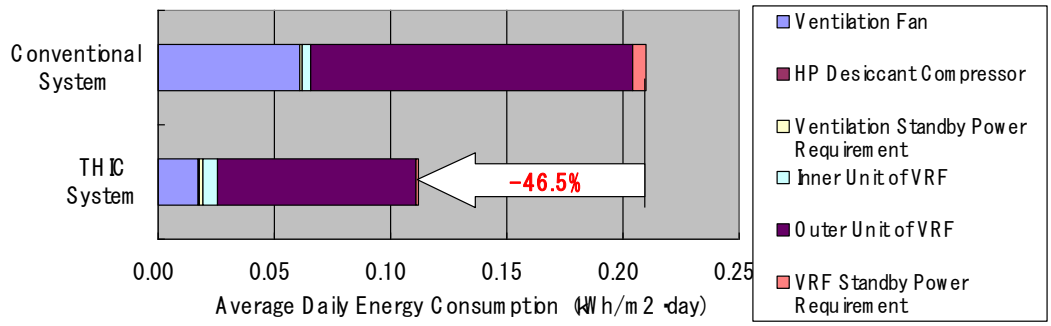

Fig. 4-24 Comparison on energy consumptions of these two systems.

4.2.4. Liquid desiccant

The air dehumidification process using liquid desiccant depends on the low vapor pressure of the solution. Solution contacts with air in packed bed of parallel-flow, counter flow or cross flow. Packing construction is used to increase heat and mass exchanger area. As the same as solid desiccant dehumidification method, liquid desiccant material need be concentrate after absorbing water from moist air. As shown in Fig. 4-25, two packed beds are used to dehumidify and regenerate respectively, and solution circles between them. To enhance dehumidification and regeneration, cooling source and heat source are usually applied.

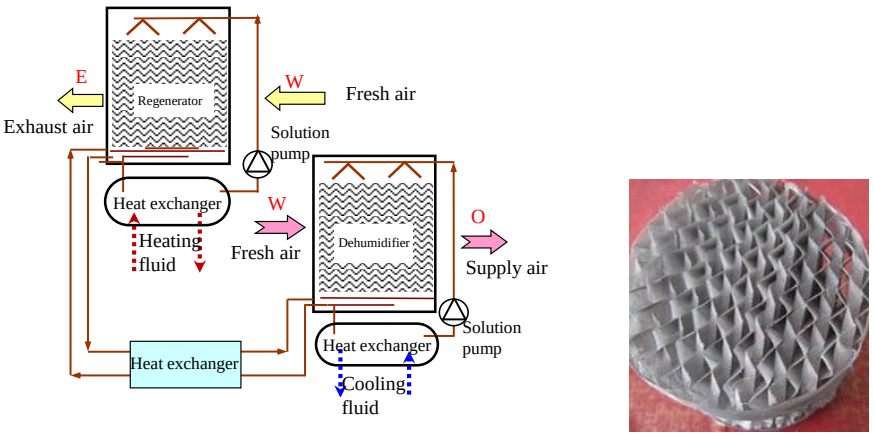

Fig. 4-25 Diagram of liquid desiccant system and ceramic structured packing

Air dehumidification methods that utilize liquid desiccant are becoming more and more popular, and heat pump-driven liquid desiccant (HPLD) systems are developing very quickly

in China. The cooling capacity from the evaporator and heat from the condenser are both utilized in HPLD systems, where the cooling capacity is used to cool the desiccant to enhance its dehumidification ability, and the heat is used to regenerate the desiccant. For HPLD systems, there are different ways to utilize the condensation heat for desiccant regeneration. The issues of how to evaluate the performances of different HPLD systems and how to pursue a process with better energy efficiency are at the center of current research efforts.

Fig. 4-26(a) and (b) show the operating schematics of two basic HPLD processes. In these processes, an adiabatic dehumidifier/regenerator is adopted. A small part of the diluted solution after dehumidification is sent into the regenerator and another small amount of concentrated solution after regeneration returns to the dehumidifier. As the variance of the desiccant concentration is usually lower than 0.5%, the mass flow rates of these two parts of the solution circulating between the dehumidifier and the regenerator are almost identical for these HPLD systems. A solution heat recovery device is used for the heat recovery between the diluted solution sent to the regenerator and the concentrated solution sent to the dehumidifier. The concentrated solution sent to the dehumidifier is then mixed with the rest of the diluted solution after dehumidification, and sent to the top of the dehumidifier with the help of a solution pump.

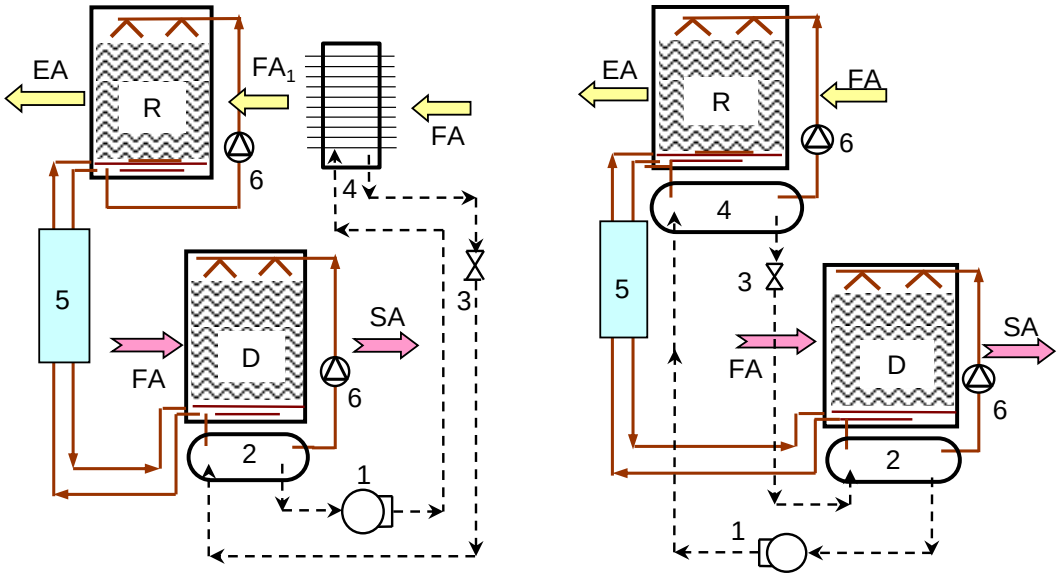

FA-fresh air; SA-supply air; FA₁-fresh air heated by the condenser; EA-exhaust air; D-dehumidifier; R-regenerator; 1-compressor; 2-evaporator; 3-expansion valve; 4-condenser; 5-solution heat exchanger; 6-pump.

(a) (b)

Fig. 4-26 Operating schematic of heat pump-driven liquid desiccant air handling processes with different regeneration modes: (a) Basic Type I: heating inlet air; and (b) Basic Type II: heating inlet solution.

In contrast to the typical adiabatic process where all the solution circulates between the dehumidifier and the regenerator, in the adiabatic dehumidifier/regenerator examined here,

most of the solution circulates only between the packed tower and the evaporator or condenser. The major difference between Basic Type I and Basic Type II systems is related to the different fluids that the condenser uses for heating. In Basic Type I, the condenser is an air-cooled type, and the regeneration air is heated by the condensation heat before flowing through the regenerator. A solution-cooled condenser is adopted in Basic Type II, and the solution is heated by the condensation heat instead of the regeneration air.

The performance discrepancy between these two systems and the primary explanations for this discrepancy are discussed here. The typical air handling processes shown are illustrated in Fig. 4-27 in a psychrometric chart. As indicated by the figure, the coupled heat and mass transfer process in the regenerator of Basic Type I proceed close to the isenthalpic line, while the process of Basic Type II is near the iso-concentration line of the liquid desiccant.

As indicated by the simulation results shown in Fig. 4-27, there are significant discrepancies in the operating performances of Basic Types I and II due to the difference between heating the regeneration air and heating the solution. Also, the inlet temperature that the solution is heated to for regeneration in basic Type II (78.8 ℃) is lower than that of the air in basic Type I (51.1 ℃). Entransy analysis is introduced in Section 4.3.3 to explain it.

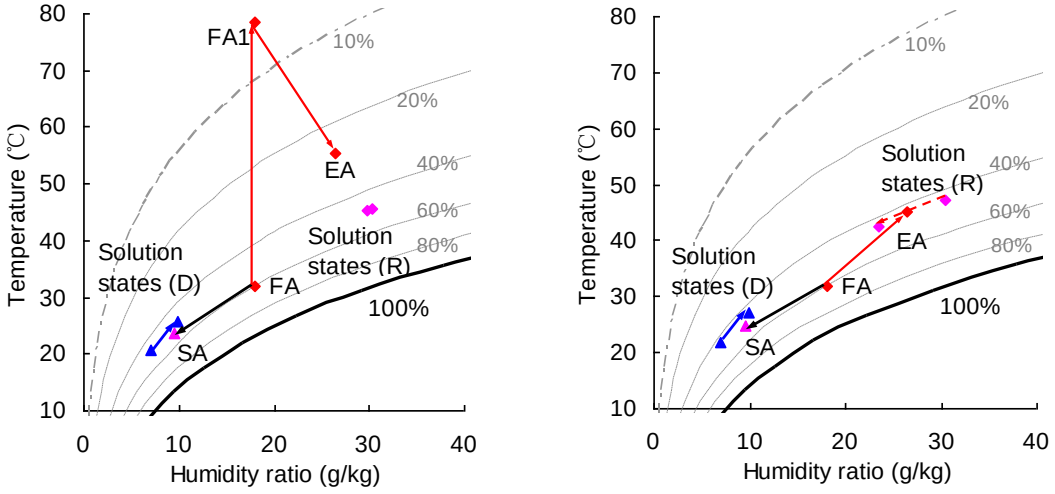

Fig. 4-27 Air and solution states of heat pump-driven liquid desiccant air handling processes shown in psychrometric chart: (a) basic Type I; and (b) basic Type II.

4.3. Entransy analysis method

The idea of entransy comes from an analogy between heat conduction and electric conduction; entransy corresponds to electric potential. The definition of entransy is based on the heat conduction equation, which is also the basis of entransy analysis. Eq. (4-1) is referred to as entransy, the ability to transfer thermal energy that results from both energy and

temperature level. And entransy dissipation rate is written as Eq. (4-2). In a reversible heat transfer process, entransy dissipation is equal to zero. For example, the heat transfer area of the counter flow heat exchanger is infinite and the heat capacity flow rates of the two sides are equal.

$$E_n = \frac{1}{2}\rho c_p T^2 \tag{4-1}$$

$$\Delta E_{n,dis} = k\left|\nabla T\right|^2 = \frac{Q^2}{UA} = Q\cdot\Delta T_m \tag{4-2}$$

T-Q chart and unmatched coefficient are useful method to analyze heat transfer or couple heat and mass transfer process, refined from entransy analysis.

For heat transfer process, take a counter flow heat exchanger as example in Fig. 4-28(a). Assuming the specific heat capacities of the fluids are constant, the temperature changes of the two fluids can be represented by the lines in a *T–Q* (temperature–heat flux) chart, as shown in Fig. 4-28(b).

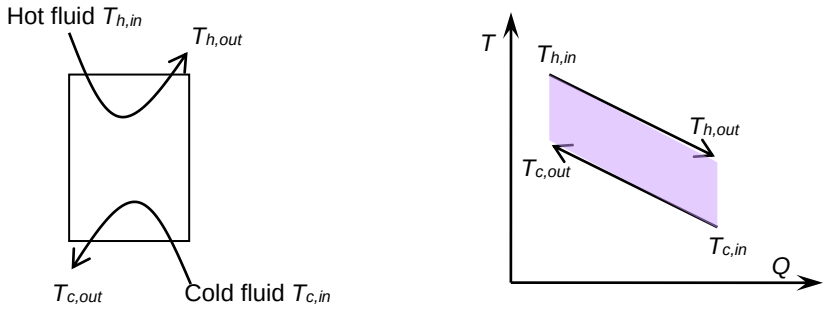

(a) (b)

Fig. 4-28 Heat transfer process in a counter-flow heat exchanger: (a) hot and cold fluids; (b) heat transfer process shown in a T-Q chart.

Entransy dissipation of this heat transfer process can be represented by the area in Fig. 4-28(b), and is calculated by Eq. (4-3), where Q is total transferred heat of this process.

$$\Delta E_{n,dis} = \frac{1}{2}(T_{h,in} + T_{h,out} - T_{c,in} - T_{c,out})Q \tag{4-3}$$

Heat resistance of the heat transfer process is:

$$R_H = \frac{\Delta E_{n,dis}}{Q^2} = \frac{(T_{h,in} + T_{h,out} - T_{c,in} - T_{c,out})}{2Q} \tag{4-4}$$

The outlet temperatures can be obtained using the ε-NTU method. The heat resistance can be expressed as Eq.(4-5), where ξ is the flow unmatched coefficient and is expressed as Eq.(4-6).

$$R_H = \frac{\xi}{UA} \tag{4-5}$$

$$\xi = \frac{P}{2} \cdot \frac{e^P + 1}{e^P - 1}, \text{ where } \quad P = UA \cdot \left(\frac{1}{c_{p,h}\dot{m}_h} - \frac{1}{c_{p,c}\dot{m}_c}\right) \tag{4-6}$$

If one of the fluids maintains a constant temperature, such as in evaporator and condenser, P can be calculated by Eq. (4-7).

$$P = \frac{UA}{c_{p,c}\dot{m}_c} \tag{4-7}$$

The flow unmatched parameter is always greater than or equal to 1, but only when the calorific capacities of the two fluids are equal will the flow unmatched parameter be equal to 1. As indicated by Eq.(4-5), 1/UA denotes the resistance caused by the limited heat transfer capacity, and the heat resistance will increase by a multiple of ξ from the base of 1/UA when the calorific capacities of the fluids are different. Thus, the heat resistance can be reduced by improving the heat transfer coefficient or increasing the heat transfer area, while flow mismatching will lead to an increase of heat resistance.

For coupled heat and mass transfer process, the entransy dissipationes of the heat transfer process and the mass transfer process are depicted in Fig. 4-29, and calculated by Eqs. (4-8) and (4-9), respectively, where Q_s is the sensible heat transferred in the device, T_l and ω_e are temperature and equivalent humidity ratio of liquid.

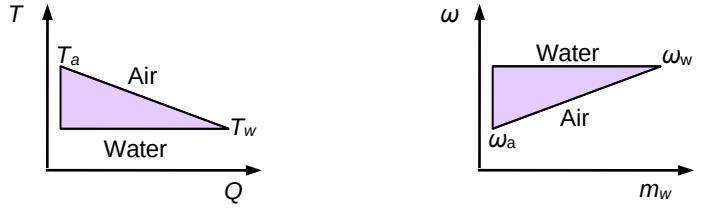

(a) (b)

Fig. 4-29 Entransy dissipationes in a coupled heat and mass transfer process, taking an air-water direct contact device as example: (a) heat transfer process shown in a *T*-*Q* chart; (b) moisture transfer process shown in an ω-m_w chart.

$$\Delta E_{n,dis,H} = \frac{Q_S}{2}(T_a - T_w) \tag{4-8}$$

$$\Delta E_{n,dis,M} = \frac{Q_S}{2r}(\omega_w - \omega_a) \tag{4-9}$$

Heat transfer resistance and mass transfer resistance are:

$$R_H = \frac{\Delta E_{n,dis,H}}{Q_S^2} = \frac{1}{UA} \cdot \frac{a_{11} \cdot (\Delta T_1)^2 + a_{12} \cdot \Delta T_1 \Delta T_2 + a_{22} \cdot (\Delta T_2)^2}{b_{11} \cdot (\Delta T_1)^2 + b_{12} \cdot \Delta T_1 \Delta T_2 + b_{22} \cdot (\Delta T_2)^2} = \frac{1}{UA} \cdot \xi_H \tag{4-10}$$

$$R_M = \frac{\Delta E_{n,dis,M}}{\dot{m}_w^2} = \frac{1}{U_M A_M} \cdot \frac{a_{11} \cdot (\Delta\omega_1)^2 + a_{12} \cdot \Delta\omega_1 \Delta\omega_2 + a_{22} \cdot (\Delta\omega_2)^2}{b_{11} \cdot (\Delta\omega_1)^2 + b_{12} \cdot \Delta\omega_1 \Delta\omega_2 + b_{22} \cdot (\Delta\omega_2)^2} = \frac{1}{U_M A_M} \cdot \xi_M \qquad (4\text{-}11)$$

4.3.1. Condensing dehumidification

For above introduced three condensing dehumidification process (conventional condensing, precooling with heat recovery, precooling with high-temperature chilled water), T-Q charts of the processes are shown in Fig. 4-30.

For the conventional process, as shown in Fig. 4-30 (a), a big triangle area is formed due to high temperature difference and unmatched flow, indicating much entransy dissipation. ξ = 1.26, more greater than 1, thus limiting heat transfer ability for the given heat exchanger area. This means that, for the dehumidification process, the heat transfer resistance caused by the unmatched flow rates increases 126% on the basis of 1/UA.

For the precooling method with heat recovery, as shown in Fig. 4-30(b), 40% enthalpy are recovered by heat recovery device from indoor exhaust air. Because indoor air flow rate is equal to outdoor air, so ξ_1 = 1, and entransy dissipation are caused by limited heat exchanger area.

The precooling method with high-temperature chilled water, similar with multi-stage chillers, can effectively improve the uniformity characteristics of temperature differences, as shown in Fig. 4-30(c).

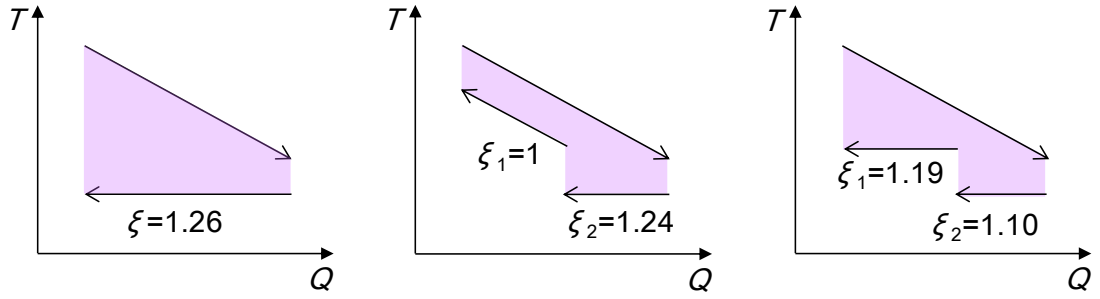

(a) (b) (c)

Fig. 4-30 *T-Q* charts and unmatched coefficient of three condensing dehumidification process: (a) conventional condensing; (b) precooling with heat recovery; (c) precooling with high-temperature chilled water.

4.3.2. Desiccant wheel

1) Desiccant wheel

Wherever air inlet conditions of two flows are, the handling process of the air is close to iso-enthalpy line. Usually there are two kinds of dehumidification wheel. Type I is with 1/2 regeneration section of the whole wheel, and Type II is with 1/4, as shown in

Fig. 4-31.

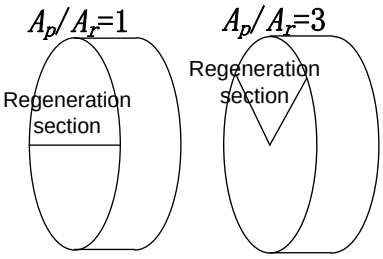

Fig. 4-31 Diagram of two kids of dehumidification wheel

Taking a typical air handling process as an example, the condition of outdoor air is 30℃ and 18g/kg, and the inlet humidity ratio of regeneration air is 10g/kg. The outdoor air flow rate is 3000m^3/h, and indoor air flow rate is the same ratio of outdoor air flow rate with area ratio. The radius and thickness of the wheel is 500mm and 200mm respectively.

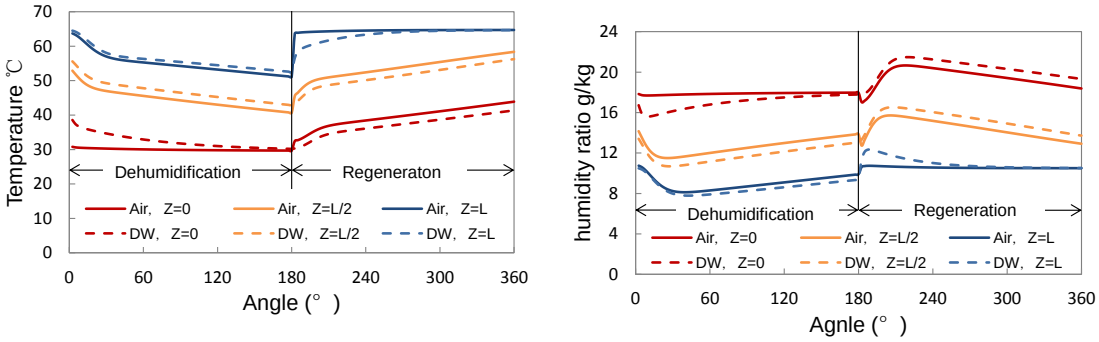

(a) Temperature (b) Humidity ratio

Fig. 4-32 Temperature and humidity ratio distribution of air and desiccant along rotary direction of Type I: (a) temperature; (b) humidity ratio.

For Type I, that a desiccant wheel that dehumidification and regeneration section are both half the wheel (Ap/Ar=1), the outdoor air flow rate and indoor exhaust air flow rate are equal. Fig. 4-32 shows the temperature and humidity ratio distribution of air and desiccant material, in three different positions along wheel thickness direction, where the humidity ratio of material means the equivalent humidity ratio. In the dehumidification section, the temperature of air is lower than that of solid desiccant material, so that the material is cooled along rotary direction. The mass transfer direction is just opposite to the heat transfer direction, so the material moisture content of material increases, tending to saturation. In a similar way, the solid desiccant material is heated and desorbing water along rotary direction in the regeneration section. And considering that the air flow direction is different with rotary direction of wheel, the temperature and humidity ratio of supply air and exhaust air is non-uniform along angles, as shown by dashed lines of Z=H in dehumidification section and

Z=0 in regeneration section in Fig. 4-32. However, throughout the whole wheel, the temperature difference and humidity ratio difference between air and material are relatively uniform, which represent the uniform heat and mass transfer driving force. And meanwhile, the ξ_m of Type I wheel is close to 1, meaning that limited heat and mass transfer area gives full play to exchange heat and moisture.

For Type II, the area of processed section is three times that of regeneration section, and processed air flow rate is also three times regeneration air flow rate. The temperature and humidity ratio distribution of air and desiccant material, in three different positions along wheel thickness direction, is shown in Fig. 4-33. Different with that of Type I, the difference of desiccant and air is not uniform along the angles. The main reason is unequal air flow rate. For Type II, the ξ_m of the whole wheel is rather more than 1, indicating that heat and mass transfer resistance caused by unmatched parameters is very much.

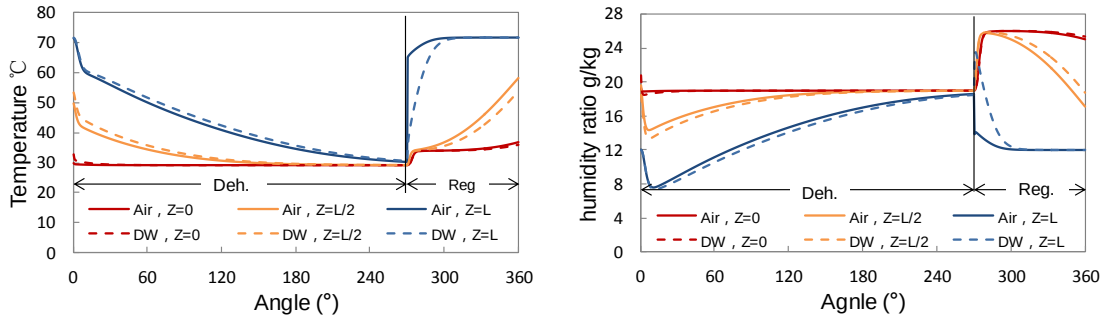

(a) Temperature (b) Humidity ratio

Fig. 4-33 Temperature and humidity ratio distribution of air and desiccant along rotary direction of Type II: (a) temperature; (b) humidity ratio.

2) System

Of desiccant wheel air-conditioning system, desiccant wheel and sensible heat exchangers are the two key components. Heat and mass transfer between the air and the solid desiccant occurs in the former, high enthalpy regeneration air makes desiccant release moisture, and dry desiccant dehumidifies the processed air. In the dehumidification part, the processed air is cooled to enhance the mass transfer process. In the regeneration part, hot air is used to input heat to supply the desiccant regenerated heat requirement. Heat and cooling is input in sensible heat exchangers before or after desiccant wheels, by constant temperature source, like evaporator and condenser, or varying temperature source, like water.

One-stage desiccant wheel system is depicted in Fig. 4-34(a), composing of one desiccant wheel, one heater, one pre-cooler and one post-cooler. If the processed air is dehumidified to degree drier than enthalpy recovery outlet, the regeneration air enthalpy inlet must be higher than the processed air enthalpy inlet. When the system is divided into two stages, the thickness of wheel, the heat transfer area of all heat exchangers and the source

flow divide equally, and two air streams flow through components in turn. The system is shown in Fig. 4-34 (b). The air handling processes in psychromatric chart are shown in Fig. 4-35. Fig. 4-35(a) presents the air handling processes of one-stage system, in which shadow region means the solid desiccant states. Throughout the wheel, equivalent humidity ratio and moisture content of desiccant material are 7.8~21.5g/kg and 7.4%~33.7%, respectively, of wide ranges. According to Fig. 4-35(b), the desiccant material states of two-stage are separately in high humidity and low humidity zones on psychrometric chart. Desiccant material of 1st-stage is ranging in 11.3~20.8g/kg and 12.7%~30.0% at Equivalent humidity ratio and moisture content, respectively. Meanwhile that of 2nd-stage is ranging in 8.5~14.5g/kg and 13.9~24.6% respectively. Thus moisture content span of desiccant material in each stage becomes narrowed, leading to lower regeneration temperature.

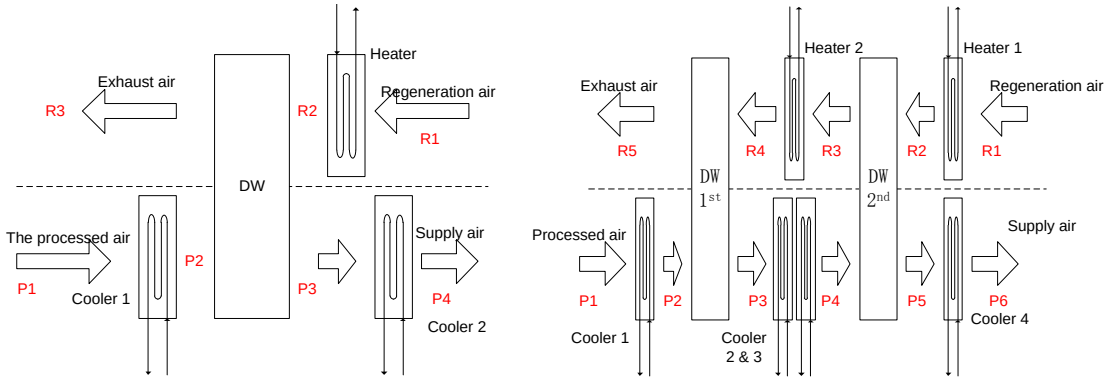

(a) (b)

Fig. 4-34 Diagram of desiccant wheel air-conditioning system: (a) one-stage; (b) two-stage.

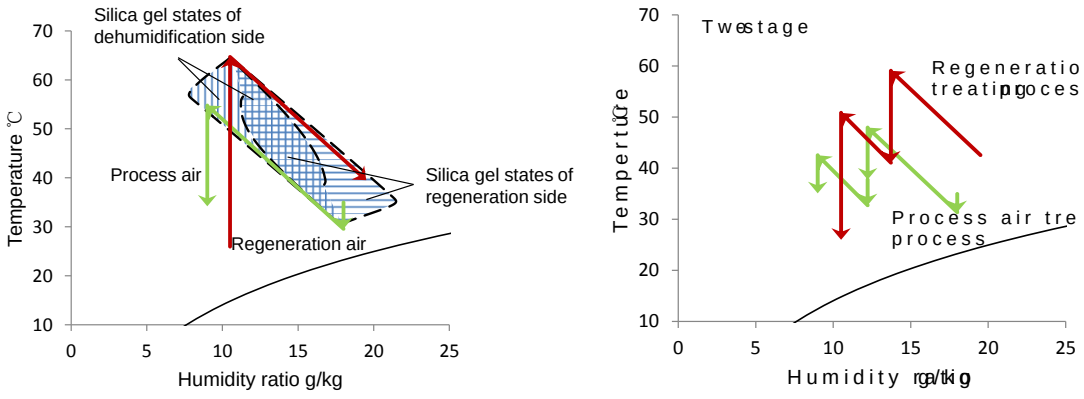

(a) (b)

Fig. 4-35 Air handling processes of two systems in psychromatric chart

Though the regeneration temperature decreases of two-stages compared with one-stage, it is found that the increasing or decreasing of required hot water temperature after dividing the desiccant wheel system depends on the water flow. Fig. 4-36 shows the required hot water temperature of one-stage and two-stage systems with various water flows. When the total hot

water flow increases from 0.12kg/s to 1.5kg/s (cold water flow of each cooler is equal to hot water flow of each heater), the required hot water of two systems both decreases. Due to different changing slopes, the critical water flow exists. When the total water flow is slower than critical value, the required hot water temperature of one-stage system is lower than that of two-stage system. And when the total water flow is higher than critical value, the required hot water temperature of two-stage system is lower. For the given system, 0.33kg/s is determined as the critical value.

At the same time, the required hot water temperature tends to a constant by increasing water flow. For the given system with limited heat exchange area, it represents the lowest heat source temperature, which can be obtained with infinite water flow or constant temperature sources.

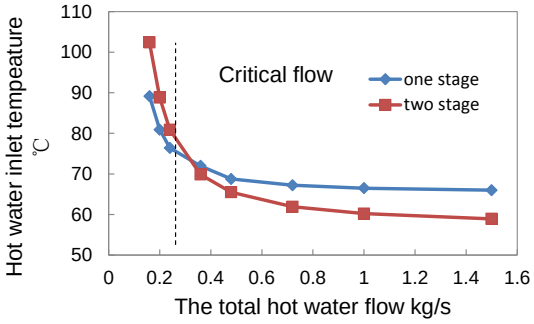

Fig. 4-36 The required hot water temperature with various water flows.

Supporting different water flow, the uniformity coefficient of the desiccant wheel has little change, and that of heaters are shown in Fig. 4-37. When the total hot water flow increases from 0.12kg/s to 1.5kg/s, the uniformity coefficient of heaters decrease first and then go up, and inflection point exists. Minimums of one-stage system and two-stage system are 0.24kg/s and 0.48kg/s, respectively, flow matching point with the air flow. As indicated in Fig. 4-37, the intersection of two lines is the same with that in Fig. 4-36. Therefore, uniformity coefficient can replace required hot water temperature as evaluation criteria. Comparing performances of heat exchangers in one-stage and two-stage system, the system with lower uniformity coefficient of heat exchangers requires lower hot water temperature.

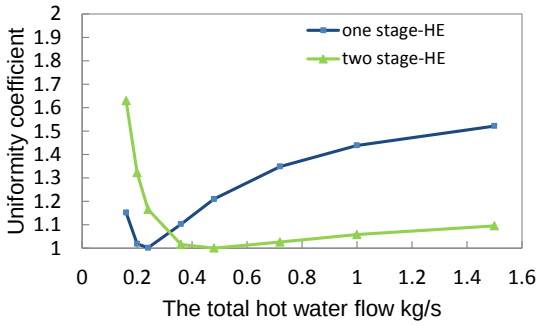

Fig. 4-37 Uniformity coefficient of heaters at different water flow.

4.3.3. Liquid desiccant

1) Solution and air inlet position's impact

Taking a typical solution state as an example, match properties varying with the typical inlet air states are shown in Fig. 4-38, where a_1 ~ a_{16} are the air inlet states around inlet solution state S (the temperature of the LiBr solution is 25 ℃, and the concentration is 45%). The mass transfer rates of a_1 ~ a_{16} varying with NTU_M in this air-desiccant process are shown in Fig. 4-39(a) and calculated by the analytical method, where the air flow rate is 1 kg/s and the heat capacity ratio of two fluids is 1. The unmatched coefficient (ξ_M) of different air inlet states is illustrated in Fig. 4-39 (b), except for a_3 and a_{11}. A comparison can be made between the heat and mass transfer processes proceeding along the isenthalpic line and those proceeding along the iso-concentration line. For the processes along the iso-concentration line (a_3-S and a_9-S), ξ_M is always 1; for the processes along the isenthalpic line (a_5-S and a_{13}-S), ξ_M is 1.08, 1.31, and 1.66 if *NTU* is 1, 2, and 3, respectively. This indicates that, for the processes along the isenthalpic line, 8%, 31%, and 66% more mass transfer capacity is required due to the unmatched parameters when *NTU* is 1, 2, and 3, respectively.

Thus, in the coupled heat and mass transfer processes between the air and liquid desiccant, the greater the unmatched coefficient, the greater the required transfer ability for certain heat or moisture transfer devices. Similarly, the effects of unmatched parameters on the processes are magnified as input heat and mass transfer capacity increase. Match properties help to examine the performance of the heat and mass transfer process between the air and desiccant, and the following section demonstrates the analysis using both a simulation method and the unmatched coefficient method.

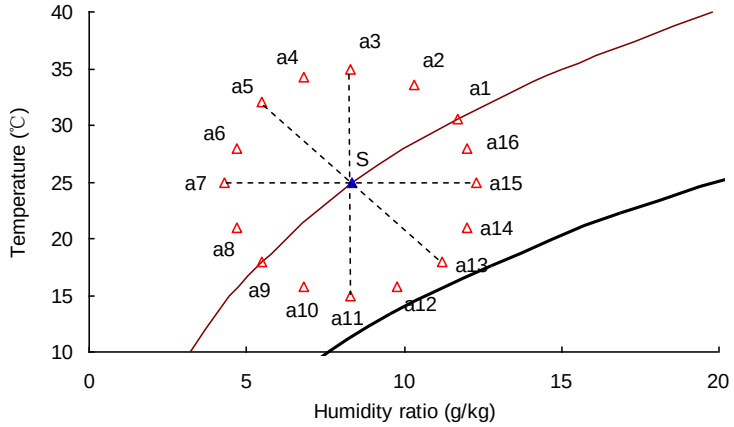

Fig. 4-38 Different air and solution inlet states shown in an air psychrometric chart (S: solution inlet state).

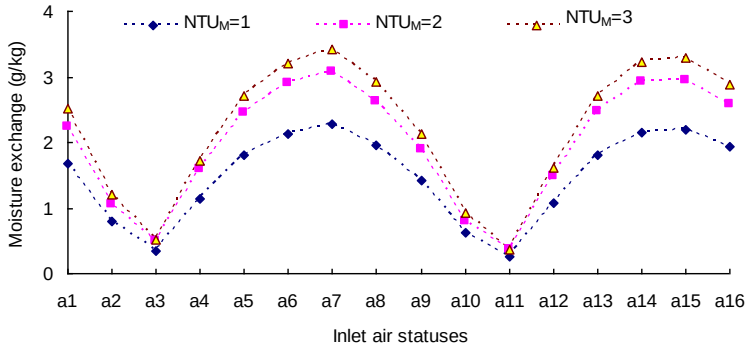

(a)

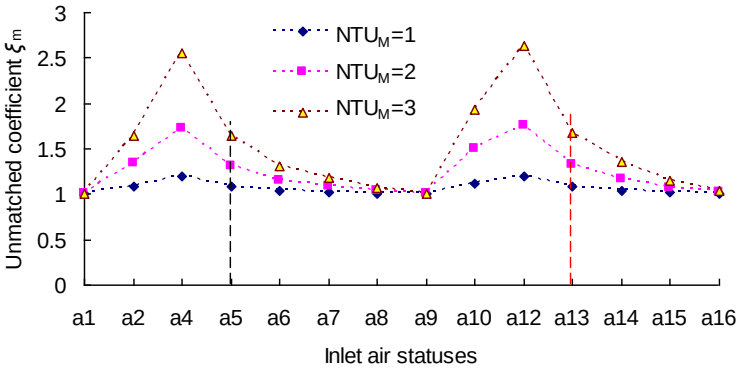

(b)

Fig. 4-39 Unmatched heat and mass transfer coefficients in an air-solution direct contact device: (a) moisture exchange; and (b) mass transfer unmatched coefficient.

2) Basic processes comparison

Based on the two basic processes introduced in Section 4.2.4, unmatched coefficients of key components for Basic Type I and Basic Type II in a typical condition are listed in Table 4-5. As indicated by the match properties of these components, the unmatched coefficients of the evaporator, the dehumidifier, and the heat exchanger are similar for Basic Types I and II. The unmatched coefficient of the dehumidifiers is 1.07 for these two HPLD systems,

indicating that the unmatched flow rates and parameters have a relatively limited effect on the dehumidification process. For the condenser and regenerator, there is significant variation in the unmatched coefficients of Basic Types I and II. In Basic Type I, ξ of the air-cooled condenser is 2.70 in this typical condition, more than two times higher than that of Basic Type II. This means that, for the air-cooled condenser of Basic Type I, the heat transfer resistance caused by the unmatched flow rates increases 170% on the basis of 1/UA. So the regeneration air in Basic Type I has to be heated to a relatively high temperature to satisfy the requirement for desiccant regeneration before flowing through the regenerator, which leads to a high ξ of the air-to-solution condenser. As a result, the unmatched coefficient of the regenerator is 1.34, still significantly higher than that of Basic Type II. This implies that, in order to overcome the mass transfer resistance caused by unmatched flow rates and parameters, more heat and mass transfer capacity or a higher heat source temperature is required in Basic Type I compared to Basic Type II. In summary, the match properties of Basic Type II are much better than those of Basic Type I.

The significant difference in unmatched coefficients of Basic Types I and II is similar to the performance discrepancy between the simulated HPLD systems. The operating parameters of the HPLD systems in this typical condition are also listed in Table 4-5, including the evaporating and condensing temperatures of the heat pump, COPhp, and COPsys. The evaporating temperatures and the supply air temperatures are similar for Basic Types I and II. However, the condensing temperature of Basic Type I (78.8 ℃) is much higher than that of Basic Type II (51.1 ℃), indicating that the condensing temperature increases due to the unmatched flow rates of the air-cooled condenser. The increase of the condensing temperature results in a COPhp of 1.89 in Basic Type I, lower than half of the COPhp of Basic Type II (4.53).

Table 4-5 Match properties and system performances of HPLD systems under a typical condition (outdoor air: 32 ℃, 18g/kg)

Type		Basic Type I	Basic Type II
Unmatched coefficients ξ (ξ_M) of key components	Condenser	2.7	1.07
	Regenerator	1.34	1.05
	Evaporator	1.07	1.05
	Dehumidifier	1.07	1.07
	Heat exchanger	1	1
Supply air parameters		23.6 ℃, 9.5 g/kg	24.7 ℃, 9.5 g/kg
Performance of the heat pump cycle	t_c	78.8 ℃	51.1 ℃

	t_e	16.5℃	17.7℃
	COP_{hp}	1.89	4.53
	COP_{sys}	1.83	4.17

4.4. Conclusion

Humid air handling process is one of the key components in the air-conditioning system, especially for the areas with a humid climate such as east part of China and Japan. The outdoor air is usually required to be handled to a state drier and colder than the indoor air before supplied to the indoor space in summer. Based on the requirements for dehumidification for humid air handling devices, condensation dehumidification method and desiccant dehumidification method are both introduced in this chapter. Performance evaluating indexes, tested results and theoretical analysis using entransy dissipation are investigated. It's indicated that condensation dehumidification method and desiccant dehumidification method are both sufficient for humid air handling requirement. To improve the energy performance of the air handling process using solid or liquid desiccant, it's recommended that the air handling process proceed along the iso-concentration line (or iso-relative humidity line) rather than the isenthalpic line. Constructing a multi-stage process for the humid air handling process is a feasible approach to increase the required cooling source temperature (for condensation dehumidification method) or lower the required regeneration heating source temperature (for desiccant dehumidification method).

5. Evaporative cooling

Evaporative cooling has been known for hundreds of years and is an attractive technology that is broadly used in the various countries including the USA, Iran, and Mexico. However, it is not a technology used as often in European countries. One reason is that the need for cooling has not been as significant a matter to address as it is in this timeframe. Another factor could be that natural and/or mechanical ventilation as well as night time cooling was sufficient to meet the cooling needs of buildings. Nevertheless, evaporative cooling has many advantages such as lower energy use than refrigerant cooling; inexpensive and simple to operate and maintain; will work as an air filter; and uses only water as a cooling agent instead of refrigerants. To illustrate the energy saving potential of evaporative cooling concerning traditional cooling, a COP parameter could be used. The COP of a traditional compressor driven cooling process would range between 3 and 4 whereas an evaporative cooling COP would be at least 10 times higher. The reason for such a high COP is the additional energy provided to the system to use evaporative cooling is proportional only to additional energy use of the fan due to pressure loss on Evaporative Cooling (EC)

components. Moreover, cooling needs for new energy efficient, air tight and very well insulated buildings are not limited only to summer months but extend to the seasonal transition and winter periods. In those timeframes, the potential for evaporative cooling increases due to a low wet bulb air temperature.

The potential of EC depends on local climatic conditions and the difference between the dry-bulb air temperature and wet-bulb temperature, which is called wet-bulb temperature depression. Due to its multi-climates, different locations in Europe might require different evaporative systems. In Section 2.3 of this report, typical components for the evaporative cooling system when integrated in a ventilation system are presented. In this chapter, some standard system solutions are presented with an investigation of the cooling potential of different EC systems including combinations for various annual climatic conditions. In this investigation, both Direct Evaporative Cooling (DEC) and Indirect Evaporative Cooling (IEC) technologies were reviewed. Both systems used sensible energy in the air to evaporate water. Additionally, these systems converted the sensible energy to latent heat. This study also investigates which system, when installed in a specific climatic location, is able to provide sufficient cooling for the range of highly probable heat loads and air change rates in buildings. The theoretical study is limited to European conditions.

The theoretical study is followed by an experimental study limited to a DEC system. In the experimental study, the sensitivity of a DEC system to water temperature, air velocity through pads and water flow is investigated. The COP of the system is calculated as part of the experimental study. To illustrate evaporative cooling potential and limitations in European weather conditions, a number of experiments were conducted for different cities located in Europe. For this investigation, climatic conditions representing the summer outdoor cooling design conditions for the 1.0 percentile of time was used.

5.1. Typical evaporative cooling systems

For the purposes of this investigation, the potential of EC systems is limited to EC when used in mechanical ventilation systems. In the study, 5 systems were chosen as presented in Fig. 5-1.

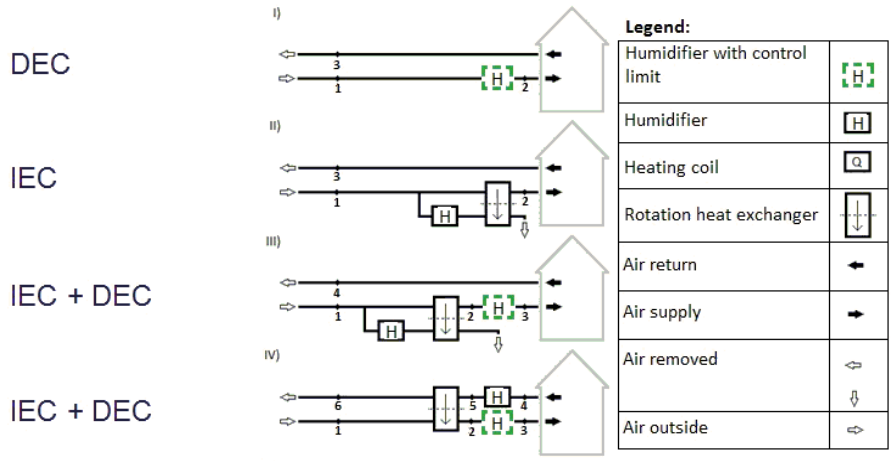

Fig. 5-1 Schematics of the evaporative cooling systems.

The symbol H in the highlighted dashed green square indicates a humidifier with control based on relative humidity of inlet air. In this investigation, these humidifiers do not humidify if inlet air humidity increases above 70%. The symbol H in the solid line square indicates humidifiers without humidity control. Typical air handling processes of system I, II and IV are illustrated as Fig. 5-2.

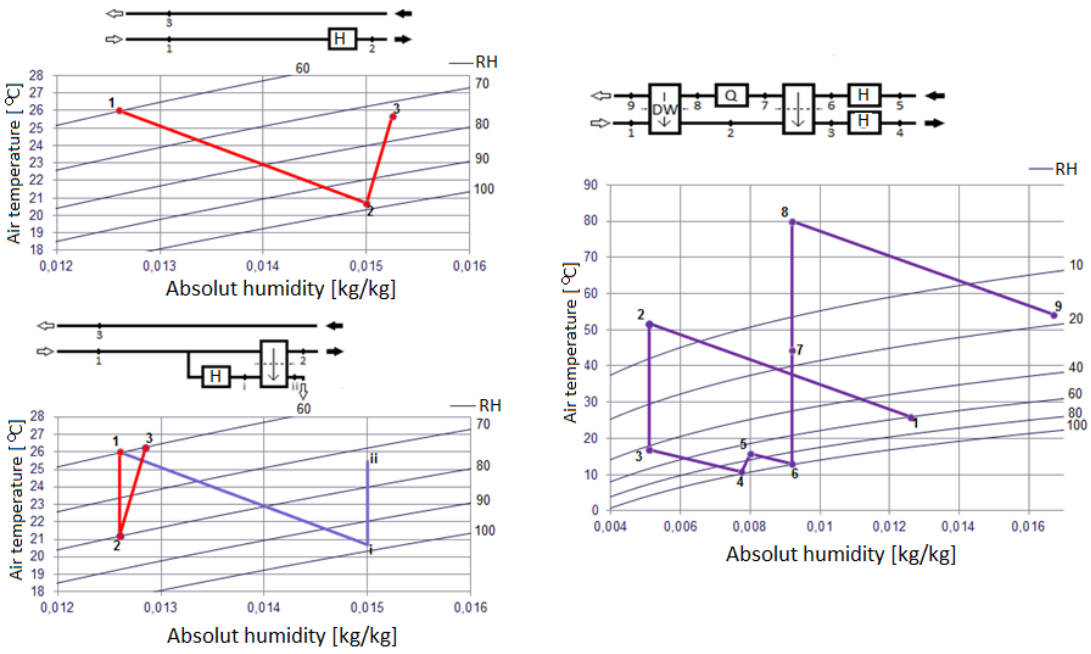

Fig. 5-2 Example of thermodynamic processes for system I, II and IV.

5.2. Calculation methodology

The performance of system I to III (respectively DEC, IEC, IEC+DEC) was independent of room air parameters while system IV (IEC+DEC) was dependent on the return air

parameters. To illustrate the process in each system, a standard case with a defined boundary condition was assumed. The performance of each component was assumed and is presented as follows:

- Humidification efficiency was chosen at 95% and temperature of the humidifying water was equal to wet bulb air temperature.
- Heat exchanger in IEC coil transfers only sensible heat and has efficiency of 90%.
- The heat transfer between the surroundings and the ventilation ducts was simplified to an adiabatic condition where the heat gain from the fans is neglected.

All calculations were performed using MATLAB. Cooling potential of evaporative systems and capacity to provide acceptable thermal comfort can be designed based on known outside conditions and assumed internal heating loads. Calculations of the presented investigation were based on hourly weather data sets for each of investigated locations. In System IV, the calculations for the inlet air into the room were solved iteratively. A method of overheating by a degree an hour above 26 ℃ was used to account for temperatures in excess of 26 ℃ and for the temperature magnitude when in excess of 26 ℃.

Table 5-1 Load cases sorted out with respect to increasing ΔT (outlet-inlet)

Load case	Δ*T*(outlet-inlet)	Inlet temp.	Outlet temp.	ACR	Heat load	Moisture load
[-]	[℃]	[℃]	[℃]	[h^{-1}]	[W/m^2]	[kg/kg]
1	3.2	23.4	26.6	7	20	0.20
2	4	22.8	26.8	5	20	0.28
3	5.7	21.4	27.1	7	40	0.20
4	6.6	20.7	27.7	3	20	0.46
5	7.9	19.7	27.6	5	40	0.28
6	8.5	19.2	27.7	7	60	0.20
7	11.9	**16.5**	28.4	5	60	0.28
8	13.2	**15.4**	28.6	3	40	0.46

In this section, some results obtained from the investigation are presented. Results should be used as guidance and indication of which of four systems have a potential to avoid overheating problems under certain load conditions.

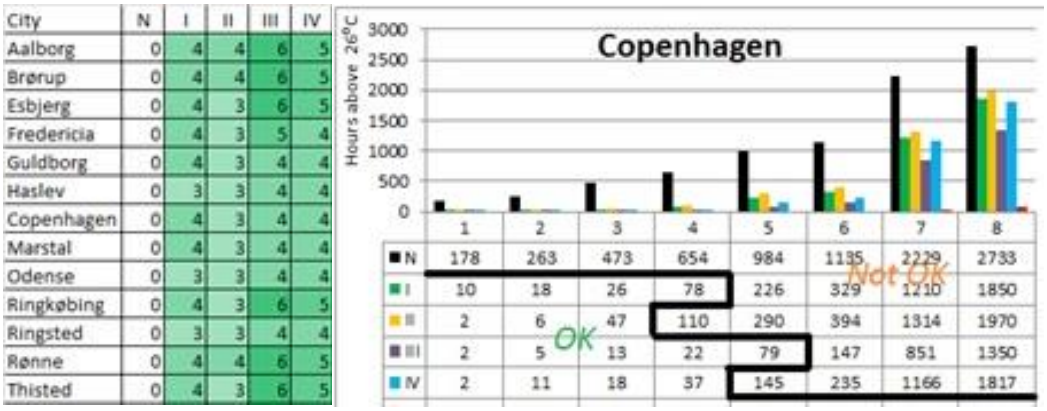

Fig. 5-3 Table indicating which system can maintain acceptable temperature up to which load case (left), example result of number of hours above 26 ℃ for Copenhagen city (right)

The results for 15 Danish cities are presented in Fig. 5-3 (table). The table indicates which system, where N is case with ventilation but without EC, can maintain acceptable temperatures for less than 100 h above 26 ℃ and up to which load case 1 to 8 shown in Table 5-1. Systems I, II, III, and IV perform similarly with System II having a slightly lower cooling capacity than System I. Additionally, System III has slightly higher capacity than system IV. On the right hand graph in Fig. 5-3, the number of hours when the temperature exceeds 26 ℃ is presented for each of the five systems and for weather conditions in Copenhagen. A bold line separates the cases that either fulfil or do not fulfill demand per Danish Building Regulations (maximum 100 h above 26 ℃).

5.3. Experimental results

In order to investigate real performance of evaporative cooling system, the DEC system presented in Fig. 5-4 was developed. In the system, three parts can be distinguished: climatic conditioner component that consists of heaters and humidifiers, the DEC component, and a straight duct with an orifice to measure air flow. In the climatic component, air from the laboratory was heated and humidified by heaters and humidifiers controlled by the Lab View program to obtain different climatic conditions. In the DEC component, air was cooled and humidified. The DEC coil was connected to a water system that was able to regulate water flow and temperature of the water that was sprayed onto the DEC pads. Wastewater dripping from the DEC coil was collected in a tank that was connected to a Brüel & Kjaer strain indicator to measure the mass of the waste and circulation water. Air temperature and humidity was measured before and after the DEC coil. The final component was equipped with an orifice and a ventilation fun to create and control airflow through the entire system.

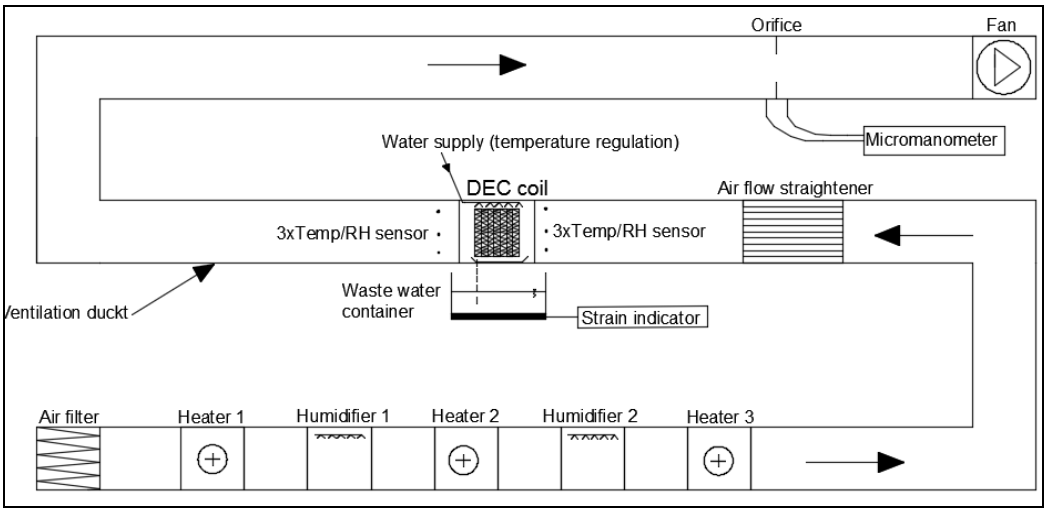

Fig. 5-4 DEC system connected

5.3.1. Sensitivity analysis of the system

In order to investigate sensitivity of the DEC system some parameters, such as air flow, water flow, and water temperature were varied. In the sensitivity analysis, the air flow parameter entering DEC coil was kept constant and for this analysis the 1% climatic cooling condition for Vienna was chosen (temperature at 29.8 ℃ and relative humidity at 41.6%).

For the DEC pad that was selected, the manufacturer's recommended air flow was 0.5 m^3/s and recommended water flow onto the pad is 0.22 m^3/h. It was decided to limit the air flow variation by ±0.1 m^3/s from the recommended air flow and to limit the water flow variation by 0.05 m^3/h from the recommended water flow. The results are listed as Table 5-2–Table 5-4. Water temperature to moisturize the DEC pad was set to following temperatures: 18 ℃, 22.5 ℃, 25.5 ℃, 28.5 ℃.

Table 5-2 Sensitivity analysis of the DEC system for an air flow of 0.4 m³/s

Air flow [m³/s]	0,40									
	Before DEC									
Air temperature [°C]	29,80									
Air humidity [%]	41,60									
Water temperature [°C]	18,00	22,50			25,50			28,50		
Water flow [m³/h]	0,22	0,17	0,22	0,27	0,17	0,22	0,27	0,17	0,22	0,27
	After DEC									
Air temperature [°C]	24,00	24,40	24,50	24,60	24,90	25,00	25,10	25,20	25,20	25,40
Air humidity [%]	62,90	63,00	63,30	63,20	63,20	63,50	63,00	63,40	63,80	63,30
Efficiency [-]	47,40	47,20	48,10	47,80	48,00	48,40	47,80	47,20	48,50	46,70
Water waste [m³/h]	0,22	0,15	0,20	0,25	0,15	0,20	0,25	0,15	0,20	0,25
Fan electricity use (without DEC-with DEC [W]	72									
Q cooling [W]	2726	2538	2491	2444	2303	2256	2209	2162	2162	2068
COP	38	35	34	34	32	31	31	30	30	29
Point on Mollier chart	**2**	**3**	**4**	**5**	**6**	**7**	**8**	**9**	**10**	**11**

Table 5-3 Sensitivity analysis of the DEC system for air flow of 0.5 m³/s (air and water parameters before the DEC are the same as Table 5-2)

Air flow [m³/s]	0,50									
	After DEC									
Air temperature [°C]	24,30	24,60	24,60	24,50	25,10	25,10	25,00	25,20	25,40	25,30
Air humidity [%]	62,20	62,10	62,00	62,20	62,30	62,30	62,50	62,80	62,30	62,60
Efficiency [-]	46,00	46,20	46,20	46,20	45,90	45,90	46,70	45,90	45,60	45,40
Water waste [m³/h]	0,22	0,15	0,20	0,25	0,15	0,20	0,25	0,15	0,20	0,25
Fan electricity use (without DEC-with DEC [W]	109									
Q cooling [W]	3231	3055	3055	3114	2761	2761	2820	2702	2585	2644
COP	45	42	42	43	38	38	39	37	36	37
Point on Mollier chart	**2**	**3**	**4**	**5**	**6**	**7**	**8**	**9**	**10**	**11**

Table 5-4 Sensitivity analysis of the DEC system for air flow of 0.6 m³/s (air and water parameters before the DEC are the same as Table 5-2)

Air flow [m³/s]	0,60									
	After DEC									
Air temperature [°C]	24,30	24,70	24,80	24,80	25,10	25,10	25,10	25,30	25,20	25,30
Air humidity [%]	61,70	61,20	61,60	61,90	61,40	61,80	61,90	61,40	61,90	62,00
Efficiency [-]	46,50	44,30	45,00	45,50	44,60	44,80	45,50	44,90	44,60	45,50
Water waste [m³/h]	0,22	0,15	0,20	0,25	0,15	0,20	0,25	0,15	0,20	0,25
Fan electricity use (without DEC-with DEC [W]	145									
Q cooling [W]	3877	3595	3525	3525	3313	3313	3313	3172	3243	3172
COP	54	50	49	49	46	46	46	44	45	44
Point on Mollier chart	**2**	**3**	**4**	**5**	**6**	**7**	**8**	**9**	**10**	**11**

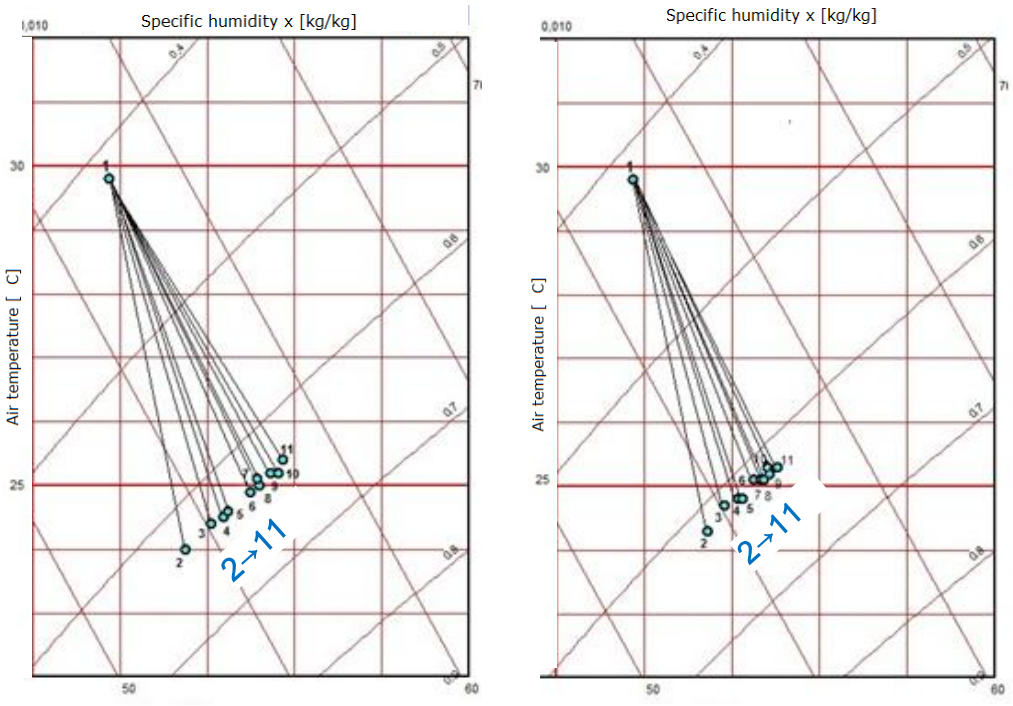

(a) (b)

Fig. 5-5 Test results of the DEC processes: (a) air flow of 0.4 m ³/s and (b) airflow of 0.6 m ³/s.

From the investigation, it can be concluded that the recommended water flow for the chosen DEC pads is too high for the climatic conditions in Vienna. Approximately one tenth of the recommended water flow should be sufficient and not result in decreased cooling capacity. Additionally, for airflow rates varying between 0.4 and 0.6 m ³/s, water consumption in the DEC is constant and independent of airflow. Finally, the COP of the system increases with an increased airflow from 0.4 to 0.6 m ³/s. For this study, the COP varied between 29 and 54 and the highest COP was obtained for the lowest water temperature. Therefore, when the water temperature is relatively high the COP will be at the low end of the range.

It can be concluded that optimum airflow for which the COP would begin to decrease due to excessive fan electricity consumption was not reached based on the investigation. Additionally, from the measurements it can be observed that the efficiency of the DEC system is almost insensitive when the design parameters were varied during the test runs. It can then be concluded that the COP of the system is mostly dependent on the pressure loss across the pad and the power consumption of the fan.

It appears that system performance is sensitive to the water temperature. In the study, the lowest water temperature used was 18 ℃, which is still a relatively high temperature in many climates. The sensitivity analysis indicated that the lower temperature the more cooling occurs through indirect evaporative cooling (IEC). It can be clearly observed that the Δx between the air before and after the DEC decreases as the water temperature deceases.

5.3.2. Experimental investigation of Climatic Potential of DEC system

In this chapter, the cooling performance of a DEC system under different climatic condition is presented. In this study, nine European cities were chosen as shown in Table 5-5. Climatic condition representing the 1% climatic cooling condition for each of the nine cities was reproduced in the set up presented in Fig. 5-4. For the climatic investigation, the water temperature was maintained at 18 ℃. The thickness of the DEC pads was 10 cm and the airflow was at 1.0 m ³⁄s.

Table 5-5 Climatic performance of a DEC in 9 European cities

	Helsinki	Copenhagen	Geneva	London	Dublin	Amsterdam	Bucharest	Vienna	Palermo
	Before DEC								
Air temperature [°C]	24,9	23,9	29	25,2	21	25,3	31,8	29,9	31,7
Air humidity [%]	39,6	49,1	30,3	45,4	65,4	51,8	31,6	42	43,9
After DEC									
Air temperature [°C]	20,4	20,8	21,6	21,5	20,2	22,4	25,8	25,1	26,3
Air humidity [%]	65,7	66,4	62,6	62	73,9	67,2	57,8	60,5	63,6	
Efficiency [-]	52,4	40,3	64	41,2	37	39	51,3	41,3	45,9
Water use [m³/h]	0,015	0,014	0,020	0,013	0,010	0,014	0,024	0,019	0,018
Fan electricity use (without DEC-with DEC [W]	602								
Q cooling [W]	5378	3718	8719	4418	969	3461	7000	5638	6303
COP	8,9	6,2	14,5	7,3	1,6	5,8	11,6	9,4	10,5
Point on Mollier chart	**1-2**	**3-4**	**5-6**	**7-8**	**9-10**	**11-12**	**13-14**	**15-16**	**17-18**

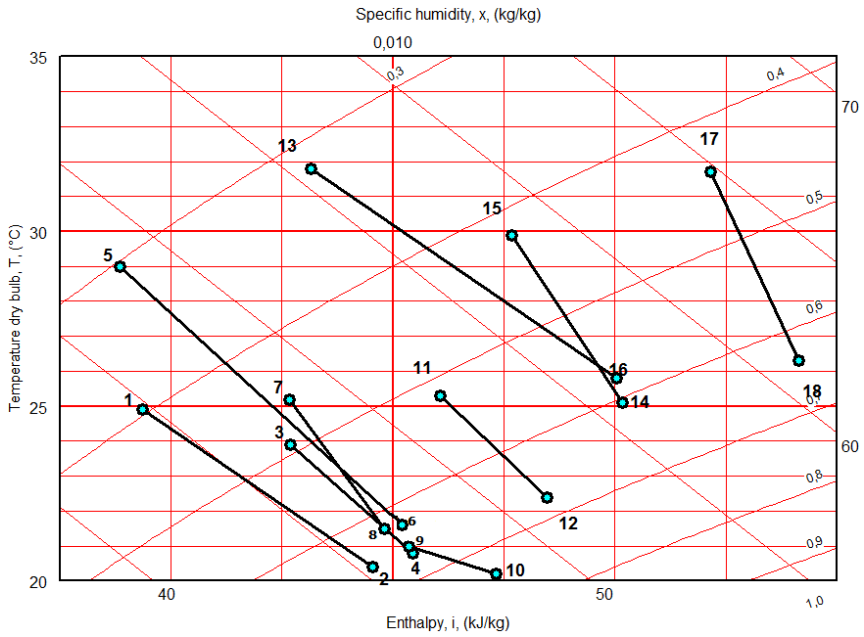

Fig. 5-6 The DEC process presented in a psychrometric chart for nine European cities.

The same cooling process was applied to nine climates and as can be observed in Table 5-5 and Fig. 5-6, performance of the system is significantly different depending on the initial climatic conditions. The system COP varies from 1.6 (Dublin) to 14.5 (Geneva). What is more,

for Bucharest, Vienna and Palermo the DEC used by itself would probably not be a suitable solution for cooling. However, the DEC could be used to precool air that would be further cooled in the coil connected to chiller, or in combination with IEC. With regards to water consumption, it can be concluded that this would vary significantly depending on the climate. For example in Dublin, water consumption would be 2 times less than in Geneva. However, this difference in water consumption would not compensate for a much lower system COP.

5.4. Conclusion

Evaporative cooling appears to be a promising cooling solution compared to traditional compressor based cooling systems. Cooling is obtained even at high water temperatures that can equal the dry bulb air temperature of cooled air. What is more, as presented in this section, the combination of a DEC and an IEC as well as a desiccant system could result in system that would successfully provide indoor thermal comfort even in very hot and humid climates. For less demanding climates, a DEC or IEC either by itself or combined together could provide the required cooling output for most load cases. Experimental study has proven that a DEC alone could be used for many European climatic conditions resulting in very high COP. For more hot and humid climates, a system using precooling or a supporting cooling system would be a better solution. When considering a DEC as a cooling system, it is necessary to determine its technical and economic potential relative to the design climatic cooling conditions it will be required to operate.

6. Conclusions

The original intention of supplying outdoor air is to meet occupants' health needs and requirements. Due to different indoor air conditions, outdoor air may increase cooling/heating and dehumidifying/humidifying loads. Furthermore, the supplied outdoor air can also help removing indoor moisture. Outdoor air handling processes or air humidity handling processes are a key issue in achieving high temperature cooling and low temperature heating in buildings. The task of choosing the appropriate approaches for humid air handling process; how to evaluate the energy performance of various air handling processors; and how to improve the processors' performances are discussed in detail in Annex 59.

Various kinds of devices can be used to handle outdoor air and different natural resources can be utilized for different climate regions. Heat recovery devices including the sensible heat recovery type and the enthalpy recovery type are a feasible solution to reduce the handling loads for an entire air-conditioning system. Evaporative cooling is a recommended approach for cooling the dry, outdoor air. Condensation dehumidification and desiccant

dehumidification are common choices for air dehumidification in summer. Many kinds of air handling processes can be constructed and investigated to provide adequate solutions.

To evaluate the energy performance of different air handling processes, the COP was chosen as the index for comparison. The COP is defined as the obtained heat/cooling capacity divided by the input power consumption. For a plate enthalpy exchanger, for example, the input power consumption is the fan. However, for systems which use compressors, the consumption includes the compressor's power used for a powering a heat pump that drives a liquid desiccant air handling processor. The appropriateness of heat recovery devices in typical cities based on the COP index systems was investigated. Experimental results for different air handling processes were also obtained to determine their performance discrepancies.

For different humid air handling approaches, performance-improving solutions were analyzed. To improve the energy performance of the air handling process using solid or liquid desiccant, it is recommended the air handling process proceed along the iso-concentration line (or iso-relative humidity line) rather than the isenthalpic line. Constructing a multi-stage process for the humid air handling process is a feasible approach to increase the required cooling source temperature (for condensation dehumidification method) or lower the required regeneration heating source temperature (for desiccant dehumidification method).

Appendix A: Outdoor air conditions

In Table A-1 are given summer outdoor cooling design condition for 0.4, 1 and 2 annual percentiles. Use of annual percentile to define design conditions ensures the same probability of occurrence in any climate. For more information about climatic design condition please refer to ASHRAE FUNDAMENTALS.

Table A-1 Outdoor cooling design condition of cities in Europe.

	Summer outdoor design					
	0.4%		**1%**		**2%**	
City	**Dry Bulb Temperature**	**Rel. Hum.**	**Dry Bulb Temperature**	**Rel. Hum.**	**Dry Bulb Temperature**	**Rel. Hum.**
Vienna	31,5	37,1	29,8	41,6	28,2	44,6
Vienna	30,6	37,9	28,9	41,2	27,3	43,5
Vienna	30,9	30,3	29,0	35,8	27,2	40,5
Innsbruck	30,0	25,0	28,1	29,0	26,5	32,3
Linz	30,2	33,4	28,6	34,6	26,9	39,4
Linz	30,4	39,7	28,6	42,2	27,0	46,0
Salzburg	30,1	29,2	28,2	33,3	26,7	37,6
Graz	30,5	33,1	28,8	39,7	27,1	43,2
Brussels	29,1	38,7	27,0	46,7	24,1	58,4
Oostende	25,9	52,0	23,6	62,6	22,0	68,3
Saint Hubert	25,2	43,7	23,6	48,6	22,0	52,2
Plovdiv	34,2	17,9	32,6	24,3	31,0	28,5
Sofia	32,0	14,3	30,0	23,0	28,2	29,1
Varna	31,0	43,1	29,3	50,6	28,1	53,6
Banja	32,9	26,0	31,0	33,1	29,2	36,8
Minsk	28,2	34,7	26,8	38,5	25,0	44,2
Geneva	30,8	24,2	29,0	30,3	27,2	36,9
Larnaca	34,1	26,5	33,1	34,6	32,1	42,4
Ostrava	30,0	32,4	28,0	37,3	26,2	42,1
Prague	29,2	29,2	27,1	36,0	25,3	41,6
Prague	29,6	29,1	27,7	36,2	26,0	41,1
Prague	30,1	25,1	28,1	31,8	26,3	36,4
Berlin	29,3	30,1	27,3	35,6	25,6	39,8
Berlin	29,6	28,5	27,7	34,0	25,8	40,1
Berlin	30,0	24,3	28,0	30,2	26,2	34,0
Berlin	30,0	25,7	28,0	31,6	26,2	37,0
Bremen	28,4	37,8	26,4	42,3	24,5	47,4
Dusseldorf	29,6	32,5	27,8	36,3	26,1	40,5
Frankfurt	30,8	23,5	28,9	30,2	27,1	36,0
Hamburg	27,8	37,7	25,9	43,2	24,0	48,3

Koln	29,9	30,3	28,0	35,2	26,1	39,7
Munich	29,5	29,0	27,7	32,6	26,1	37,5
Munich	29,4	28,8	27,6	33,9	25,9	40,2
Stuttgart	29,3	29,4	27,6	35,3	25,8	40,8
Stuttgart	29,6	32,5	27,8	35,6	26,1	40,5
Copenhagen	25,5	44,1	24,0	49,1	22,2	54,9
Barcelona	30,2	57,6	29,1	62,8	28,2	64,2
Madrid	36,2	1,1	34,9	4,8	33,3	7,6
Madrid	36,8	0,9	35,1	5,2	33,8	7,2
Palma	33,2	35,3	31,9	42,8	30,6	48,6
Santander	26,0	52,1	24,4	62,5	23,4	67,1
Sevilla	39,9	10,1	38,0	11,2	36,1	15,3
Valencia	33,1	26,3	31,7	36,7	30,2	46,2
Helsinki	26,7	36,9	24,9	39,6	23,2	44,2
Tampere	26,7	31,9	24,9	38,1	23,0	43,1
Bordeaux	32,8	27,8	30,8	33,5	28,9	39,2
Brest	26,0	49,2	23,8	58,1	21,9	64,2
Clermont-Ferrand	32,1	25,5	30,0	32,4	28,1	38,8
Dijon	31,2	29,4	29,3	36,2	27,8	40,5
Lyon	33,6	13,8	31,7	22,3	30,0	28,4
Lyon	32,4	22,7	30,7	28,7	28,9	35,0
Montpellier	32,1	28,7	30,8	34,2	29,2	38,9
Nancy	30,7	30,7	28,8	36,3	27,0	43,1
Nancy	30,2	29,3	28,2	34,7	26,6	39,7
Nantes	30,8	32,2	28,9	38,5	26,9	43,7
Nice	29,5	55,6	28,5	59,5	27,7	62,4
Paris Orly	30,9	29,0	28,9	35,7	27,0	40,9
Strasbourg	31,1	33,3	29,2	38,2	27,6	43,1
Aberdeen	21,9	60,2	20,2	63,5	18,8	66,5
Aughton	24,4	49,6	22,4	55,9	20,6	62,2
Belfast	22,6	56,1	20,9	63,3	19,4	67,0
Birmingham	26,7	36,9	24,5	43,6	22,8	50,0
Finningley	26,1	40,5	24,2	46,3	22,4	51,9
Hemsby	23,7	57,2	22,1	62,8	20,7	66,5
Leuchars	22,2	53,3	20,6	57,2	19,2	61,6
London Gatwick	27,2	39,8	25,2	45,2	23,8	49,6
Oban	23,0	49,4	21,0	55,1	19,2	61,6
Andravida	33,1	30,1	31,9	35,6	30,8	40,8
Athens	35,1	15,0	33,8	19,1	32,4	26,6
Thessaloniki	34,1	22,7	32,8	29,1	31,2	33,4
Debrecen	31,7	32,8	30,0	36,5	28,4	42,0
Szombathely	31,2	31,4	29,2	38,2	27,6	42,4
Belmullet	21,3	67,8	19,3	75,6	18,1	79,2

Birr	23,8	51,2	21,9	59,4	20,4	63,7
Clones	23,0	58,9	21,2	62,8	19,8	67,4
Dublin	22,1	60,4	20,7	64,8	19,5	68,8
Kilkenny	24,1	51,5	22,4	56,7	20,9	61,7
Malin	19,8	71,6	18,5	76,8	17,4	79,7
Valentia Observatory	21,6	64,8	19,9	70,8	18,6	76,8
Reykjavik	16,0	64,7	14,9	68,4	14,0	71,5
Jerusalem	32,9	10,1	31,2	16,9	30,1	20,4
Brindisi	32,6	43,6	31,0	56,3	29,9	62,1
Genova	29,9	54,6	28,9	62,7	28,0	66,9
Messina	32,8	42,5	31,3	50,6	30,3	56,3
Milan	33,0	44,0	31,6	45,7	30,2	48,2
Milan	31,9	38,9	30,6	42,6	29,2	45,0
Naples	33,5	38,2	32,1	43,0	31,0	47,0
Palermo	33,5	30,0	31,6	43,7	30,1	59,5
Pisa	32,2	34,7	31,0	39,7	29,9	44,5
Rome	31,0	46,4	30,0	52,7	29,0	58,6
Rome	33,2	29,0	32,1	33,3	30,9	37,6
Torino	28,2	46,0	27,1	49,0	25,9	52,7
Torino	31,0	44,4	29,8	47,1	28,3	50,3
Venice	31,1	50,4	29,9	54,0	28,8	55,6
Kaunas	27,8	38,4	26,1	43,4	24,4	46,5
Amsterdam	27,8	43,4	25,6	51,7	23,7	56,5
Groningen	28,2	43,2	25,9	51,3	23,7	58,0
Bergen	23,0	43,9	21,0	52,7	19,1	58,9
Bergen	24,2	42,4	22,3	48,6	20,5	53,7
Oslo Fornebu	26,8	35,6	25,0	40,5	23,2	43,4
Kolobrzeg	26,2	42,1	23,8	54,3	22,0	64,3
Krakow	29,7	36,8	27,8	42,7	25,9	46,1
Poznan	30,0	27,7	28,0	32,3	26,2	37,7
Warsaw	29,6	35,3	27,6	41,0	25,9	43,2
Braganca	33,6	5,0	31,8	10,7	30,1	15,7
Coimbra	33,7	22,1	31,3	30,2	29,2	37,5
Evora	35,7	5,6	33,7	9,6	31,8	15,9
Evora	37,8	-5,5	36,0	-0,5	34,1	5,2
Faro	31,9	24,6	30,2	33,4	29,0	38,6
Lajes	27,0	64,0	26,1	66,2	25,2	68,4
Porto	26,0	66,1	25,2	67,7	24,8	68,2
Bucharest	33,2	28,4	31,8	31,6	30,1	35,3
Bucharest	33,8	22,3	32,0	29,3	30,2	33,4
Cluj-Napoca	30,0	35,8	28,4	38,5	26,8	43,6
Constanta	29,7	59,9	28,2	63,5	27,1	65,5
Craiova	33,4	31,8	31,8	36,8	30,1	41,3

Galati	32,4	34,3	30,8	37,5	29,3	41,7
Timisoara	33,5	23,1	31,9	27,8	30,0	33,1
Arhangelsk	27,0	43,8	24,8	47,8	22,7	53,0
Moscow	28,4	42,7	26,6	49,1	25,0	51,8
Saint-Petersburg	27,3	42,0	25,5	46,4	23,8	50,4
Samara	31,5	25,9	29,6	32,5	27,8	37,7
Belgrade	33,7	22,1	32,1	27,4	30,4	31,6
Belgrade	33,8	25,4	32,0	32,5	30,1	38,0
Podgorica	36,0	15,8	34,8	21,3	33,1	26,9
Bratislava	32,0	26,0	30,1	32,6	28,5	35,9
Kosice	30,0	35,1	28,3	40,5	26,6	44,0
Ljubljana	30,2	34,0	28,8	39,0	27,0	43,8
Ljubljana	31,3	30,9	29,6	35,3	28,0	39,4
Goteborg Landvetter	26,0	33,0	24,1	39,2	22,3	43,8
Karlstad	25,7	41,4	24,0	47,5	22,2	50,8
Kiruna	22,0	36,1	20,0	43,0	18,0	49,7
Ostersund Froson	23,9	35,9	21,9	40,8	20,0	48,9
Stockholm Arlanda	27,1	31,7	25,2	37,0	23,2	42,6
Damaskus	39,1	-16,8	37,8	-13,6	36,2	-9,1
Istanbul	31,1	36,6	30,0	41,9	28,9	45,4
Izmir	36,2	14,9	34,9	19,0	33,8	21,6
Izmir	37,0	5,4	35,5	8,9	34,2	12,9
Kiev	29,4	36,4	27,8	40,5	26,2	45,0
Odessa	31,2	28,1	29,8	33,5	28,0	40,1

Fig. A-1. Map indicating location of cities listed in Table A-1.

Table A-2 Outdoor design condition of cities in China

Cities	Summer outdoor design		Winter outdoor design (AC)	
	Dry bulb Temperature ℃	Humidity ratio g/kg	Dry bulb Temperature ℃	Humidity ratio g/kg
Beijing	33.5	19.3	-9.9	0.70
Tianjin	33.9	19.7	-9.6	0.91
Shijiazhuang	35.1	19.4	-8.8	0.97
Taiyuan	31.5	17.5	-12.8	0.67
Hohhot	30.6	13.8	-20.3	0.41
Shenyang	31.5	18.2	-20.7	0.35
Changchun	30.5	17.1	-24.3	0.28
Harbin	30.7	16.5	-27.1	0.23
Shanghai	34.4	21.5	-2.2	2.32
Nanjing	34.8	21.7	-4.1	2.01
Hangzhou	35.6	21.1	-2.4	2.33
Hefei	35	21.7	-4.2	2.00
Fuzhou	35.9	21.3	4.4	3.82
Nanchang	35.5	21.8	-1.5	2.55
Jinan	34.7	19.5	-7.7	1.03
Zhengzhou	34.9	20.7	-6	1.38

Wuhan	35.2	22.2	-2.6	2.31
Changsha	35.8	20.7	-1.9	2.65
Guangzhou	34.2	21.4	5.2	3.91
Haikou	35.1	21.7	10.3	6.66
Nanning	34.5	21.7	5.7	4.43
Chengdu	31.8	21.2	1	3.54
Chongqing	35.5	19.5	2.2	3.79
Guiyang	30.1	17.4	-2.5	2.77
Kunming	26.2	16.0	0.9	3.42
Lhasa	24.1	10.8	-7.6	0.86
Xi'an	35	18.5	-5.7	1.59
Lanzhou	31.2	13.3	-11.5	0.90
Xining	26.5	11.6	-13.6	0.68
Yinchuan	31.2	15.6	-17.3	0.51
Urumchi	33.5	8.4	-23.7	0.38

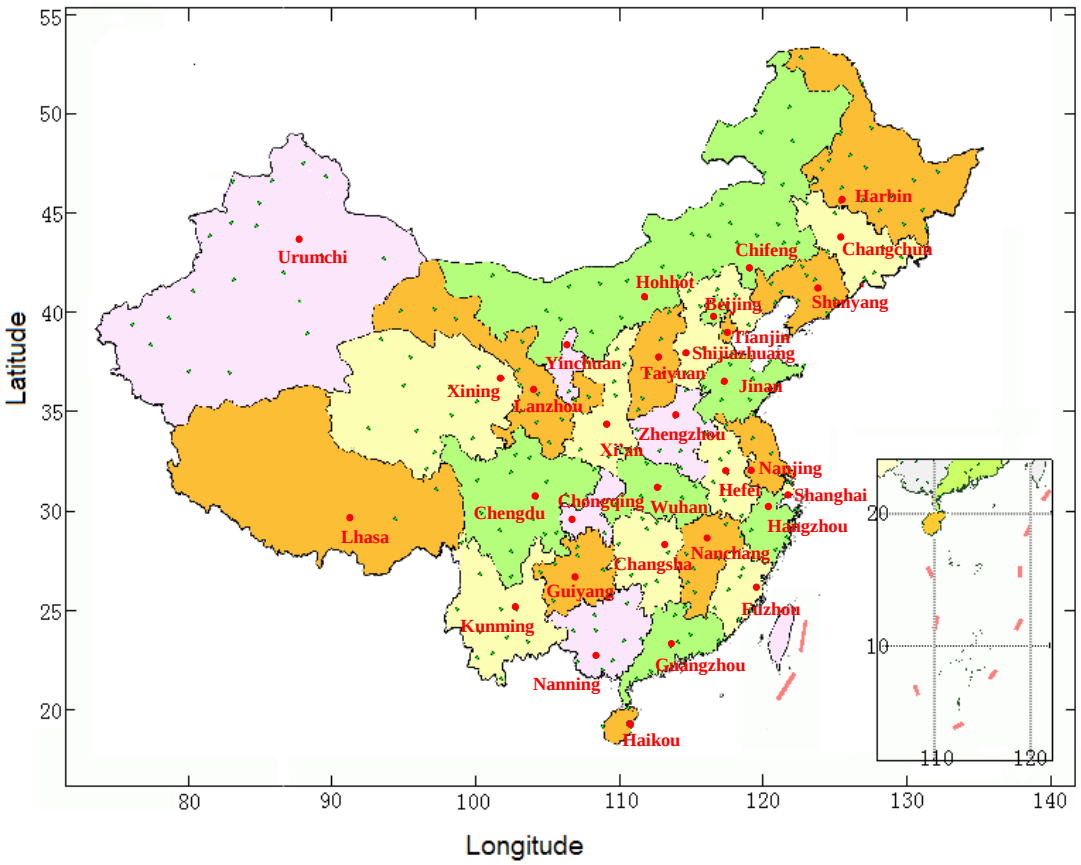

Fig. A-2 Cities' locations on map of China.

Appendix B: Dehumidification desiccant wheel model

B.1 Solid desiccant material

Solid desiccant material can be used to adsorb water vapor molecules in the air to achieve dehumidification, and the water vapor pressure difference between the air and the desiccant surface is the driving force for this moisture transfer process. Adsorption isotherms can indicate adsorbing characteristics of desiccant materials, and they can be divided into different types (as shown in Fig. B-1): Type I (including IE and IM), type II, and type III (including IIIE and IIIM). For dehumidification processes using desiccant wheels, desiccant materials with adsorption isotherms of type I and II are usually preferred.

Solid desiccant materials commonly used for dehumidification include silica gel, activated aluminum oxide, molecular sieves, calcium chloride, zeolite, etc. When the solid desiccant and humid air reach equilibrium, their water vapor pressures are identical. The state of the desiccant can be represented in a psychrometric chart according to the equilibrium of the air state with the desiccant. Fig. B-2depicts the states of RD silica gel in a psychrometric chart. It can be observed that, for the iso-water-content line, lowering the temperature helps to lower the vapor pressure and strengthen its adsorption ability. In the process of dehumidification, the driving force for mass transfer is the vapor pressure difference between the desiccant and the air. Reducing the desiccant's temperature and water content helps to increase the mass transfer driving force. The regeneration process is similar to the dehumidification process, but with an opposite mass transfer direction.

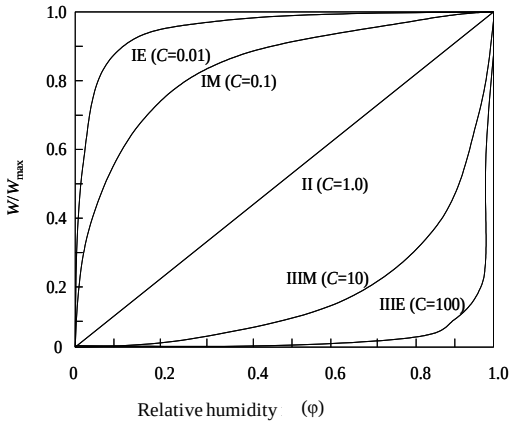

Fig. B-1 Adsorption isotherms of ideal adsorbents [reference].

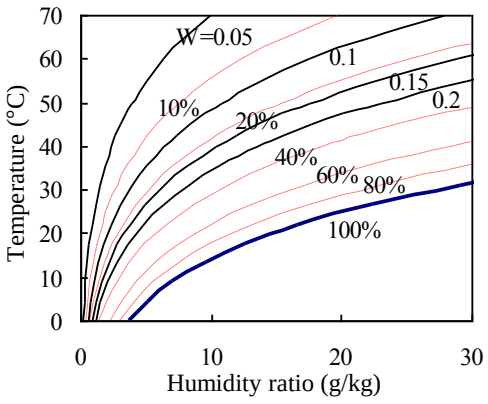

Fig. B-2 Usual solid desiccant states shown in air psychrometric chart (RD silica gel)

B.2 Model introduction and experiment validation

The model in this study belongs to the second type of desiccant wheel model, in which D_A and D_S are considered at the same time. Heat and mass transfer processes between the air and the solid with a honeycomb structure are simulated. The control unit of the desiccant

wheel in the mathematical model is shown in Fig. B-3. The model is set up based on the following assumptions: 1) the axial heat conduction and mass diffusion in the air flow are neglected; 2) the channels are equal and uniformly distributed throughout the wheel; 3) the thermodynamic properties in the solid are constant and uniform; and 4) the desiccant and substrate are the same temperature in the wall thickness direction.

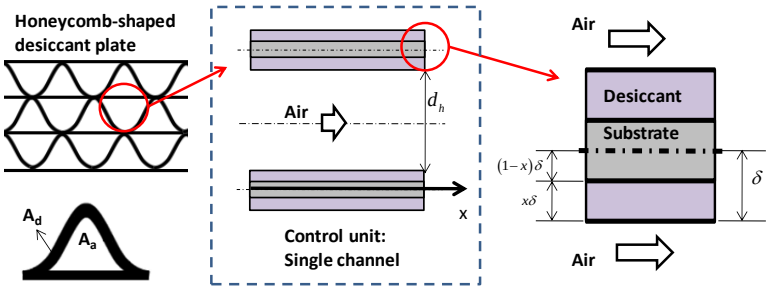

Fig. B-3 Control unit of the desiccant wheel in the mathematical model.

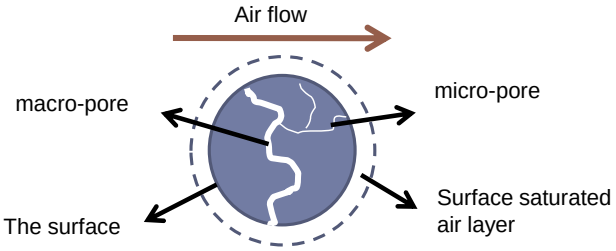

Fig. B-4 Mass transfer between air flow and silica gel.

Energy conservation and mass conservation of the air are as follows:

$$\frac{1}{u_a}\frac{\partial T_a}{\partial \tau}+\frac{\partial T_a}{\partial z}=\frac{4h}{\rho_a c_{pa} u_a d_h}\left(T_d-T_a\right) \tag{B-1}$$

$$\frac{1}{u_a}\frac{\partial Y_a}{\partial \tau}+\frac{\partial Y_a}{\partial z}=\frac{4h_m}{\rho_a u_a d_h}\left(Y_d-Y_a\right) \tag{B-2}$$

where T_a and T_d are the temperatures of the main stream air and the desiccant material, respectively; Y_a and Y_d are the humidity ratio of the main stream air and the equilibrium humidity ratio of the desiccant, respectively; d_h is the hydraulic diameter of the honeycombed channel; u_a is the face velocity of the air; and h and h_m are the convective heat transfer coefficient and the convective mass transfer coefficient, respectively. As indicated in the two conservation equations, the air states vary with the wheel's angle (expressed by τ) and the wheel thickness direction (z direction).

Energy conservation and mass conservation of the desiccant plate are

$$\rho_d\left(c_{pd}+\frac{\rho_{ad}x}{\rho_d}c_{pw}W\right)\frac{\partial T_d}{\partial \tau}+x\rho_{ad}c_{pw}T_d\frac{\partial W}{\partial \tau}=k_d\frac{\partial^2 T_d}{\partial z^2}+r_s\rho_{ad}x\frac{\partial W}{\partial \tau}+\frac{4h}{d_h f}\left(T_a-T_d\right) \tag{B-3}$$

$$\varepsilon\rho_a \frac{\partial Y_d}{\partial \tau} + \rho_{ad} \frac{\partial W}{\partial \tau} = \rho_a \varepsilon D_A \frac{\partial^2 Y_d}{\partial z^2} + \rho_{ad} D_S \frac{\partial^2 W}{\partial z^2} + \frac{4h_m}{x d_h f}\left(Y_a - Y_d\right) \tag{B-4}$$

Where ρ_d and c_{pd} are the equivalent density and the heat capacity of the solid, respectively, i.e., the weighted values of the substrate (subscript *m*) and the desiccant material (subscript *ad*), respectively, calculated by Eqs. (B-5) and (B-6), respectively; *x* is the volume ratio of the desiccant material in the solid, which is combined with the substrate and desiccant material; and *f* is the frontal area ratio of the solid and air in the control unit, calculated by Eq. (B-7). k_d is heat conductivity, and substrate and desiccant material are assumed of the same heat conductivity.

$$\rho_d = x\rho_{ad} + \left(1-x\right)\rho_m \tag{B-5}$$

$$c_{pd} = xc_{pad} + \left(1-x\right)c_{pm} \tag{B-6}$$

$$f = \frac{A_d}{A_a} \tag{B-7}$$

Gas diffusion D_A and surface diffusion D_S are calculated by the following equations (Majumdar, 1988):

$$D_A = \frac{\varepsilon}{\xi}\left(\frac{1}{D_{AO}} + \frac{1}{D_{AK}}\right)^{-1}, \text{ where } D_{AO} = 1.758\times10^{-4}\frac{T_d^{1.685}}{P_a}, D_{AK} = 97a\left(\frac{T_d}{M}\right)^{1/2} \tag{B-8}$$

$$D_S = \frac{1}{\xi} D_0 \exp\left(-0.974\times10^{-3} r_s / T_d\right) \tag{B-9}$$

A dehumidification desiccant wheel from a manufacturer is experimentally evaluated in labs. The experimental setup is shown in Fig. B-5. The diameter and thickness of wheel is 370mm and 200mm. A quarter of the wheel is for regeneration, and air flow rate of processed air and regeneration air are 610m^3/h and 170m^3/h, respectively. Integrating the wheel and air states of experiments into the mathematic model, and a comparison of the simulation results and the experimental results is shown in Fig. B-6. It can be seen that the simulation results accord well with the experimental results, and thus, this model can be adopted for further research on dehumidification wheels.

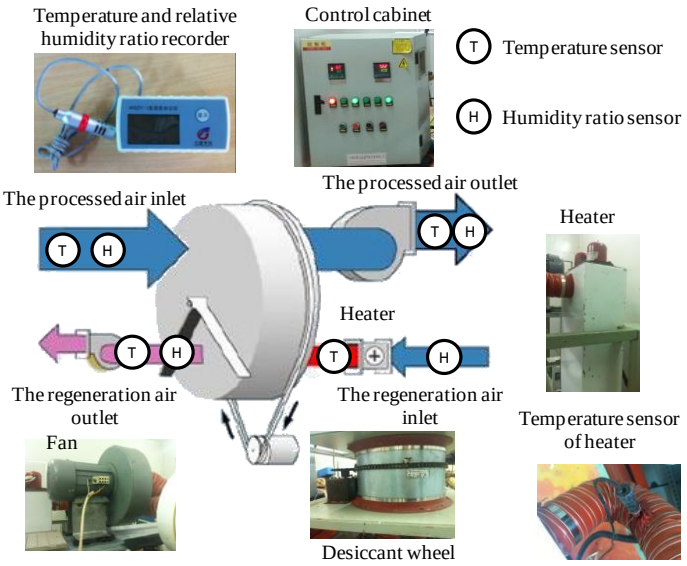

Fig. B-5 Experimental setup of desiccant wheel

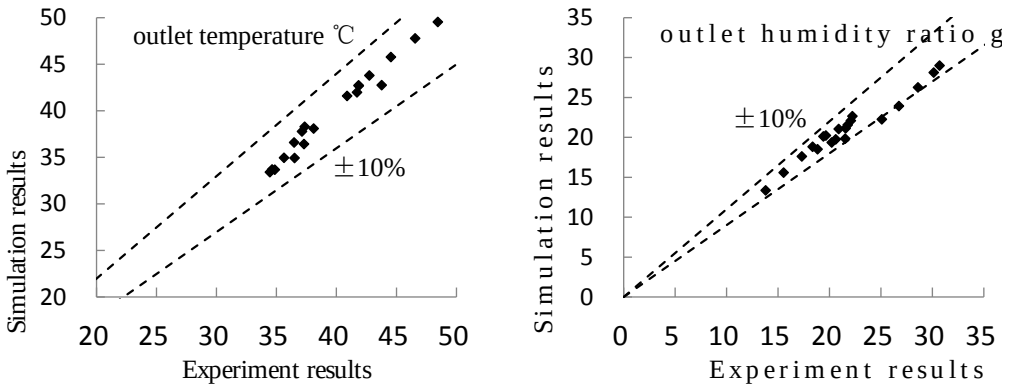

Fig. B-6 Comparison of experimental results and simulation results of the dehumidification wheel..

Appendix C: Liquid desiccant dehumidication model

C.1 Liquid desiccant material

The most common liquid desiccants used nowadays are lithium bromide (LiBr), lithium chloride (LiCl), and calcium chloride ($CaCl_2$) aqueous solutions. For these commonly used liquid desiccants, the boiling points of the solutes and water are rather different. Under atmospheric pressure, the boiling points of LiBr, LiCl, and $CaCl_2$ are all above 1200 ℃, while that of water is only 100 ℃. As a result, the vapor pressure of the salt solutions is approximately equal to the partial pressure of the water vapor. As the liquid desiccant makes direct contact with the air and reaches equilibrium, the temperature and the water vapor pressure of the solution are equal to those of the air. The equivalent humidity ratio of the solution is defined as the humidity ratio of the air in equilibrium with the solution state. The states of the solution can be represented in a psychrometric chart according to the states of the air in equilibrium with the aqueous solution. Fig. C-1(a)~(c) show the corresponding states of the LiBr, LiCl, and $CaCl_2$ aqueous solutions, respectively, where ξ represents the mass concentration of the solution (equal to the mass of solute divided by the mass of the solution), and φ represents the relative humidity of the air. As indicated by these figures, the lower the solution temperature, the lower its equivalent humidity ratio at the same desiccant concentration, and the stronger the dehumidification ability. Furthermore, the iso-concentration line of the solution almost coincides with the iso-relative humidity line of the moist air. For example, the concentrations with the iso-concentration lines of the LiBr solution, LiCl solution, and $CaCl_2$ solution corresponding to the 40% iso-relative humidity line of the moist air are 46%, 31%, and 40%, respectively. Due to the limitation of crystallization, the solution states cannot cover certain regions on the left side of the crystal line in the psychrometric chart. Among these three desiccants, the reachable air handling area of the $CaCl_2$ solution is the narrowest, while the LiBr and LiCl solutions can process the air to a similar lower humidity ratio. As a result, the dehumidification ability of the LiBr and LiCl solutions is better than that of the $CaCl_2$ solution.

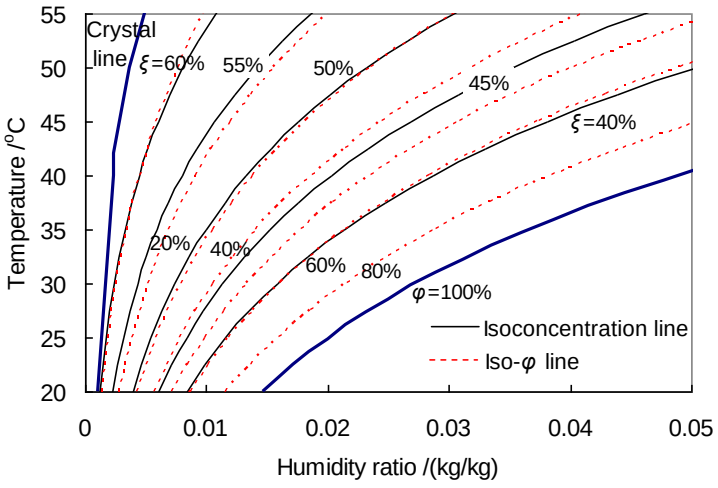

(a)

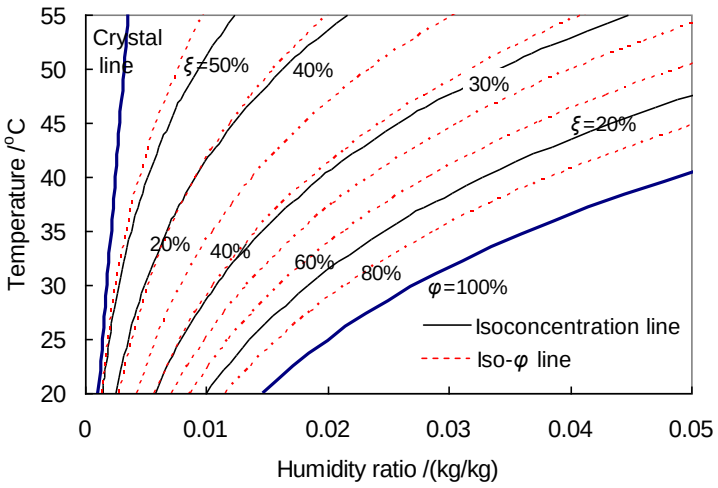

(b)

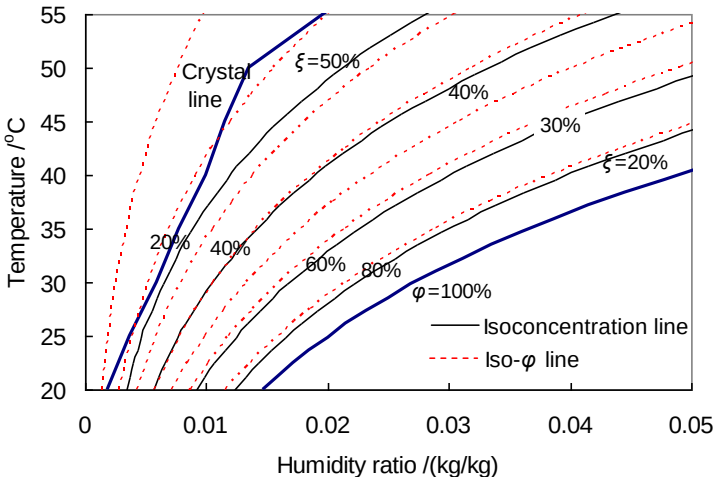

(c)

Fig. C-1 States of commonly used liquid desiccants shown in psychrometric chart: (a) LiBr aqueous solution; (b) LiCl aqueous solution; and (c) $CaCl_2$ solution.

C.2 Model and experiment validation

The schematics of parallel flow and counter flow packed bed dehumidifier or regenerator

are shown in Fig. C-2. Energy conservation and mass conservation relations are observed in the packed bed dehumidifier or regeneration.

The energy conservation equation is shown in Eq. (C-1), where m_a and m_s are the air and desiccant mass flow rates, respectively; h_a and h_s are the air and desiccant enthalpies, respectively. Desiccant enthalpy is the sum of the solute enthalpy, water enthalpy and the mixing heat when the solute and water are mixed.

$$\dot{m}_a \mathrm{d}h_a + \mathrm{d}(\dot{m}_s h_s) = 0 \tag{C-1}$$

Mass conservation relations include water content mass conservation and solute mass conservation, as shown in Eqs. (C-2) and (C-3), where ω_a is the air humidity ratio and X is the desiccant concentration

$$\dot{m}_a \mathrm{d}\omega_a + \mathrm{d}\dot{m}_s = 0 \tag{C-2}$$

$$\mathrm{d}(\dot{m}_s X) = 0 \tag{C-3}$$

The total energy transfer and mass transfer between the air and the liquid desiccant are shown as Eqs. (C-4) and (C-5), where H is the height of the dehumidifier/regenerator; and he and ω_e are the air enthalpy and air humidity ratio in equilibrium with the desiccant, respectively. The status of typical liquid desiccant in equilibrium with air is shown in the psychrometic chart, as indicated in Fig. C-1. The desiccant iso-concentration line is almost coincident with the air iso-relative humidity line

$$\frac{\partial h_a}{\partial z} = \frac{NTU \cdot Le}{H} \cdot \left[\left(h_e - h_a \right) + \lambda_{Ts} \left(\frac{1}{Le} - 1 \right) \cdot \left(\omega_e - \omega_a \right) \right] \tag{C-4}$$

$$\frac{\partial \omega_a}{\partial z} = \frac{NTU}{H} \cdot \left(\omega_e - \omega_a \right) \tag{C-5}$$

As indicated by the energy conservation and transfer Eqs. (C-1) and (C-4), the temperature changes alone cannot express the entire energy change, since vaporization latent heat is released or absorbed along with the mass transfer process. As indicated by the mass conservation and transfer Eqs. (C-2), (C-3) and (C-5), the humidity ratio difference (ω_a - ω_e) is the mass transfer driving force. The changes of ω_a can express the water content change in the air, yet the changes of ω_e cannot express the water content change in the desiccant. The water content change in the desiccant should be expressed by the change of desiccant mass flow rate or desiccant concentration.

The model is about the same for three flow patterns. Parallel flow and counter flow patterns can be calculated by one-dimensional model, while cross flow pattern by two-dimensional model, as shown in Fig. C-2.

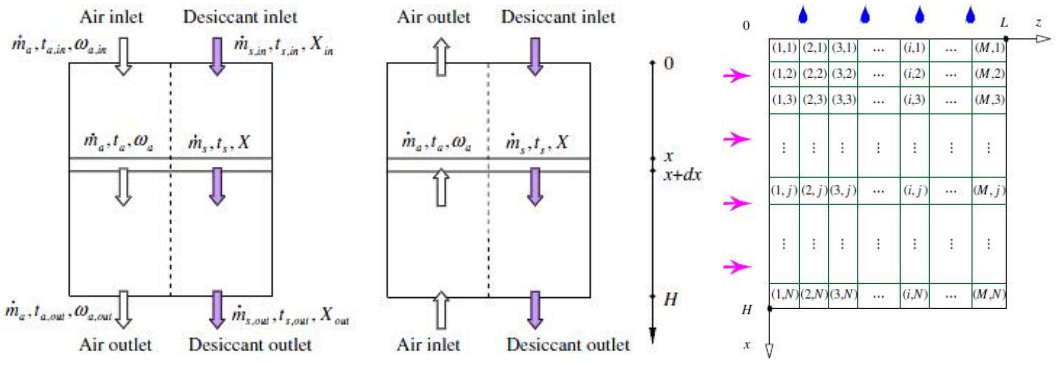

(a) (b) (c)

Fig. C-2 Model schematic of the three flow patterns.

I: cross flow experiments

The schematic of the cross-flow-pattern experimental setup is shown in Fig. C-3. The packed module was the core device of the setup, in which the cross flowing air and desiccant exchanged heat and moisture. The module used Celdek structured packing with the specific surface area of 396m^2/m^3. Its height, length and width were 0.55m, 0.40m and 0.35m, respectively. The air handling system, liquid desiccant system and cooling water system provided the air and desiccant to the packed module with certain parameters. The air handling system consisted of the cooling coil, the heater A, the humidifier and the fan. The liquid desiccant system consisted of solution tanks A and B, the solution pump, solution valve and heat exchanger. A lithium bromide aqueous solution was used as the desiccant in the system. The cooling water system supplied cooling water to the heat exchanger to adjust the desiccant temperature coming into the packed module.

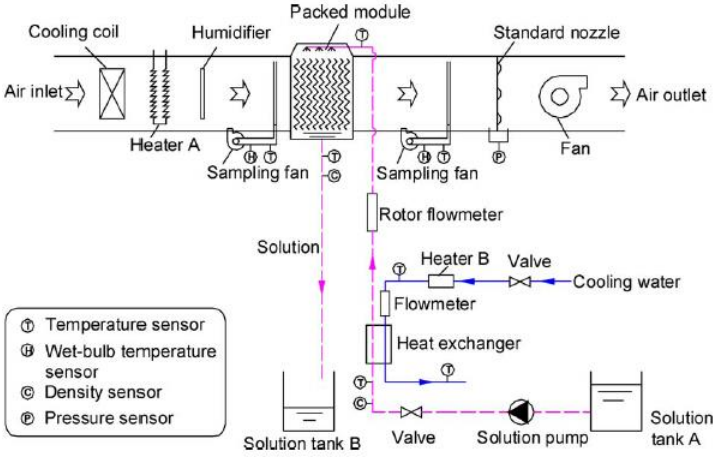

Fig. C-3 Schematic diagram of the cross flow pattern experimental rig.

Totally, 179 experimental runs were conducted with the following parameter ranges: air flow rate of 0.31–0.47kg/s, air inlet temperature of 24.7–33.9 ℃, air humidity ratio of

0.01–0.021kg/kg, desiccant flow rate of 0.30–0.64kg/s, desiccant inlet temperature of 20.1–29.5 ℃ and desiccant concentration of 42.6–48.3%.

Experiments are conducted aiming at researching influence of desiccant flow rate, air flow rate, desiccant inlet temperature and concentration, air inlet temperature and humidity ratio. The results are shown in . Moisture removal rate and dehumidifier effectiveness were used as the performance indices of the mass transfer process, calculated by Eqs. (C-6) and (C-7). It was found that the moisture removal rate increased with increasing air and desiccant flow rate, air inlet humidity ratio and desiccant inlet concentration; decreased with desiccant inlet temperature; and changed very little with air inlet temperature. The dehumidifier effectiveness increased with increasing desiccant flow rate and inlet temperature and decreased with air flow rate but was affected little by the other three inlet parameters, including the air inlet temperature and humidity ratio and desiccant inlet concentration.

$$m_w = G \cdot A \cdot (\omega_{a,in} - \omega_{a,out}) \tag{C-6}$$

$$\eta = \frac{\omega_{a,in} - \omega_{a,out}}{\omega_{a,in} - \omega_{e,in}} \tag{C-7}$$

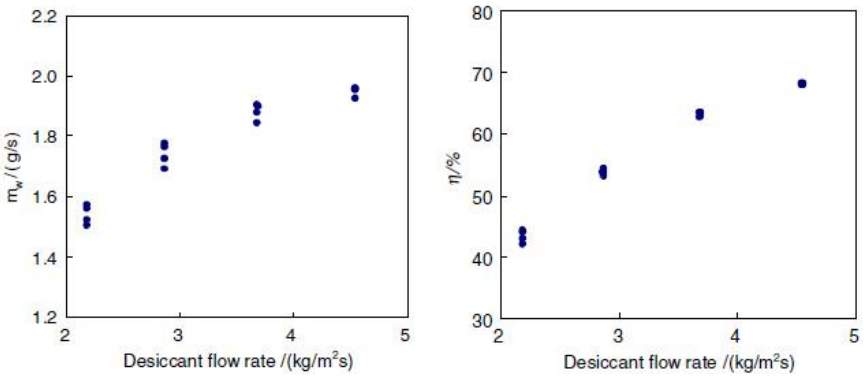

Fig. C-4 Effect of desiccant flow rate on moisture removal rate and dehumidifier effectiveness.

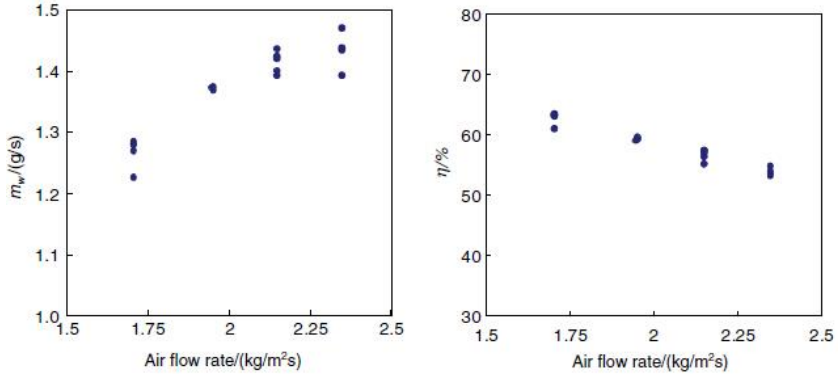

Fig. C-5 Effect of air flow rate on moisture removal rate and dehumidifier effectiveness

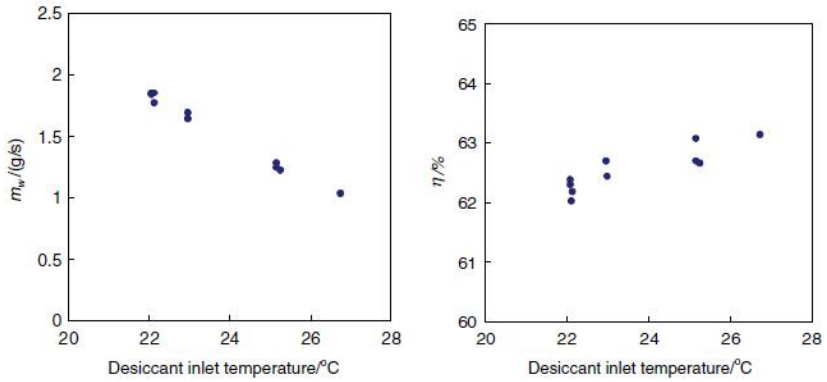

Fig. C-6 Effect of desiccant inlet temperature on moisture removal rate and dehumidifier effectiveness.

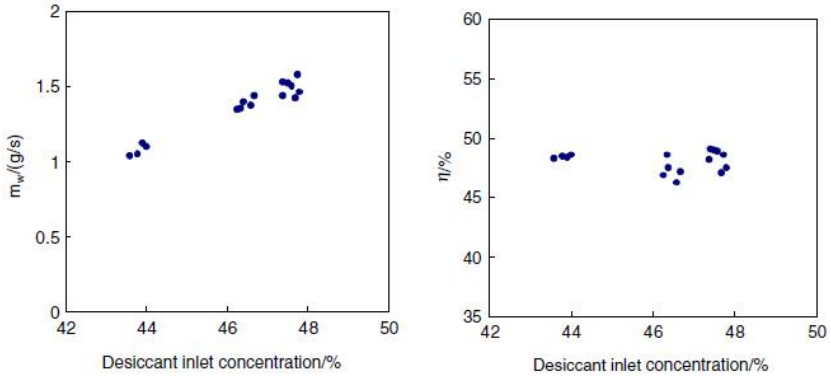

Fig. C-7 Effect of desiccant inlet concentration on moisture removal rate and dehumidifier effectiveness.

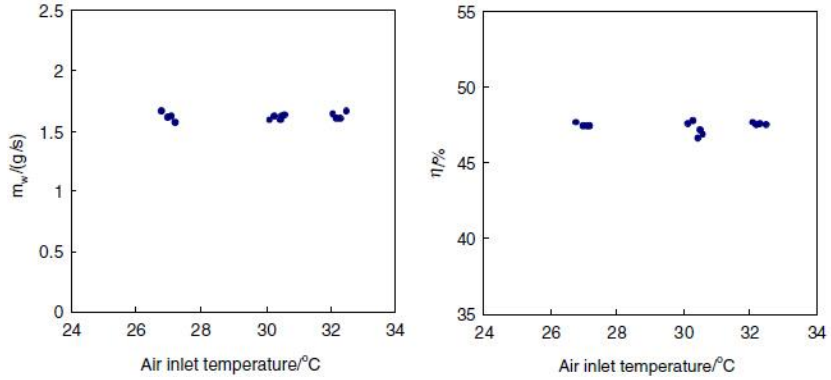

Fig. C-8 Effect of air inlet temperature on moisture removal rate and dehumidifier effectiveness.

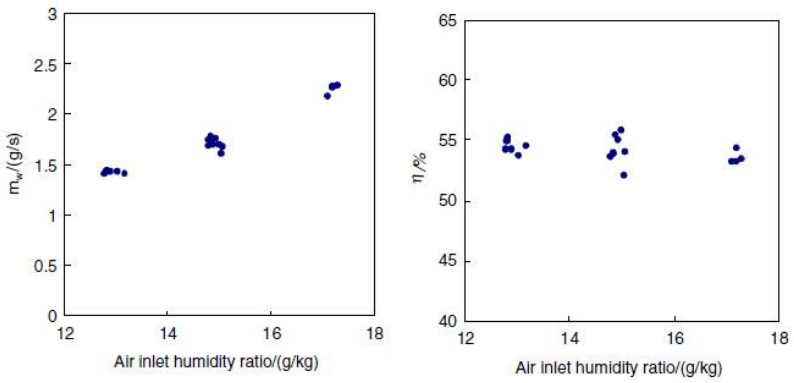

Fig. C-9 Effect of air inlet humidity ratio on moisture removal rate and dehumidifier effectiveness.

II: counter flow experiments

Experimental setup is shown in Fig. C-10. The module used ceramic structured paper packing. Its height, length and width were 0.7m, 0.4m and 0.4m, respectively, and one layer and three layers (2.1m high) are both measured. Lithium bromide aqueous solution was used as the desiccant in the system. Dehumidification working condition and regeneration working condition are measured at intervals.

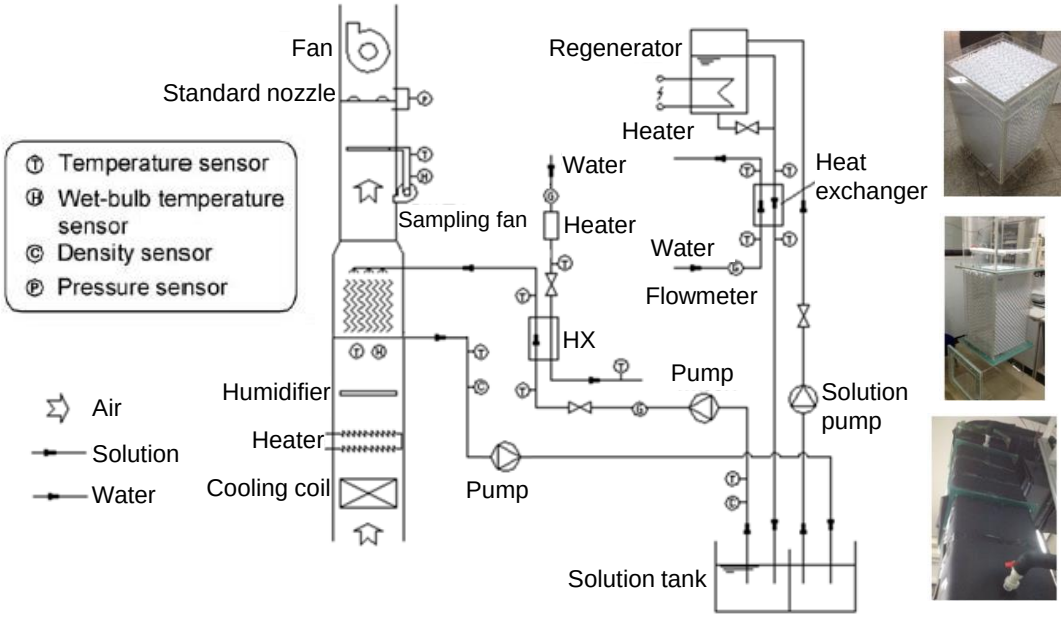

Fig. C-10 Schematic diagram of the counter flow pattern experimental rig.

The operating parameters are shown in Table C-1. As indicated from experimental results, effectiveness of dehumidification and regeneration are 50~60% and 35%~60% respectively for one layer, and those are 60~85% and 50~70% for three layers.

Table C-1 Operating parameters of counter flow pattern packing

Dehumidification	Regeneration

Air inlet parameters	30~44 ℃, 13~30g/kg	Air inlet parameters	16.5~28.0 ℃, 9~14g/kg
Air flow rate	570~1260m^3/h	Air flow rate	410~1240 m^3/h
solution inlet parameters	17~25 ℃, 29%~46%	solution inlet parameters	30~42 ℃, 30%~47%
Solution flow rate	1.1~1.4m^3/h	Solution flow rate	1.0~1.4m^3/h
mass flow rate ratio ($\dot{m}_s / \dot{m}_a$)	1.1~2.4	mass flow rate ratio ($\dot{m}_s / \dot{m}_a$)	1.1~3.2

Utilizing mathematics model and experimental data, volumetric mass transfer coefficient (h_mA) and number of mass transfer units (NTU_m) can be derived. As shown in Fig. C-11, NTU_m can is 1.0~1.5 for a layer of packed tower, and 3.0~4.5 for three layers. Air flow rate has much impact on volumetric mass transfer coefficient, the coefficient changes from 1.0~4.0 kg/m^{3}s with air flow rate increasing from 1.0 to 3.0 kg/m^{3}s. Correlation of volumetric mass transfer coefficient is

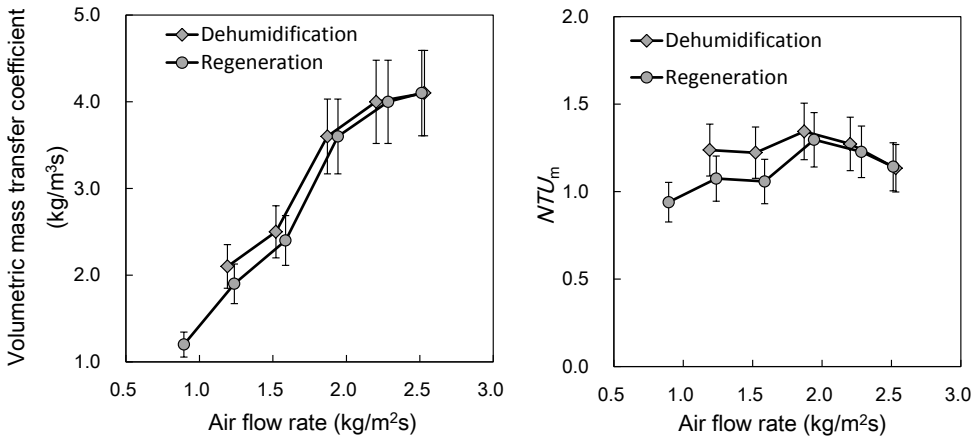

(a) one layer (0.7m high)

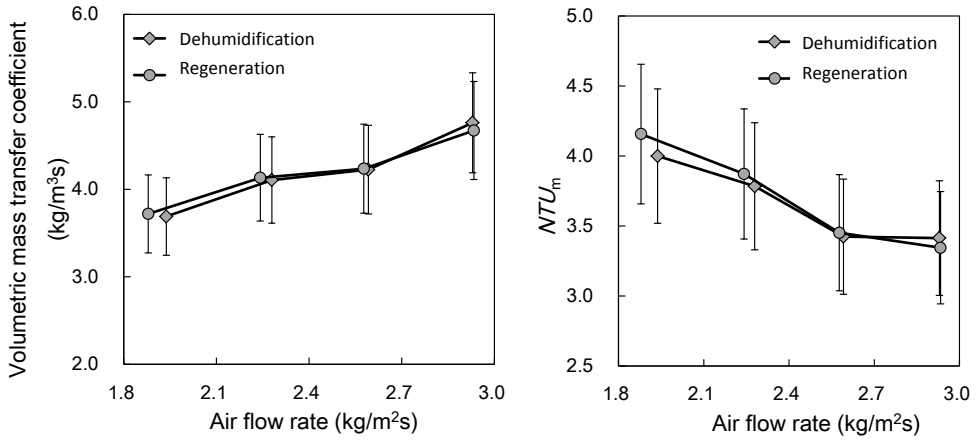

(b) three layers (2.1m high)

Fig. C-11 Volumetric mass transfer coefficient and number of mass transfer units (NTU_m) from experimental data.

h_mA is correlated with air velocity v_a (m/s), solution spray velocity v_s (mm/s) and

equivalent relatively humidity of solution inlet $\varphi_{e,in}$, by power exponent relates. To correlate with experimental data, Eq. (C-8) can be obtained. Then for this kind of packing material, h_mA can be predicted by equation, and NTU_m can be calculated with it and packing size and air volume.

$$h_m a = 0.9845 \times v_a^{0.7467} \times v_s^{0.2428} \times \varphi_{e,in}^{0.1878} \quad \text{(C-8)}$$

III: validation

Results comparison between experimental data and predicted values calculated by above mentioned model are shown in Fig. C-12 and Fig. C-13. It can be seen that the simulation results accord well with the experimental results, and thus, this model can be adopted for further research on dehumidification using liquid and solid desiccant.

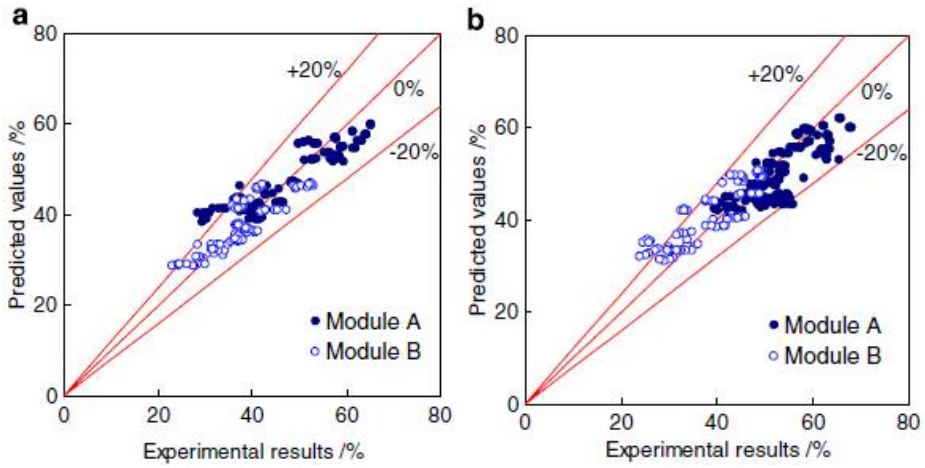

Fig. C-12 Comparison of simulation results with the experimental findings for cross flow dehumidification processes: (a) enthalpy effectiveness and (b) moisture effectiveness

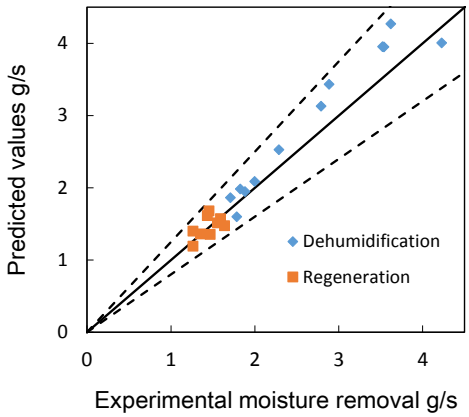

Fig. C-13 Comparison of simulation results with the experimental findings for counter flow dehumidification processes

References

[1] ASHRAE. ASHRAE Handbook- Fundamentals. Atlanta: American Society of Heating Refrigerating and Airconditioning Engineer, Inc., 2009.

[2] ASHRAE. ASHRAE Standard 62.1 Ventilation for Acceptable Indoor Air Quality. Atlanta: American Society of Heating, Refrigerating and Air-Conditioning Engineers, Inc., 2010.

[3] ASHRAE Handbook. Chapter 27 Climatic Design Information.

[4] MOHURD, AQSIQ. GB50736-2012 Code for design of heating ventilation and air conditioning. Beijing: China Architecture & Building Press; 2012 (in Chinese).

[5] Meteorological Information Center of China Meteorological Administration, Tsinghua University. Dedicated meteorological data sets for thermal built environment analysis in China. Beijing: China Architecture & Building Press; 2005 (in Chinese).

[6] Heat recovery equipment selection and installation for air-conditioning system, China Architecture & Building Press, 2006

[7] Pesaran AA, Mills AF. Moisture transport in silica gel packed beds 1: theoretical study. International Journal of Heat and Mass Transfer, 1987;30:1037-1049.

[8] Munters. Samples of desiccant wheels. 2004.

[9] Subramanyam N, Maiya MP, Murthy SS. Application of desiccant wheel to control humidity in air-conditioning systems. Applied Thermal Engineering, 2004;24:2777-2788.

[10] Aynur TN, Hwang Y, Radermacher R. Integration of variable refrigerant flow and heat pump desiccant systems for the cooling season. Applied Thermal Engineering, 2010;30:917-927.

[11] Jeong J, Yamaguchi S, Saito K, Kawai S. Performance analysis of four-partition desiccant wheel and hybrid dehumidification air-conditioning system. International Journal of Refrigeration, 2010;33:496-509.

[12] Guo ZY, Zhu HY, Liang XG. Entransy - a physical quantity describing heat transfer ability. International Journal of Heat and Mass Transfer, 2007;50:2545-2556.

[13] Cheng XT, Liang XG. Computation of effectiveness of two-stream heat exchanger networks based on concepts of entropy generation, entransy dissipation and entransy-dissipation-based thermal resistance. Energy Conversion and Management, 2012;58:163-170.

[14] Liu XH. Combined heat and mass transfer characteristic in air handling process using liquid desiccant. Doctoral dissertation, Tsinghua University, Beijing, 2007 (in Chinese).

[15] Liu XH, Zhang Y, Qu KY, Jiang Y. Experimental study on mass transfer performances of cross flow dehumidifier using liquid desiccant. Energy Conversion and Management, 2006; 47(15-16):2682-2692.

[16] Liu XH, Jiang Y, Chang XM, Yi XQ. Experimental investigation of the heat and mass

transfer between air and liquid desiccant in a cross-flow regenerator. Renewable Energy, 2007; 32(10):1623-1636.

[17] Zhang T, Liu XH, Zhang L, Jiang Y. Match properties of heat transfer and coupled heat and mass transfer processes in air-conditioning system. Energy Conversion and Management, 2012;59:103-113.

[18] Zhang T, Liu XH, Jiang Y. Performance comparison of liquid desiccant air handling processes from the perspective of match properties. Energy Conversion and Management, 2013;75:51-60.

[19] Beccali M, Butera F, Guanella R, Adhikari R S. Simplified models for the performance evaluation of desiccant wheel dehumidification. International Journal of Energy Research 2002;27: 17-29

[20] pr/EN 15251. Indoor environmental input parameters for design and assessment of energy performance of buildings addressing indoor air quality, thermal environment, lighting and acoustics. 2007.

[21] Technical potential of evaporative cooling in Danish and European condition, Proceedings of the 6th International Building Physics Conference 2015.

[22] Chua KJ, Chou SK, Yang WM, Yan J. Achieving better energy-efficient air conditioning – A review of technologies and strategies. Applied Energy 104 (2013) 87–104.

[23] Liu XP, Niu JL. An optimal design analysis method for heat recovery devices in building applications. Applied Energy 129 (2014) 364–372.

[24] Lu YQ. Practical design manual for heating and air-conditioning. 2nd ed. Beijing: China Architecture & Building Press; 2008.

[25] Fehrm M, Reiners W, Ungemach M. Exhaust air heat recovery in buildings. International Journal of Refrigeration 25 (2002) 439–449.

[26] Besant RW, Simonson C. Air-to-air exchangers. ASHRAE Journal 45 (2003) 42–52.

[27] Perez-Lombard L, Ortiz J, Maestre IR. The map of energy flow in HVAC systems. Applied Energy 88 (2011) 5020–5031.

[28] Cuce PM, Riffat S. A comprehensive review of heat recovery systems for building applications. Renewable and Sustainable Energy Reviews, 2015, 47:665–682.

[29] Beccali M, Finocchiaro P, Nocke B. Energy performance evaluation of a demo solar desiccant cooling system with heat recovery for the regeneration of the adsorption material. Renew Energ 2012;44:40-52.

[30] Henning HM, Pagano T, Mola S, Wiemken E. Micro tri-generation system for indoor air conditioning in the Mediterranean climate. Appl Therm Eng 2007;27:2188-94.